· INEEL/EXT-99-01322

The Preparation and Characterization of INTEC Phase 2b Composition Variation Study Glasses

B. A. Staples
B. A. Scholes
D. K. Peeler
L. L. Torres
J. D. Vienna
C. A. Musick
B. R. Boyle

Published February 2000

Idaho National Engineering and Environmental Laboratory
High-Level Waste Operations
Idaho Falls, Idaho 83415

Prepared for the
U.S. Department of Energy
Office of Science and Technology
Under DOE Idaho Operations Office
Contract DE-AC07-99ID13727

DISCLAIMER

ABSTRACT

The second phase of the composition variation study (CVS) for the development of glass compositions to immobilize Idaho Nuclear Technology and Engineering Center (INTEC) high level wastes (HLW) is complete. This phase of the CVS addressed waste compositions anticipated primarily from the direct vitrification of calcine, whereas the first phase of the CVS addressed waste composition of high activity waste fractions (HAW) from the initial separations flowsheet. Updated estimates of INTEC calcined HLW compositions and of high activity waste fractions (HAW) proposed to be separated from dissolved calcine were used as the waste component for this CVS phase. These wastes are of particular interest because high aluminum, calcium, zirconium, fluorine, potassium, and low iron and sodium content places them outside the vitrification experience in the Department of Energy (DOE) complex. Because of the presence of calcium and fluorine, two major zirconia calcine components not addressed in Phase 1, a series of scoping tests, designated Phase 2a, were performed. The results of these tests provided information on the effects of calcium and fluoride solubility and their impacts on product properties and composition boundary information for Phase 2b. Details and results of Phase 2a are reported separately. Through application of statistical techniques and the results of Phase 2a, a test matrix was defined for Phase 2b of the CVS. From this matrix, formulations were systematically selected for preparation and characterization with respect to visual and optical homogeneity, viscosity as a function of melt temperature, liquidus temperature (T_L), and leaching properties based on response to the product consistency test (PCT). The results of preparing and characterizing the Phase 2b glasses are presented in this document. Based on the results, several formulations investigated have suitable properties for further development. A full analysis of the composition-product characteristic relationship of glasses being developed for immobilizing INTEC wastes will be performed at the completion of composition-property relationship phases of the CVS. Contributions were made to this phase of the CVS by personnel working at the Idaho National Engineering and Environmental Laboratory (INEEL), Pacific Northwest National Laboratories (PNNL), and the Savannah River Technology Center (SRTC).

EXECUTIVE SUMMARY

One option for immobilizing and reducing the volume of HLW vitrification is being considered for the immobilizing HLW being stored at INTEC is to dissolve calcined waste then separate the radionuclides. The separated fraction hosting radionuclides is known as HAW, and it is proposed to immobilize HAW by vitrification. The separation process also retains a significant amount of aluminum and zirconium in the HAW from the dissolved calcine. The separation process also adds phosphate and potassium to the HAW. The concentrations of these elements in the HAW place its composition outside those of wastes expected to be immobilized in the DOE complex. Another option for immobilizing INTEC calcined waste is direct vitrification. Zirconia calcines contain high amounts of zirconium, calcium and fluorine. Alumina calcines contain high amounts of aluminum. These concentrations place calcine compositions outside those of expected wastes to be immobilized in the DOE complex.

A cooperative CVS conducted at the INEEL, PNNL and SRTC is in progress to observe the composition-product characteristic relationships of the glasses formed from the HAW and the calcine. This study is a precursor to defining vitrifying formulations for the waste. The multi-year scope of the CVS provides opportunity to adjust the overall compositional envelope as HAW and calcine composition estimates improve or separation processes are refined. It also allows the observation of composition-product property relationships in enough phases to acquire information necessary to optimize formulations for use in process development activities. The first CVS phase (Phase 1 and Phase 1b) was completed in FY98. The results are given in "The Preparation and Characterization of INTEC HLW Phase 1 Composition Variation Study Glasses," INEEL/EXT-98-00970, Rev. 1. The experience of preparing and characterizing the second phase of the CVS glasses, known as Phase 2b glasses, is discussed in this document.

Phase 2a was a series of scoping tests designed to evaluate the solubility and resultant effects of calcium and fluorine on product homogeneity, durability as defined by the PCT and viscosity. Both these elements are major components of zirconia calcine, and neither they nor their effects were addressed in Phase 1. The results of completing Phase 2a are reported elsewhere, but were used in establishing compositional boundaries of the Phase 2b matrix. Using updated HAW and calcine compositions estimates, and information from conducting Phase 2a, mixture analysis techniques were applied to derive the Phase 2b formulation matrix. Formulations for preparation and characterization with respect to viscosity profile, liquidus temperature (T_L) and leaching response to the PCT were derived from this matrix through systematic selection described in Section 2.2. These formulations are given in Tables 3 and 4. Most formulations selected for preparation and characterization would be vitrified at 1150°C. Others were known to require higher vitrification temperatures and were prepared to evaluate the potential advantages of high melt temperatures on waste loading. These glasses requiring higher vitrification temperatures were also selected for preparation and characterization.

The specific melt conditions used to fabricate the Phase 2b glasses are given in Section 4.2 and summarized in Table 6. Table 7 summarizes the "as-measured" compositions. Table 8 presents the homogeneity properties of air quenched Phase 2b glasses. Characterization of these glasses for visual homogeneity and x-ray diffraction analysis are given in Section 5.1 and summarized in Table 6. Table 9 presents the results of the canister centerline cooling experiment conducted on some Phases 2b glasses. Sections 5.2, 5.3 and 5.4 discuss the determination of T_L, leaching response to the PCT, and viscosity-melt temperature relationship data, respectively. Tables 10, 12 and 13 summarize the respective results. Table 14 presents a summary of Phase 2b glass characteristics compared to performance criteria.

Most Phase 2b formulations yielded optically homogeneous products after vitrification at 1150°C and cooling by air quenching. Some did not yield optically homogeneous products when vitrified at temperatures as high as 1500°C. Observations herein are that the concentration of certain INTEC HAW and calcine components have a major influence on vitrification temperature. Reduced waste loading could also decrease the concentration impact on melt temperature from some of these components. Through the results of canister centerline cooling (CCC) heat treatment experiments, it was observed that either devitrification or amorphous phase separation tendency was increased by the presence of components such as calcium and fluorine.

Fluorapatite is the primary phase formed at T_L in optically homogeneous glasses containing calcium, fluorine and phosphorous. For those glasses requiring temperatures higher than 1150°C to yield optically homogeneous products, a larger variety of primary crystalline phases were observed at T_L. The crystalline species observed in the T_L tests on Phase 2b glasses are significantly different than those in Phase 1b and can be attributed to the difference in waste compositions investigated in each phase. It is also the reason for observing effects on T_L as estimates of INTEC HLW composition improve. All but four Phase 2b glasses performed better than the Environmental Assessment (EA) glass with respect to leachability of major components when subjected to the PCT. Viscosity as a function of melt temperature was observed on optically homogeneous Phase 2b glasses. The viscosity at 1150°C of most of the Phase 2b glasses was in the range of 2-10 Pascal-seconds (Pa-sec.). Most of those not achieving this viscosity range were glasses added in the matrix to investigate the potential advantages of vitrification at temperatures higher than 1150°C.

Most of the Phase 2b products have characteristics that make further efforts to develop INTEC waste vitrifying formulations practical. A full analysis of the information obtained in this phase of the CVS glasses will be made at the conclusion of the composition-property relationship investigations. A complete analysis is needed for planning the optimization of the glass formulations for vitrifying HAW and calcine.

A more thorough estimate of INTEC calcined waste compositions was made after Phase 2b of the INTEC CVS began. Compositions with respect to major and minor components as well as radionuclides are included in this updated estimate. The estimates do not include the chemical and phase composition of undissolved solids within the calcines. Nevertheless, these

newest INTEC calcined waste composition estimates must be used in developing surrogates for use in future phases of this CVS. Each of the components by themselves, or in combination with others present, could have significant effects on the processability and acceptability for disposal of the glasses being developed.

Recommendations for other important areas of attention with respect to the five processing and product performance properties investigated in Phase 2b CVS for INTEC HLW glasses include:

1. Obtaining more data for the definition of primary phase fields of the crystalline species that determine T_L of glasses investigated.

2. Studying the effects of composition changes on durability.

3. Defining the influence of composition and phase changes on the ability to retain a homogeneous product.

4. Defining the influence of composition on glass viscosity-melt temperature profile.

5. Performing electron microscopy and durability testing of glasses cooled at the CCC heat treatment.

ACKNOWLEDGMENTS

The authors acknowledge the guidance and funding provided for this multi-institutional task by the DOE's Tanks Focus Area (TFA). The following personnel from the indicated institutions made significant technical contributions towards the completion of this task.

Tommy Edwards, SRTC

Bill Holtzscheiter, SRTC

Carol Jantzen, SRTC

Irene Reamer, SRTC

Jarrod Crum, PNNL

Pavel Hrma, PNNL

Greg Piepel, PNNL

Mike Schweiger, PNNL

Carol Geis, INEEL

Ron Harris, INEEL

Jill Kugler, INEEL

Duane Lundholm, INEEL

Dennis Nielsen, INEEL

Arlin Olson, INEEL

Rich Tillotson, INEEL

The following individuals made significant contributions toward the issue of this report.

Sharla Mickelsen and Ina Moore, INEEL

David Best, Eric Frickey, Sherry Vissage and Debbie Marsh, SRTC Mobile Laboratory

We also acknowledge the contributions of Jim Rindfleisch (INEEL), Jeff Laug (INEEL), Jay Roach (INEEL), and Jim Herzog (INEEL).

Funding to perform this task, Technical Task Plan ID-77WT-31, Subtask B, was provided by the U.S. Department of Energy's Office of Science and Technology.

CONTENTS

ABSTRACT i

EXECUTIVE SUMMARY iv

ACKNOWLEDGMENTS vii

ACRONYMS xi

1. INTRODUCTION 1

2. BASIS 4

2.1 Waste Stream Compositions 4
2.2 Approach 10

2.2.1 Determination of Composition Region Boundaries 11
2.2.2 Derivation of Models for Screening the Phase 2b Matrix 11
2.2.3 Phase 2a Testing 11
2.2.4 Phase 2b Experimental Design 12

3. PERFORMANCE AND PROCESSING CRITERIA 16

3.1 Properties Influencing Glass Processability 16

3.1.1 Liquidus Temperature 16
3.1.2 Viscosity 16

3.2 Properties Influencing Glass Waste Form Acceptability 16

3.2.1 Durability 16
3.2.2 Homogeneity 17

4. GLASS PREPARATION AND OBSERVATIONS DURING FORMATION 18

4.1 Preparation Sequence 18
4.2 Physical Conditions of Preparation 18
4.3 Composition and Homogeneity Characterization 19
4.4 Liquidus Temperature 25
4.5 Durability 25
4.6 Viscosity Characterization 26

5. CHARACTERIZATION RESULTS AND DISCUSSION 27

5.1 Composition and Homogeneity Results 27

5.1.1 Composition 27
5.1.2 Homogeneity of Air Quenched Glasses 27
5.1.3 Homogeneity of Glasses Subjected to CCC Heat Treatment 30

5.2 Liquidus Temperature Results....30
5.3 Durability Results....36

5.3.1 Results from the Multi-Element Solution Standard....36
5.3.2 Normalized PCTs Using As-Targeted Glass Compositions....37

5.4 Viscosity Characterization....41

6. Summary of Phase 2b Glass Characteristics....45

7. CONCLUSIONS AND RECOMMENDATIONS....47

7.1 Obtaining More Data for the Definition of Primary Phase Fields of the Crystalline Species That Determine T_L of Glasses Investigated....47
7.2 Studying the Effects of Composition and Phase Changes on Durability....47
7.3 Defining the Influence of Composition on the Ability to Retain a Homogeneous Product....47
7.4 Defining the Influence of Composition on Glass Viscosity-Melt Temperature Profile....47
7.5 Performing Electron Microscopy and Durability Testing of Glasses Cooled at the CCC Heat Treatment....47

8. REFERENCES....50

Appendix A — X-Ray Diffraction Patterns for Air Quenched Glasses and for those Cooled at Canister Centerline Heat Treatment

Appendix B — Raw Data from PCT Leachate Analyses of INTEC Phase 2b CVS Glasses

Appendix C — Raw Data form Viscosity Measurements on Phase 2b Glasses

FIGURES

1. Typical INTEC calcined solids storage bin set....1

2. Plot of cooling curve applied to simulate canister centerline cooling conditions for Phase 2b glasses20

3. Micrograph (1994 X) of crystalline structure in glass IG2-07 formed by air quenching....29

4. SEM micrograph (1000X) of fluorapatite crystal and adjacent glass matrix in IG2-20 with spectra taken from fluorapatite crystal....33

5. Elemental map of fluorapatite crystal and adjacent glass in IG2-20....33

6. SEM micrograph (1000X) of IG2-04 displaying NiO and Na_2ZrO_3 crystallinity with spectra taken from Na_2ZrO_3 crystal....34

7. Elemental map of nickel oxide and sodium zirconate crystals and adjacent glass in IG2-04....34

8. SEM micrograph (500X) of IG2-24 displaying ZrO_2 crystallinity....35

9. Elemental map of zirconia crystal identified in IG2-24 showing distribution of calcium, oxygen, silicon, and zirconium....35

10. Fit of Arrhenius equation to IG2-19 viscosity data 42

11. Fit of Arrhenius equation to IG2-27 viscosity data 42

12. Fit of Arrhenius equation to IG2-27 viscosity data showing discontinuity 43

TABLES

1. Mean estimates of bin set contents 5

2. Composition of HAWs use to derive Phase 2b experimental glass composition region 9

3. Composition of others 12

4. Phase 2a test matrix of batching compositions (mass fraction) for Phase 2b glasses 13

5. Mass fraction boundaries of Phase 2b glass components 15

6. Vitrification conditions required to achieve visually homogeneous products 19

7. Result of spectrochemical analysis of Phase 2b glasses 21

8. Homogeneity properties of air quenched glasses formed in this study 28

9. Homogeneity and phase formation in glasses subjected to CCC experiment 30

10. Results of liquidus temperature measurements (^{o}C) performed on Phase 2b glasses 32

11. Analytical results from multi-element solution standard 36

12. PCT an leachate pH results for Phase 2b glasses normalized by "as targeted" composition 38

13. Viscosity Profile at T_M °C using Arrhenius model 43

14. Summary of Phase 2b glass characteristics compared to performance criteria 45

ACRONYMS

CCC	Canister centerline cooling
CVS	Composition Variation Study
DOE	Department of Energy
DWPF	Defense Waste Processing Facility
EA	Environmental Assessment glass
FLAAS	Flame atomic absorption spectrometry
GCER	Glass composition experimental range
HAW	High activity waste
HLW	High level waste
ICP	Inductively coupled plasma emission spectrometry
INEEL	Idaho National Environmental and Engineering Laboratory
INTEC	Idaho Nuclear Technology and Engineering Center, formerly Idaho Chemical Processing Plant (ICPP)
LMITCO	Lockheed Martin Idaho Technologies Company
NBS	National Bureau of Standards
Pa-sec.	Pascal-seconds
PCT	Product consistency test
PNNL	Pacific Northwest National Laboratory
RCRA	Resource Conservation and Recovery Act
SBW	Sodium bearing waste
SEM	Scanning electron microscope
SRS	Savannah River Site
SRTC	Savannah River Technology Center
TEM	Transition Electron Microscopy
TFA	Tanks Focus Area
T_A	Lowest observed temperature where glass remains amorphous
T_C	Highest observed temperature where glass remains crystalline
T_L	Liquidus temperature
T_M	Nominal melter operating temperature
USDOE	United States Department of Energy

WAPS	Waste Acceptance Product Specifications
WCUR	Waste composition uncertainty region
WVDP	West Valley Demonstration Plant
XRD	X-ray Diffraction Analysis

The Preparation and Characterization of INTEC HAW Phase 2 Composition Variation Study

1. INTRODUCTION

As a result of four decades of nuclear fuels reprocessing at the Idaho Nuclear Technology and Engineering Center (INTEC), large volumes of radioactive wastes have been collected. Since 1963 these wastes have been converted to a granular form through fluidized bed calcination. These calcined high level wastes (HLW), totaling to about 4,000 m^3 in volume, are currently being stored on site in stainless steel bin sets. Figure 1 provides a view of a typical INTEC calcine storage bin set. During the span of INTEC operations, secondary radioactive liquid wastes high in alkali oxide have also been collected and stored. These wastes originate from decontamination, laboratory and fuels storage activities. Collectively, these liquid wastes are known as "sodium bearing wastes (SBW)." They can not be directly calcined because of their high alkali content. Historically they have been blended with reprocessing wastes or non-radioactive aluminum nitrate prior to calcination. Because fuel reprocessing is no longer being performed at INTEC, the option of waste blending to deplete SBW inventory is eliminated. Consequently, about 5.7 million liters of SBW are temporarily stored in stainless steel tanks at INTEC.

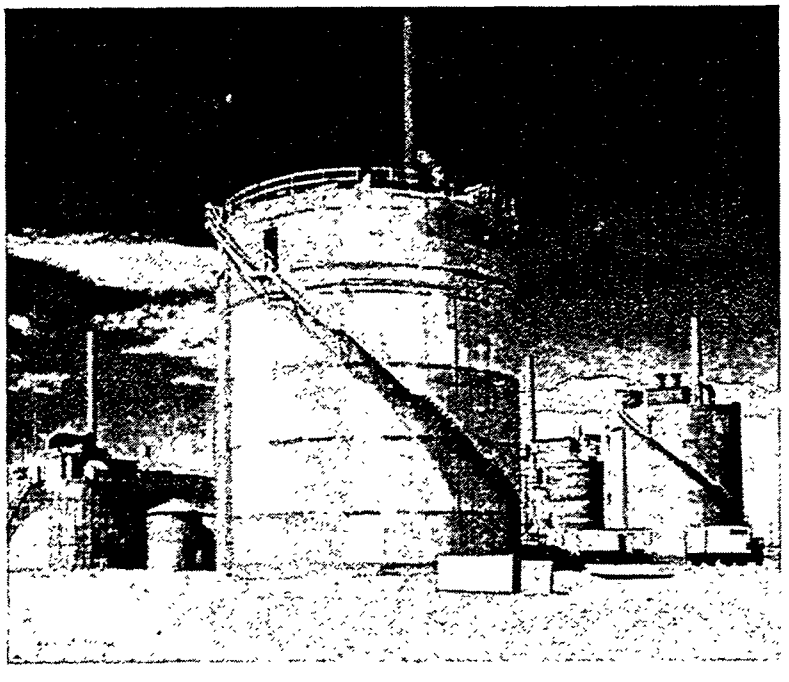

Figure 1. Typical INTEC calcined solids storage bin set.

The Batt Settlement Agreement was established in August 1995, between the U.S. Navy, the State of Idaho and the U.S. Department of Energy (DOE). Section E.6 of the Agreement states that all HLW stored at the Idaho National Engineering and Environmental Laboratory (INEEL) will be rendered ready (immobilized) for transport to a suitable repository by the end of year 2035. More immediately, immobilization technology, including the results of this composition variation study (CVS), must be applied to provide information for the beginning of design of the HLW treatment facility in year 2007. This design supports the Settlement Agreement milestone of submitting a Resource Conservation and Recovery Act (RCRA) Part B permit application in year 2012 and the Site Treatment Plan operational date of September 30, 2019. Vitrification is considered the "Best Demonstrated Available Technology" for immobilizing HLW.[1] Therefore, vitrification is being studied for the purpose of immobilizing INTEC HLW. Precedents for the vitrification of INTEC HLW into borosilicate glass are established by the production scale operation of the Defense Waste Processing Facility (DWPF) at the Savannah River Site (SRS), the West Valley Demonstration Project (WVDP) at West Valley, New York, and certain European facilities.

Efforts are in progress at the INEEL to investigate processes and immobilizing formulations for vitrifying HLW stored as calcines or as liquid. The *Idaho High Level Waste and Facilities Disposition Environmental Impact Statement* is under development and evaluates various options for immobilizing INTEC HLW.[2] These options include vitrification of INEEL HLW either as calcines or as the high activity waste fraction (HAW) separated from the calcine. The HAWs and calcines have unique chemical compositions. These respective compositions differ significantly from those wastes being vitrified at the DWPF, the WVDP and planned for vitrification at Hanford. Production scale technologies exist with vitrifying formulations for the waste chemistries at these plants. However, it is uncertain that the frit formulations developed for vitrifying waste compositions at these sites could vitrify the INTEC wastes in a cost-effective manner.

Insufficient data exists on the composition-product property relationships for glasses formed from INTEC wastes to develop glass formulations. Thus the major purpose of this study is to collect information on these relationships in borosilicate glass compositions prepared using current estimates of HAW and calcine composition ranges. Data is also needed to demonstrate that HAW or calcine can be vitrified in a full-scale process. Thus another goal of the CVS is to provide information to the developing separation process for determining how HAW compositions must be altered to obtain cost effective vitrification. Also, the composition-product property information obtained in the CVS will be the foundation for establishing the extensive data base required for developing formulations for use in glass composition optimization, pretreatment and staging plans, plant design, and plant operation.

A capability for developing glass formulations on a small scale has been in progress through years of active HLW management programs at the INTEC.[2] At the Savannah River Technology Center (SRTC) and at Pacific Northwest National Laboratory (PNNL), expertise exists to apply vitrification technology on a production and engineering scale respectively. These sites have established and refined glass formulation development and implementation through the entire scale-up process. Also established is an extensive database and operating experience on vitrification in joule-heated ceramic brick melters.

In FY97, the DOE Tanks Focus Area-Immobilization Program (TFA-Immobilization) sponsored a task at PNNL and SRTC to investigate the effects of INTEC glass composition on product properties and process variables impacting the corrosion of melter materials. Also in 1997, TFA brought experts from the INEEL, PNNL and SRTC together to define a path forward for developing glass formulations for the INTEC HAW. These persons collaborated in FY98 to:

1. Provide the best estimate of HAW compositions,

2. Define an approach to develop glass formulations for immobilizing HAWs, and

3. Prepare and characterize initial glasses to begin CVS data base development.

As a result of this collaboration a phased approach was adopted to allow participants to adjust the compositional envelope as INTEC waste stream composition estimates are improved. Phase 1 of the CVS was performed using only contemporary HAW estimates based on the preliminary separations flowsheet. Phase 1 was completed, and its results were presented in March 1999.[3] Phase 2 was performed to evaluate the potential for developing formulations for the direct vitrification of INTEC calcined wastes in addition to the vitrification of HAW. Preparation and characterization of glasses making up Phase 2b of the INTEC CVS has been completed. This document relates the details and results of these actions.

Extensive glass property-composition databases were developed to support the processability and acceptability for repository disposal of the glasses produced at DWPF, Hanford and WVDP. These data do not cover the composition region expected in INTEC HAW or calcine glasses. A benefit of this CVS is the data acquisition that can test the versatility of models established at PNNL and SRTC for assessing the acceptability and processing characteristics of vitrified wastes. Testing the models' capability to address the immobilization of wastes outside of Hanford or SRS compositions enhances their suitability to address the immobilization of radioactive wastes existing throughout the DOE complex.

2. BASIS

2.1 Waste Stream Compositions

During FY98 and FY99, more information became available on the composition of INTEC calcines and SBW, including a better identification of the minor components and an updated estimate of the major component contents. This information adjusts the separations flowsheet which alters the HAW fraction composition removed from the calcines. Through review of separations flowsheet development, increased interest has resulted in direct vitrification of INTEC calcined waste. Direct vitrification offers simpler pretreatment facilities, but may result in a larger volume of vitrified waste.

Because of the interest in radionuclide separations and direct vitrification, both HAW and calcine compositions were used to define CVS Phase 2 glass compositions. The calcined waste composition estimates as of March 1999 and their component ranges are given in Table 1. These are known as the "March 1999 composition estimates." Because of the preliminary nature of the separations flowsheets, and the incomplete knowledge of calcine compositions, assumptions based on current process knowledge were made and applied in estimating waste compositions for use in Phase 2 of this task.

Six bin sets hold the calcined wastes produced and stored at INTEC. The number of bins in each bin set ranges from four to seven. Most bins hold calcine in layers, and these layers are of different compositions. In its current development stage, the INTEC High Level Waste Management Program (HLWMP) does not have the resources needed to perform the analysis for the various calcine compositions in each bin nor to determine the location of interfaces between calcine of different compositions. Thus the elemental composition estimates used in this study were obtained indirectly from processing knowledge, and the data given in Table 1 are mean estimates for the contents of each bin set. Significant future efforts in the HLWMP must be devoted to defining the amounts and limits of each calcine composition.

Composition-product characteristics of vitrified INTEC HLW must be understood before optimizing formulations for use in process development. Optimized formulations and a thorough knowledge of the amounts and locations of various calcine compositions within the INTEC storage bins will provide the basis for developing a calcine retrieval strategy suitable for successful immobilization.

Table 1. Mean estimates of bin set contents.

Bin Set 1				
	Average Wt%	Std Dev Wt%	Minimum Wt%	Maximum Wt%
Al	47.64	0.83	46.76	49.71
B	0.25	0.02	0.18	0.26
Ca	0.00	0.00	0.00	0.00
Fe	0.88	0.41	0.27	1.36
Cs	0.03	0.00	0.02	0.04
Hg	1.89	0.21	0.99	2.06
K	0.00	0.00	0.00	0.00
Mg	0.00	0.00	0.00	0.00
Na	1.34	0.25	0.99	1.60
Sr	0.02	0.00	0.01	0.02
CO_3	0.00	0.00	0.00	0.00
NO_3	2.21	0.62	0.99	2.85
PO_4	0.95	0.36	0.00	1.15
SO_4	1.63	0.18	0.78	1.75
O	43.14	0.66	42.52	44.70

Bin Set 2 Al				
	Average Wt%	Std Dev Wt%	Minimum Wt%	Maximum Wt%
Al	47.16	2.13	42.67	49.42
B	0.19	0.04	0.14	0.25
Ca	0.78	1.01	0.00	2.86
Fe	0.09	0.07	0.06	0.24
Cs	0.02	0.00	0.02	0.03
Hg	0.03	0.00	0.02	0.03
K	0.08	0.16	0.00	0.48
Mg	0.47	0.61	0.00	1.73
Na	1.57	0.51	1.20	2.88
Sr	0.02	0.00	0.01	0.02
CO_3	2.33	3.04	0.00	8.56
NO_3	2.89	1.08	2.14	5.65
PO_4	0.85	0.39	0.17	1.28
SO_4	1.33	0.58	9.27	1.80
O	42.17	1.82	38.20	44.07

Table 1. (continued).

	Bin Set 2 Zr			
	Average Wt%	Std Dev Wt%	Minimum Wt%	Maximum Wt%
Al	15.34	9.74	7.17	41.27
B	0.72	0.18	0.23	0.89
Ca	24.02	7.49	4.99	31.14
Cr	0.20	0.07	0.03	0.29
Fe	0.13	0.04	0.07	0.21
Hg	0.00	0.01	0.00	0.03
K	0.11	0.23	0.00	0.96
Mg	0.27	0.32	0.00	0.97
Mn	0.00	0.00	0.00	0.00
Na	0.19	0.35	0.00	1.21
Ni	0.06	0.02	0.01	0.08
Sr	0.26	0.08	0.05	0.34
Sn	0.23	0.08	0.03	0.33
Zr	14.23	4.79	1.99	20.75
Cl	0.00	0.00	0.00	0.00
F	21.10	6.92	3.01	27.32
CO_3	1.34	1.57	0.00	4.77
NO_3	0.46	0.83	0.00	2.79
PO_4	0.12	0.08	0.06	0.49
SO_4	0.19	0.13	0.10	0.73
O	21.01	6.51	15.42	38.23

	Bin Set 3			
	Average Wt%	Std Dev Wt%	Minimum Wt%	Maximum Wt%
Al	11.94	4.11	8.23	39.47
B	0.82	0.07	0.46	1.00
Ca	24.83	4.18	5.45	29.01
Cr	0.21	0.03	0.08	0.26
Fe	0.23	0.08	0.11	0.48
Hg	0.00	0.00	0.00	0.01
K	0.16	0.25	0.00	0.81
Mg	0.65	0.44	0.00	1.81
Mn	0.02	0.03	0.00	0.11
Na	0.84	1.11	0.00	3.23
Ni	0.06	0.01	0.03	0.07
Sr	0.26	0.06	0.03	0.31
Sn	0.23	0.04	0.03	0.30
Zr	14.48	2.43	2.08	18.53
Cl	0.03	0.05	0.00	0.16
F	20.50	3.05	3.32	24.71
CO_3	3.17	2.17	0.00	8.94
NO_3	1.66	2.19	0.00	6.63
PO_4	0.91	2.62	0.05	14.33
SO_4	0.51	0.52	0.09	2.94
O	18.50	2.70	14.45	36.35

Table 1. (continued).

	Bin Set 4			
	Average Wt%	Std Dev Wt%	Minimum Wt%	Maximum Wt%
Al	9.74	0.98	7.99	12.73
B	0.90	0.05	0.73	1.06
Ca	27.99	1.19	24.04	29.77
Cd	0.00	0.00	0.00	0.00
Cr	0.24	0.02	0.18	0.28
Fe	0.48	0.34	0.21	2.03
K	0.41	0.14	0.16	0.67
Mg	0.29	0.40	0.00	2.03
Mn	0.00	0.00	0.00	0.00
Na	1.69	0.56	0.65	2.71
Nb	0.00	0.00	0.00	0.00
Ni	0.08	0.01	0.06	0.10
Sr	0.29	0.02	0.23	0.32
Sn	0.22	0.03	0.05	0.26
Zr	13.88	1.08	10.70	16.23
Cl	0.09	0.06	0.01	0.24
F	19.91	1.31	15.21	23.94
CO_3	1.41	1.97	0.00	10.01
NO_3	3.45	1.14	1.33	5.55
PO_4	0.07	0.01	0.05	0.10
SO_4	0.11	0.01	0.09	0.16
O	18.75	0.43	17.37	19.29

	Bin Set 5			
	Average Wt%	Std Dev Wt%	Minimum Wt%	Maximum Wt%
Al	11.19	4.17	4.94	19.21
B	0.87	0.13	0.55	1.22
Ca	23.83	3.34	14.34	27.85
Cd	2.77	1.93	0.00	5.64
Cr	0.12	0.05	0.05	0.23
Fe	0.48	0.39	0.14	1.62
K	0.64	0.11	0.26	0.83
Mg	0.48	0.59	0.00	3.53
Mn	0.02	0.03	0.00	0.08
Na	3.23	0.85	1.68	5.33
Nb	0.22	0.43	0.00	1.67
Ni	0.03	0.02	0.01	0.08
Sr	0.25	0.04	0.11	0.30
Sn	0.16	0.04	0.07	0.26
Zr	10.01	2.58	4.40	16.52
Cl	0.13	0.06	0.04	0.32
F	15.91	3.28	5.08	25.33
CO_3	2.31	2.89	0.00	17.42
NO_3	6.44	1.57	3.28	10.25
PO_4	0.18	0.04	0.09	0.23
SO_4	1.92	1.20	0.17	3.63
O	18.79	2.94	14.24	23.72

Table 1. (continued).

Bin Set 6				
	Average Wt%	Std Dev Wt%	Minimum Wt%	Maximum Wt%
Al	27.80	5.62	18.96	34.09
B	0.53	0.09	0.43	0.74
Ca	9.77	4.29	4.44	16.23
Cd	1.04	0.63	0.29	2.02
Cr	0.15	0.06	0.05	0.23
Fe	0.76	0.22	0.33	1.06
K	1.33	0.57	0.53	1.99
Mg	0.69	0.65	0.00	2.27
Mn	0.04	0.03	0.00	0.08
Na	5.17	0.90	3.08	6.60
Ni	0.06	0.04	0.01	0.11
Sr	0.03	0.04	0.00	0.12
Sn	0.04	0.03	0.01	0.11
U	0.03	0.01	0.01	0.04
Zr	2.75	2.04	0.62	6.76
Cl	0.15	0.04	0.09	0.21
F	4.73	2.58	1.62	8.86
CO_3	3.42	3.19	0.00	11.19
NO_3	10.62	2.13	6.13	13.78
PO_4	0.26	0.93	0.01	7.19
SO_4	1.31	0.27	1.03	1.96
O	29.31	4.07	23.08	33.98

The current HAW composition estimates and their low and high limits are given in Table 2. These limits were estimated from calculated flowsheet distributions and experience with laboratory scale tests. The HAW separations process consists first of dissolving the calcine, most likely in a nitric acid system, then applying organic extractants to remove radionuclides from the bulk of calcine matrix components. As this process develops, and as assumptions with respect to it are verified, modified or rejected, the estimates of HAW compositions will improve.

Table 2. Composition of HAWs used to derive Phase 2b experimental glass composition region.

	Alumina calcine HAW			Zirconia calcine HAW			SBW HAW		
	Low Wt %	Expected Wt %	High Wt %	Low Wt %	Expected Wt %	High Wt %	Low Wt %	Expected Wt %	High Wt %
Al	23.51	23.43	23.30	3.85	3.67	3.52	1.68	1.17	0.95
B	0.12	0.12	0.12	0.36	0.34	0.32	2.79	1.94	1.53
Ba	0.02	0.02	0.02	0.05	0.16	0.16	0.05	0.05	0.06
Ca				11.12	10.61	10.18	0.85	0.59	0.47
Cd + Ni							1.52	1.05	0.83
Ce + TRU	1.00	1.00	0.99	0.26	0.25	0.23	0.14	0.09	0.08
Cl	0.31	0.31	0.31	0.04	0.04	0.04	2.60	1.81	1.43
Cr				0.10	0.09	0.09	0.21	0.15	0.12
Cs	1.02	1.02	1.01	0.32	0.31	0.29	0.10	0.07	0.05
Cu							0.15	0.10	0.08
Eu	0.02	0.02	0.02						
F				23.23	22.15	21.16	2.49	1.73	1.37
Fe				0.21	0.30	0.48	2.35	1.67	1.04
Gd				0.00	0.01	0.00			
K				0.34	0.67	0.93	6.57	12.36	14.78
Li							0.15	0.10	0.08
Mg				0.10	0.10	0.09	1.51	1.05	0.83
Mn							0.36	0.25	0.20
Mo	10.43	10.53	10.42	5.06	4.84	4.62	5.31	3.84	3.04
Na	3.64	3.63	3.91	2.31	6.25	2.42	6.65	11.09	13.43
Nb							0.14	0.10	0.08
Nd	1.70	1.70	1.68	0.41	0.39	0.37	0.16	0.11	0.09
Pb				0.01	0.01	0.02	0.37	0.41	0.33
Pd							0.09	0.06	0.05
PO_4	53.84	53.66	53.10	40.52	38.65	36.92	35.52	24.70	19.55

Table 2. (continued).

	Alumina calcine HAW			Zirconia calcine HAW			SBW HAW		
	Low Wt %	Expected Wt %	High Wt %	Low Wt %	Expected Wt %	High Wt %	Low Wt %	Expected Wt %	High Wt %
Pr	0.47	0.47	0.47	0.11	0.10	0.10	0.04	0.03	0.02
Rh	0.01	0.01	0.01				0.15	0.10	0.08
Ru	0.01	0.01	0.01				1.51	1.05	0.83
Si							3.82	2.65	2.10
Sm	0.33	0.33	0.33	0.05	0.05	0.04	0.03	0.02	0.02
Sn				0.09	0.09	0.08	0.75	0.52	0.41
Sr	0.59	0.58	0.58	5.85	5.58	5.33	0.05	0.03	0.03
SO_4	0.81	0.80	0.79	0.05	0.05	0.04	13.70	9.59	7.59
Tc	0.06	0.06	0.06	0.02	0.02	0.02	0.01	0.01	
Ti							0.15	0.10	0.08
Zn							0.15	0.10	0.08
Zr	1.69	1.87	1.85	5.51	5.28	12.51	7.81	21.27	27.39

2.2 Approach

Phase 2 of the INTEC CVS was developed to investigate composition-property relationships within a glass composition region that includes the expected range for HAW and calcine glasses. The March 1999 calcine and HAW composition estimates (see Tables 1 and 2) were applied in its development. Zirconia calcine types make up about three-quarters of the mass of INTEC calcined HLW, and calcium fluoride is the major component of these types. Calcium and fluorine were not considered in Phase 1 of this CVS because the separations process mostly eliminates them from HAW. It was therefore determined to conduct Phase 2 in two stages: Phase 2a and Phase 2b. The first stage, Phase 2a, was a scoping study performed to acquire data on the solubility of these two components in a glass melt. Details of preparing and characterizing the glasses in the Phase 2a matrix are given in T. B. Edwards, et al.[4] Testing in this stage evaluated the effects of these components on product homogeneity, viscosity and durability, as estimated by the Product Consistency Test (PCT).[5] The results of Phase 2a were used to set composition bounds for CaO and F in the larger Phase 2b matrix, the second stage of this study, which investigated composition-property relationships within a glass composition region that includes the expected range for HAW and calcine glasses. The Phase 2b matrix was statistically designed following the strategy discussed in Piepel et al.[6] and applied as in Phase 1b.[3] In Phase 1, 1150°C was assumed to be the nominal INTEC melter processing temperature, thus glasses within its matrix were processed at this temperature.[3] Therefore, the Phase 2b matrix contained glasses intended to be processed at 1150°C as well as some glasses intended to be processed at higher temperatures. Phase 2b would also produce data on components that changed in concentration or were added in the newest HAW composition estimates (P_2O_5, K_2O, MoO_3 and SrO) based on revised HAW separations flowsheets. A synopsis of its derivation and application follows.

2.2.1 Determination of Composition Region Boundaries

Review of the newest INTEC bin set composition estimates identified major and minor waste components that must be varied in the glass composition experimental region (GCER). Likewise, glass forming oxides added to the wastes must also be varied in the GCER. On completion of the review, twelve major glass forming additives and waste components were selected to define the compositional boundaries. These included Al_2O_3, B_2O_3, K_2O, Li_2O, Na_2O, P_2O_5, SiO_2, and ZrO_2, as in Phase 1 of the CVS, and CaO, F, Fe_2O_3, MoO_3, NiO, and SrO added because of the newest calcine composition estimates. The upper and lower boundaries for these components were established based on available data from Phases 1 and 2a of this study, data from other sources and glass formulation experience. From this information a layered design was created for the initial Phase 2b GCER through applying mixture analysis techniques which provided upper and lower boundaries for the twelve components in each layer. The inner layer was constrained with respect to composition ranges to increase the probability of yielding glasses that would meet an arbitrary set of processing and performance specifications. The software applied also defined extreme vertices (corner points) of each layer to be screened for use in the Phase 2b formulation matrix.

2.2.2 Derivation of Models for Screening the Phase 2b Matrix

Screening of extreme compositional vertices was performed using glass formulation experience and available linear compositional models. Linear durability (normalized B release from the PCT) and viscosity models were applied as constraints on the compositional ranges of the inner and outer layers to define formulations with the best potential for acceptable processing and performance characteristics. Data from the performance of homogeneous Phase 1b glasses were used in these models which were linear functions with respect to the eight major oxide components investigated in Phase 1a. Coefficients for NiO and Fe_2O_3 were obtained from previous studies.[7]

2.2.3 Phase 2a Testing

Calcium and fluorine exist primarily as CaF_2 in zirconia calcine. For developing vitrifying formulations, however, these were expressed as CaO and F. Phase 2a scoping tests were performed to evaluate the effects of both on primary processing and acceptance criteria and to minimize the potential of producing a large number of unacceptable glasses in Phase 2b. A constraint of 20 mass % loading was used for major components other than CaO and F in the direct vitrification of a Bin Set 4 zirconia calcine. Then CaO and F were varied independently to find their upper and lower component limits. Details of defining the Phase 2a formulation matrix are given in Edwards, et al.[4] These formulations were prepared using standard batching and melting techniques.[a]

Phase 2a products were characterized with respect to fluoride content, viscosity as a function of temperature and durability as defined by response to the PCT. The results of this testing indicated that targeted fluoride content in glasses could be attained, and fluoride volatility occurring could be attributed to increased surface area to volume ratio in smaller sized melts. Homogeneity observations suggested that CaO and F contents up to 9.18 and 4.59 mass % respectively are soluble in the glass samples tested. Viscosity values of the glasses tested were in the acceptable range of 2-10 Pa-sec at 1150°C. These values were applied to define model coefficients for implementing durability and viscosity constraints on the compositional range of the Phase 2b matrix. The results of subjecting Phase 2a glasses to the PCT indicate that all products have normalized boron releases less than 0.6 g/L. The PCT results, however,

---

a. Procedure for Glass Batching and Melting, PSL-417-GBM, Pacific Northwest National Laboratory.

were not completed in time for use in defining model coefficients for constraining the compositional relationship applied in developing the Phase 2b matrix. Results from previously completed studies were used for this purpose. Based on the Phase 2a property-composition relationships obtained, the upper limits for CaO and F in the Phase 2b matrix were defined as 12.0 and 6.0 mass % respectively.

2.2.4 Phase 2b Experimental Design

The models discussed in Subsection 2.2.2 were applied to refine durability and viscosity acceptability regions within the two layers of the Phase 2b GCER. In addition, upper limit constraints on the Al_2O_3+ZrO_2 contents were applied to ensure that glasses would form. Also, total alkali content lower limit constraints were applied to decrease the probability of producing low durability glasses.

Waste components present in very small quantities were collected into an "Others" component. The "Others" component composition is given in Table 3. This component was added in the amount of 0.0072 mass fraction to all glasses in the test matrix except for one centroid and two formulations (IG1-07 and IG1-38) taken from the Phase 1b matrix to provide an opportunity for observing reproducibility between phases. The components making up "Others" are thought to be present in such small concentrations that they are not likely to have a significant effect on the process/product acceptability region. Thus, the effects on the properties due to "Others" are not being fully evaluated. The only insight on "Others" being offered by the Phase 2b test matrix is through the one centroid composition that is not being spiked. Property measurements for this glass can be compared against those from its spiked counterparts to check for gross differences due to "Others." If significant differences are observed, components within the "Others" mix may have an effect on the properties of interest, and additional testing would be required to identify those critical components.[4]

Details are given in Edwards, et al.[4] with respect to selecting optimal sets of 14 glasses from the extreme vertices of each layer. A pseudo-center derived from the average composition of inner and outer layer centroids was added twice with the "others" component (see Table 3) and once without to these 28 glasses. The pseudo center with 0.5% and with 2.0% MoO_3 and with 2% and 4% SrO were also included. With the addition of the two Phase 1b glasses identified above, these 37 glasses completed the Phase 2b matrix given in Table 4. Table 5 summarizes the component boundaries of the glasses in the Phase 2b matrix.

Table 3. Composition of others.

Oxide	Weight %	Oxide	Weight %	Oxide	Weight %
BaO	0.60	MoO_3	0.92	Sm_2O_3	0.38
Ce_2O_3	0.70	Nb_2O_5	2.89	SnO_2	7.20
Cl^-	3.995	Nd_2O_3	1.15	SO_3	30.33
Cr_2O_3	8.992	PdO	0.20	SrO	7.59
Cs_2O	0.51	Pr_2O_3	0.32	TeO_2	0.27
I^-	0.31	Rb_2O	0.32	Y_2O_3	0.22
La_2O_3	0.34	ReO_2	0.62	Total	100.00
MgO	29.64	Rh_2O_3	0.34		
MnO	1.61	RuO_2	0.56		

Table 4. Phase 2a test matrix of batching compositions (mass fraction) for Phase 2b glasses.

Glass ID	Al_2O_3	B_2O_3	CaO	F	Fe_2O_3	K_2O	Li_2O	Na_2O	NiO	P_2O_5	SiO_2	ZrO_2	Others
IG2-01	0.19860	0.04960	0.00000	0.05960	0.00000	0.00000	0.00000	0.19860	0.01490	0.00000	0.47150	0.00000	0.00720
IG2-02	0.19860	0.17870	0.11910	0.00000	0.00000	0.00000	0.00000	0.04960	0.00000	0.02980	0.41700	0.00000	0.00720
IG2-03	0.03470	0.17870	0.00000	0.03970	0.07940	0.00000	0.00000	0.04960	0.01490	0.00000	0.59580	0.00000	0.00720
IG2-04	0.19860	0.17870	0.00000	0.00000	0.00000	0.09930	0.08940	0.04960	0.01490	0.00000	0.34740	0.01490	0.00720
IG2-05	0.03470	0.04960	0.11910	0.00000	0.07940	0.00993	0.00000	0.19860	0.01490	0.00000	0.34760	0.13900	0.00720
IG2-06	0.06450	0.17870	0.00000	0.00000	0.07940	0.00000	0.08940	0.04960	0.01490	0.02980	0.34750	0.13900	0.00720
IG2-07	0.07940	0.04960	0.11910	0.05960	0.00000	0.09929	0.00000	0.04964	0.01490	0.02980	0.35250	0.13900	0.00720
IG2-08	0.03470	0.17870	0.11910	0.00000	0.00000	0.09929	0.00000	0.12680	0.00000	0.00000	0.43420	0.00000	0.00720
IG2-09	0.19860	0.04960	0.11910	0.05960	0.07940	0.00000	0.07360	0.04960	0.00000	0.00000	0.36330	0.00000	0.00720
IG2-10	0.03470	0.04960	0.00000	0.05960	0.07940	0.09929	0.08340	0.04960	0.00000	0.02980	0.50740	0.00000	0.00720
IG2-11	0.03470	0.04960	0.07460	0.00000	0.00000	0.00000	0.08940	0.15880	0.01490	0.02980	0.54100	0.00000	0.00720
IG2-12	0.03470	0.17870	0.00000	0.05960	0.00000	0.00000	0.00520	0.19860	0.00000	0.00000	0.40440	0.11160	0.00720
IG2-13	0.04850	0.07060	0.00000	0.00000	0.00000	0.00000	0.08940	0.04960	0.00000	0.00000	0.59570	0.13900	0.00720
IG2-14	0.19860	0.06130	0.00000	0.00000	0.07940	0.09929	0.00000	0.14890	0.00000	0.02980	0.35560	0.01990	0.00720
IG2-15	0.07940	0.05960	0.03970	0.00990	0.00500	0.02979	0.05960	0.14890	0.00500	0.01990	0.49630	0.03970	0.00720
IG2-16	0.10920	0.11910	0.03970	0.00990	0.00500	0.02979	0.02980	0.14890	0.00500	0.01990	0.39710	0.07940	0.00720
IG2-17	0.07940	0.05960	0.07940	0.02480	0.00600	0.02979	0.02980	0.09930	0.00500	0.01990	0.48140	0.07940	0.00720
IG2-18	0.11910	0.05960	0.03970	0.00990	0.02980	0.05957	0.02980	0.14890	0.00500	0.00990	0.40210	0.07940	0.00720
IG2-19	0.07940	0.05960	0.03970	0.00990	0.00500	0.02979	0.05960	0.14890	0.00990	0.01990	0.49140	0.03970	0.00720
IG2-20	0.07940	0.05960	0.03970	0.00990	0.00500	0.05957	0.02980	0.14890	0.00990	0.01990	0.49140	0.03970	0.00720
IG2-21	0.07940	0.05960	0.07940	0.00990	0.01990	0.05957	0.02980	0.09930	0.00990	0.00990	0.49640	0.03970	0.00720
IG2-22	0.11910	0.05960	0.03970	0.01080	0.00500	0.02979	0.05960	0.14890	0.00500	0.01990	0.41600	0.07940	0.00720

Table 4. (continued).

Glass ID	Al_2O_3	B_2O_3	CaO	F	Fe_2O_3	K_2O	Li_2O	Na_2O	NiO	P_2O_5	SiO_2	ZrO_2	Others
IG2-23	0.10500	0.11910	0.03970	0.01410	0.00500	0.02979	0.02980	0.14890	0.00500	0.01990	0.39710	0.07940	0.00720
IG2-24	0.11910	0.05960	0.07940	0.00990	0.00500	0.05957	0.05640	0.09930	0.00990	0.00990	0.40530	0.07940	0.00720
IG2-25	0.11910	0.05960	0.07940	0.00990	0.00500	0.05957	0.05760	0.09930	0.00500	0.00990	0.40900	0.07940	0.00720
IG2-26	0.07970	0.05960	0.03970	0.00990	0.00500	0.05957	0.04930	0.09930	0.00500	0.00990	0.49640	0.07940	0.00720
IG2-27	0.09810	0.05960	0.07943	0.02480	0.00500	0.02979	0.03100	0.09930	0.00990	0.01990	0.49630	0.03970	0.00720
IG2-28	0.07940	0.05960	0.07350	0.00990	0.02980	0.05957	0.02980	0.09930	0.00990	0.00990	0.49240	0.03970	0.00720
IG2-29	0.09800	0.09150	0.04890	0.02070	0.02540	0.04369	0.03920	0.11540	0.00740	0.01440	0.43610	0.05790	0.00000
IG2-30	0.15010	0.15010	0.00000	0.00000	0.00000	0.00000	0.08450	0.05000	0.00000	0.00000	0.53070	0.03010	0.00450
IG2-31	0.03750	0.12500	0.00000	0.00000	0.00000	0.02498	0.06310	0.08750	0.00000	0.01250	0.53960	0.10500	0.00480
IG2-32	0.09800	0.09080	0.04850	0.02070	0.02540	0.04370	0.03890	0.11460	0.00730	0.01430	0.43310	0.05750	0.00720
IG2-33	0.09800	0.09080	0.04850	0.02070	0.02540	0.04370	0.03890	0.11460	0.00730	0.01430	0.43310	0.05750	0.00720
IG2-34	0.09600	0.08900	0.04760	0.02030	0.02490	0.04280	0.03810	0.11230	0.00720	0.01400	0.42430	0.05630	0.02720
IG2-35	0.09310	0.08630	0.04610	0.01970	0.02410	0.04150	0.03700	0.10880	0.00700	0.01360	0.41100	0.05460	0.00770
IG2-36	0.09600	0.08900	0.04760	0.02030	0.02490	0.04280	0.03810	0.11230	0.00720	0.01400	0.42430	0.05630	0.02720
IG2-37	0.09400	0.08720	0.04660	0.01990	0.02440	0.04190	0.03730	0.11000	0.07100	0.01370	0.41550	0.05520	0.04720

Table 5. Mass fraction boundaries of Phase 2b glass components.

Component	Lower Boundary	Upper Boundary
Al_2O_3	0.0347	0.1986
B_2O_3	0.0496	0.1787
CaO	0.0000	0.1191
F	0.0000	0.0596
Fe_2O_3	0.0000	0.0794
K_2O	0.0000	0.0993
Li_2O	0.0000	0.0894
MoO_3	0.0000	0.0200
Na_2O	0.0496	0.1986
NiO	0.0000	0.0149
P_2O_5	0.0000	0.0298
SiO_2	0.3474	0.5958
SrO	0.0000	0.0400
ZrO_2	0.0000	0.1390
Others	0.0000	0.0072

Because of the interest in direct vitrification, availability of updated estimates of calcine composition and the results of the INTEC CVS Phase 1, a forum was required to establish final details in the approach to conducting Phase 2b of the CVS. This forum was provided by the Phase 2 INTEC CVS Workshop held in Idaho Falls, March 30-31, 1999.[8] The workshop had the purpose of:

1. Presenting the most recent ("March 1999 composition estimates") estimates of calcine and HAW compositions,

2. Reviewing recent progress in the separations process flowsheet,

3. Reviewing the results of Phase 2a of the INTEC CVS,

4. Finalizing the Phase 2b matrix, and

5. Establishing a preparation and characterization protocol for the Phase 2b glasses.

The remainder of this document describes the fabrication and characterization of the Phase 2b glasses within the INTEC CVS.

3. PERFORMANCE AND PROCESSING CRITERIA

Certain properties are of major significance in determining the suitability of a glass as a waste form. These properties influence glass processability and its acceptability as a waste form. Processing properties have operational constraints. Those properties affecting the suitability of a waste form for repository disposal have regulatory constraints. Properties investigated during the characterization of glasses prepared in this study are given below.

3.1 Properties Influencing Glass Processability

3.1.1 Liquidus Temperature

Liquidus temperature (T_L) is defined as the maximum temperature at which equilibrium exists between a molten glass and its primary crystalline phase.[9] If the nominal melt temperature is below T_L, (or cold spots exist within the melter) crystallization may occur and can impact processing. For example, crystallization can plug the melter drain tube or riser. Product performance such as durability can be affected if crystals are present in the glass product. To avoid the potential negative effects of crystallization within the melter, a T_L criterion of 100°C below the nominal melt temperature (T_M) is usually adopted (i.e., $T_M > T_L + 100°C$).[10] The 100°C differential provides an adequate buffer to avoid crystallization while considering variations or uncertainties in melter temperature, composition and T_L measurement.

3.1.2 Viscosity

Molten glass viscosity is strongly dependent on temperature and composition. Glass viscosity influences cold cap formation, and inversely affects volatilization from the melt. Glass viscosity also inversely affects melt reactivity, melt corrosion, devitrification rate on cooling, and pouring properties. Glass viscosity can also influence the rate of primary phase crystallization at T_L and can influence the annealing properties of a glass product poured into a can for storage.[11]

Through the DWPF operating experience, a glass viscosity range of between 20 and 100 Poise (2-10 pascal-seconds) has been recommended for joule heated, ceramic brick lined glass melters operating at 1150°C.[3] Maintaining the glass viscosity within this range minimizes processing problems (pouring, corrosion) associated with viscosity. Thus, it is necessary to characterize the viscosity as it relates to melt temperature before processing in a full-scale melter.

3.2 Properties Influencing Glass Waste Form Acceptability

3.2.1 Durability

Durability of a waste form primarily refers to its ability to resist degradation by aqueous processes. Degradation by these processes over geologic time is the most likely mechanism to result in loss to the environment of the hosted radionuclides and hazardous species. Therefore, a waste form must display certain durability properties in order to qualify for repository storage. In support of DWPF product qualification, product specifications on the glass waste form require extensive characterization to ensure that a durable and consistent glass was produced at the DWPF.[12] The PCT was developed to ensure that a glass shown to be durable is consistently produced by measuring the concentrations of the chemical species released from a representative crushed glass sample to a test solution.[5] The WAPS specify upper acceptability limits for normalized releases of boron, lithium, and sodium from waste glasses, as

determined by the PCT. Because of this precedent, and in order to enhance the database of responses of glasses of various compositions, the PCT was applied to the glasses formed in this study.

3.2.2 Homogeneity

A homogeneous glass consists of a single vitreous phase. Thus, a glass that is devitrified or phase separated is not homogeneous. The WAPS does not exclude an inhomogeneous glass from disposal if all acceptance criteria are met. For example, spinel formation is not prohibited in HLW glasses as long as durability, as determined by the PCT, meets the criteria with adequate certainty. However, qualifying an inhomogeneous glass for storage is expensive and time consuming because the presence and composition of each phase must be measured for each waste form package. In addition, the producer must also report the glass composition to within 0.5 mass % and the thermal stability of all phases present.[12]

All glasses formed in this study were air quenched onto a stainless steel plate. Several of those yielding homogeneous products after quenching as determined by x-ray diffraction analysis (XRD) were subjected to anticipated DWPF canister centerline cooling (CCC) heat treatments. The CCC is the slowest cooling rate that glass inside a full scale DWPF canister will experience.[13] Subjecting a glass to this treatment provides opportunity to observe the effects on homogeneity of the slowest expected cooling rate during processing. All glasses subjected to the CCC heat treatments were inspected visually and by optical microscopy to observe product homogeneity. All were analyzed for crystallinity by XRD. Certain inhomogeneous quenched glasses were characterized for response to the PCT, T_L and viscosity profile to obtain information on these properties at the limit of homogeneity.

4. GLASS PREPARATION AND OBSERVATIONS DURING FORMATION

Preparation of the Phase 2b glasses was performed using modified standard procedures.[14, 15] The target compositions of these glasses are given in Tables 3 and 4. A goal of Phase 2b was not only to prepare most glasses using the same melt time and temperature (1150°C), but to also include some glasses requiring higher melt temperatures and have potential for higher waste loading.

4.1 Preparation Sequence

The pseudo-center formulation (IG2-33) was prepared first and characterized with respect to viscosity profile and homogeneity. Composition analysis was also performed to verify fluorine retention. When it was observed that these properties compared well with the same version prepared at PNNL and SRTC, the remaining glasses in the Phase 2b matrix were prepared in random order, then characterized.

4.2 Physical Conditions of Preparation

Phase 2b glass batches were prepared to produce 250 grams of glass. Each batch was ground and mixed in an agate mill to sub-micron particle size before melting. Each ground, mixed batch was added incrementally at low melting temperature to a 250-mL high form 90%Pt/10%Rh crucible with a lid. This permitted total containment of a batch for one hour at 1150°C. After this time, the resulting glass was poured onto a stainless steel quench plate to form a pour patty. On cooling, the internal surfaces of each crucible and pour patties were inspected visually and optically (up to 70X) for inhomogeneity. After recording the results of the inspection, the quenched and residual crucible glass was ground and mixed to sub-micron particle size in a tungsten carbide mill and returned to its crucible. The crucible was covered and the contents melted for another hour at 1150°C. The resulting glass was poured onto a stainless steel quench plate to form a pour patty. On cooling, the patty and crucible internal surface were inspected visually and optically (up to 70X) for homogeneity. The results of the inspection were recorded and the pour patty was used as a sampling stock for characterization. Pour patties were typically about six inches (15.24 cm) in diameter and about 1/4-inch (0.64 cm) thick. Foaming only occurred during the first heat-up to 1150°C and was attributed to the release of CO_2 from the conversion of carbonate frit components (Cs_2CO_3, K_2CO_3, Li_2CO_3, Na_2CO_3) to oxides. No glassy residue was observed on the inside surface of crucible lids after melting indicating minimal component release. Most formulation batches taken through this protocol produced homogeneous products after the second melt at 1150°C. Formulation batches not yielding homogeneous products after this protocol are identified in Table 6. These were again ground and mixed, half of the pour patty at a time to a smaller particle size in a tungsten carbide mill, then heated to higher temperatures in a covered 250-mL high form 90%Pt/10%Rh crucible for another hour in an effort to achieve vitrification. The temperatures of the third melt and observations are also given in Table 6.

Table 6. Vitrification conditions required to achieve visually homogeneous products.

Glass	First melt Temp., °C	Observations	Second melt Temp., °C	Observations	Third melt Temp., °C	Observations
IG2-1	1150	Inhomogeneous, Yellow surface film	1150	Inhomogeneous, less yellow surface film, cryolite present	1250	Inhomogeneous, surface film gone
IG2-2	1250	Homogeneous, high viscosity	1350	Homogeneous, still high viscosity		
IG2-3	1450	Inhomogeneous, high viscosity	1550	Inhomogeneous, high viscosity		
IG2-5	1150	Inhomogeneous, low viscosity	1150	Inhomogeneous, low viscosity	1250	Inhomogeneous, lower viscosity
IG2-6	1150	Inhomogeneous, low viscosity	1150	Inhomogeneous, low viscosity	1250	Inhomogeneous, lower viscosity
IG2-7	1150	Inhomogeneous, high viscosity	1150	Inhomogeneous, high viscosity, zirconia and fluorite present	1250	Inhomogeneous, lower viscosity
IG2-10	1050	Inhomogeneous, low viscosity	1150	Inhomogeneous, lower viscosity		
IG2-13	1250	Inhomogeneous, high viscosity	1250	Homogeneous, high viscosity		
IG2-14	1250	Homogeneous, high viscosity	1250	Homogeneous, high viscosity		
IG2-17	1250	Inhomogeneous, average viscosity	1250	Inhomogeneous, average viscosity		
IG2-18	1150	Inhomogeneous, average viscosity	1150	Inhomogeneous, average viscosity	1250	Homogeneous, low viscosity
IG2-22	1150	Inhomogeneous, average viscosity	1150	Inhomogeneous, average viscosity	1250	Homogeneous, low viscosity
IG2-24	1150	Inhomogeneous, low viscosity	1150	Inhomogeneous, low viscosity, present zirconia	1250	Homogeneous, low viscosity
IG2-25	1150	Inhomogeneous, low viscosity	1150	Inhomogeneous, low viscosity	1250	Homogeneous, low viscosity
IG2-27	1150	Inhomogeneous, high viscosity	1150	Inhomogeneous, high viscosity	1250	Inhomogeneous, average viscosity
IG2-34	1150	Inhomogeneous, average viscosity	1150	Inhomogeneous, average viscosity	1250	Inhomogeneous, low viscosity

4.3 Composition and Homogeneity Characterization

The composition of Phase 2b glasses was determined by fusion and spectrochemical analysis on duplicate samples at the SRTC mobile laboratory (SRTC-ML).[16] Peroxide fusions were prepared on each glass and dissolved for boron and lithium analysis by inductively coupled plasma emission spectrometry (ICP). Lithium metaborate fusions were prepared on each glass and dissolved for aluminum, calcium, iron, molybdenum, nickel, phosphorous, potassium, silicon, sodium, strontium and zirconium analyses.

Potassium and sodium analyses were performed by atomic emission spectroscopy (AES), and analyses for other elements were performed by ICP. Fluoride was analyzed in duplicate using an adaptation of a potassium hydroxide fusion method.[17] Preparation began with weighing 100 mg of sample and two grams of potassium hydroxide into a ceramic crucible. All samples were fused at a maximum temperature of 425°C. The samples were then dissolved in a final water dilution of 500 mL. Sample solutions were filtered and analyzed for fluoride using a Dionex DX-500 ion chromatograph. Table 7 summarizes the "as-measured" compositions. Compositions were determined to verify that the "as batched" compositions given in Tables 3 and 4 were adequately achieved. Particularly important in this verification was the determination of fluorine because of its potential volatility during melting.

Applying the CCC heat treatment to a molten glass at melter operating temperature allows the formation of any phases tending to crystallize or to separate within the time a full-scale canister cools to storage temperature. Thus twelve Phase 2b homogeneous air quenched glasses with lowest observed T_L were selected and remelted for the CCC heat treatment. This test was performed to observe the tendency to remain homogeneous under practical cooling conditions. Sixty grams of each glass sample was remelted in 100-mL high form 90%Pt/10%Rh crucibles with lids at 1150°C then subjected to the CCC. Figure 2 is a plot of the cooling curve used in the test. This curve is based on the CCC observed in the prototype DWPF canister formed during the eighth campaign of the scaled glass melter.[12] The results of applying the CCC heat treatment to these glasses are given in Section 5.1.3 of this document.

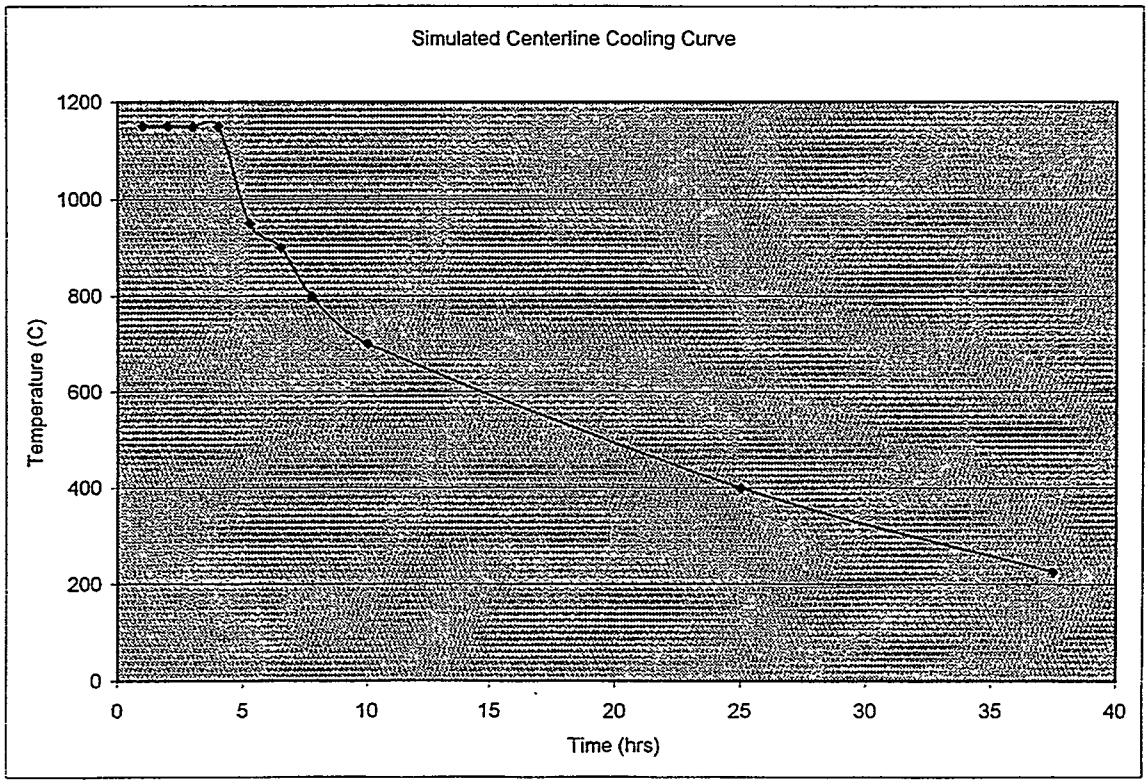

Figure 2. Plot of cooling curve applied to simulate canister centerline cooling conditions for Phase 2b glasses.

Table 7. Result of spectrochemical analysis of Phase 2b glasses.

Sample	IG2-1	IG2-2	IG2-3	IG2-4	IG2-5	IG2-6	IG2-7	IG2-8	IG2-9	IG2-10	IG2-11
	Oxide wt%	Oxide wt%	Oxide wt%	Oxide wt%	Oxide wt%	Oxide wt%	Oxide wt%	Oxide wt%	Oxide wt%	Oxide wt%	Oxide wt%
B_2O_3	5.22	19.0	18.1	20.1	5.49	20.4	5.73	18.8	5.43	6.61	5.43
SiO_2	47.8	42.5	59.3	34.1	36.5	36.3	37.8	44.5	38.4	49.1	54.5
Li_2O	<0.100	<0.100	<0.100	9.31	<0.100	10.67	<0.100	<0.100	7.56	9.21	9.11
Na_2O	20.0	5.41	5.08	5.63	19.9	5.12	5.23	14.7	5.81	6.69	17.9
K_2O	<0.010	<0.010	<0.010	13.0	1.18	<0.010	11.9	11.1	<0.010	8.68	<0.010
MoO_3	<0.010	<0.010	<0.010	<0.010	<0.010	<0.010	<0.010	<0.010	<0.010	<0.010	<0.010
P_2O_5	<0.010	2.86	0.052	<0.010	<0.010	2.88	2.80	<0.010	<0.010	3.06	2.81
NiO	1.55	<0.010	1.53	1.48	1.48	1.42	1.46	<0.010	<0.010	<0.010	1.45
Fe_2O_3	0.019	0.026	8.20	0.026	7.81	7.66	0.016	0.020	7.56	7.01	0.019
ZrO_2	<0.010	<0.010	<0.010	1.47	14.1	13.4	12.8	<0.010	<0.010	<0.010	<0.010
CaO	0.043	11.3	0.039	0.018	11.7	0.027	10.4	11.5	11.40	0.06	7.29
Al_2O_3	20.7	19.9	3.64	19.9	3.68	6.49	8.48	3.56	20.0	3.79	3.79
SrO	0.034	0.033	0.036	0.032	0.038	0.032	0.033	0.038	0.024	0.033	0.036
F	6.07	NM**	1.38	NM	NM	NM	5.48	NM	5.91	5.65	NM
Total	101	101	97.4	105	102	104	102	104	102	100	102

**NM = Not Measured

Table 7. (continued).

Sample	IG2-12	IG2-13	IG2-14	IG2-15	IG2-16	IG2-17	IG2-18	IG2-19	IG2-20	IG2-21	IG2-22
	Oxide wt%	Oxide wt%	Oxide wt%	Oxide wt%	Oxide wt%	Oxide wt%	Oxide wt%	Oxide wt%	Oxide wt%	Oxide wt%	Oxide wt%
B_2O_3	20.07	7.84	6.59	8.33	12.7	6.41	6.30	6.47	6.20	6.05	6.48
SiO_2	39.4	59.7	34.5	50.5	39.1	48.8	42.2	51.3	48.2	48.9	38.1
Li_2O	0.60	9.64	<0.100	5.79	2.94	3.06	3.09	6.31	2.90	3.26	6.09
Na_2O	22.4	5.54	15.7	15.9	14.2	10.4	16.6	16.6	17.0	9.80	1.39
K_2O	<0.010	<0.010	10.9	3.25	3.13	3.20	6.07	3.11	6.12	6.97	20.9
MoO_3	<0.010	<0.010	<0.010	<0.010	<0.010	<0.010	<0.010	<0.010	<0.010	<0.010	<0.010
P_2O_5	<0.010	<0.010	2.75	1.81	1.92	1.76	0.933	1.72	1.81	0.868	1.67
NiO	<0.010	<0.010	<0.010	0.474	0.460	0.485	0.463	0.916	0.933	0.929	0.426
Fe_2O_3	0.019	0.035	7.61	0.500	0.498	0.469	2.77	0.508	0.483	1.66	0.477
ZrO_2	11.6	13.6	1.95	3.85	7.99	7.68	7.91	3.99	3.82	3.80	7.44
CaO	0.022	0.066	0.030	4.00	3.89	6.75	3.97	3.83	3.96	7.59	3.74
Al_2O_3	3.85	4.94	19.4	8.02	10.7	7.21	11.5	7.68	7.93	7.91	11.3
SrO	0.033	0.033	0.029	0.033	0.035	0.029	0.032	0.034	0.033	0.032	0.032
F	5.81	NM	NM	0.949	0.950	2.09	0.829	0.889	0.837	0.914	0.910
Total	104	101	99.4	101	98.6	98.4	103	103	100	98.7	99.0

Table 7. (continued).

Sample	IG2-23	IG2-24	IG2-25	IG2-26	IG2-27	IG2-28	IG2-29	IG2-30	IG2-31
	Oxide wt%	Oxide wt%	Oxide wt%	Oxide wt%	Oxide wt%	Oxide wt%	Oxide wt%	Oxide wt%	Oxide wt%
B_2O_3	11.8	5.82	5.73	5.38	5.57	5.64	10.7	14.7	13.0
SiO_2	38.0	40.8	39.5	47.3	48.4	48.2	42.5	49.6	52.3
Li_2O	2.99	5.89	5.36	5.54	3.38	2.73	3.90	9.70	5.99
Na_2O	16.0	9.75	9.51	10.5	9.69	10.6	12.8	5.13	8.77
K_2O	3.59	6.62	6.16	6.09	3.27	6.96	4.80	<0.010	2.62
MoO_3	<0.010	<0.010	<0.010	<0.010	<0.010	<0.010	<0.010	<0.010	<0.010
P_2O_5	1.87	0.900	0.863	0.891	1.73	0.890	1.32	<0.010	1.23
NiO	0.472	0.937	0.458	0.457	0.915	0.901	0.703	<0.010	<0.010
Fe_2O_3	0.473	0.588	0.512	2.24	0.480	2.68	2.61	0.141	<0.010
ZrO_2	7.77	7.79	7.40	7.78	3.91	3.82	5.56	2.94	10.6
CaO	3.82	6.62	6.40	2.51	7.65	7.00	4.66	0.118	0.220
Al_2O_3	10.1	10.5	10.6	7.72	9.92	7.61	9.62	14.8	4.15
SrO	0.033	0.027	0.030	0.031	0.031	0.034	<0.010	<0.010	<0.010
F	1.32	0.910	0.920	<0.100	2.31	0.970	2.03	NM	NM
Total	98.2	97.2	93.5	96.4	97.3	98.0	101	97.1	98.8

Table 7. (continued).

Sample	IG2-32	IG2-33	IG2-34	IG2-35	IG2-36	IG2-37
	Oxide wt%	Oxide wt%	Oxide wt%	Oxide wt%	Oxide wt%	Oxide wt%
B_2O_3	9.66	9.24	9.92	9.70	9.09	8.29
SiO_2	44.9	44.3	45.1	43.3	39.0	39.7
Li_2O	4.25	4.24	3.70	3.60	3.67	3.57
Na_2O	11.2	11.5	10.8	12.2	11.0	10.2
K_2O	4.66	4.39	4.31	4.89	4.47	4.61
MoO_3	<0.010	<0.010	1.91	0.502	<0.010	<0.010
P_2O_5	1.43	1.39	1.37	1.42	1.40	1.30
NiO	0.711	0.741	0.704	0.736	0.727	0.729
Fe_2O_3	2.59	2.51	2.48	2.53	2.44	2.44
ZrO_2	5.73	5.57	5.43	5.46	5.54	5.26
CaO	4.76	4.89	4.81	4.85	4.86	4.78
Al_2O_3	10.0	9.68	9.92	10.0	9.80	9.70
SrO	0.025	0.026	0.026	0.025	1.48	3.00
F	1.95	1.93	1.77	1.99	1.95	1.95
Total	102	100	102	101	95.5	95.6

4.4 Liquidus Temperature

The T_L was measured optically on all homogeneous Phases 2b glasses using the uniform temperature method described by Vienna et al (1998).[18] In this method, glass samples were placed in 90% Pt/10%Rh boxes with tight lids and heat treated at constant temperature for no less than 22 hours. The samples were quenched and analyzed using transmitted light optical microscopy at roughly 40X to 100X magnifications to determine if crystals are present. New samples of each glass were heat treated to progressively narrow the temperature difference between the highest temperature where melt and crystals coexist (T_C), and the lowest temperature where the melt remains amorphous (T_A). Higher magnification optical microscopy (up to 400X), SEM, and XRD were applied to detect crystallinity in various glasses formed in this phase of the CVS. The T_L measurement furnaces used were calibrated using the National Bureau of Standards (NBS) T_L standard reference material No. 773.

XRD and optical analyses were made on samples with the greatest density of crystals to identify the primary crystalline phase at T_L. Generally, too few crystals were present near T_L to detect with certainty where the primary crystalline phase formed. In a few glasses, other crystalline phases formed at temperatures below T_L. These glasses were also analyzed optically and by XRD to confirm the phase forming at T_L. Scanning electron microscopy (SEM) was also applied to these glasses to observe elemental associations in these glasses heat treated at T_A, T_C, and below to help verify the identity of the phase crystallizing at T_L. A R. J. Lee Group Personal SEM was used in the T_L investigation, which was conducted at INTEC. The results of performing T_L determinations are given in Section 5.2 of this document.

4.5 Durability

The PCT Method B, as described in ASTM C1285-94, was performed in duplicate on each quenched Phase 2b glass.[5] The test parameters used were a time of seven days, a temperature of 90 ± 2°C and a ASTM Type I water leachant. The PCT was also conducted on duplicate samples of the Environmental Assessment (EA) glass and the Approved Reference Material (ARM-1) glass standards. A set of field blanks was also subjected to the PCT with each batch of cleaned leach vessels. The test was performed under static conditions in TFE-fluorocarbon vessels on crushed glass of particle size between 75 and 150 μm (-100, +200 mesh). Particles (1.5 grams) cleaned of adhered fines, were placed in TFE-fluorocarbon vessels into which 15 ml of ASTM Type I water was added. The vessels were sealed and placed with blanks and standards into a constant temperature oven at 90 ± 2°C. After the 7-day test, the vessels were allowed to cool to room temperature. The final weight of each vessel and the solution pH were recorded on a data sheet. The leachates were then filtered through a 0.45-μm syringe filter. Each leachate was acidified to 1% HNO_3 to minimize cation hydrolysis. Solutions, standards and blanks were then analyzed for various elemental concentrations using ICP. The elements analyzed for in the leachate included aluminum, boron, calcium, chlorine, chromium, fluorine, iron, lithium, magnesium, nickel, phosphorous, potassium, silicon, sodium, strontium, sulfur, tin and zirconium.

Elemental leaching results determined by the PCT were normalized with respect to the amount of that element "as-targeted" in the waste form. This allows that result to be reported as a portion of the weight fraction of that element in the waste form. The results are discussed in Section 5.3. Table B3 of Appendix B presents the solution analyses (μg/mL) on leachates of the Phase 2b glasses.

4.6 Viscosity Characterization

Viscosity as a function of temperature was obtained on all the HAW CVS glasses, except IG2-03, using a method consistent with the ASTM standard procedure.[19] In this procedure, viscosity is systematically taken at equal increments around a central temperature. For the purpose of viscosity characterization of the Phase 2b glasses, 1150°C was established as the central temperature because most Phase 2b formulations resulted in homogeneous products when melted there. Glasses that were melted at higher temperatures than 1150°C (see Table 5) were measured over the range of 950°C to 1350°C. Viscosity readings were taken at 50°C increments first going below 1150°C to 950°C before increasing temperature past 1150°C, on to 1250°C, or above in the case of glasses that melted at higher temperatures, and back down to a final reading at 1150°C. The profile was performed in this manner because of the unknown magnitude of fluoride volatility from the glass. Because of this uncertainty, beginning viscosity measurements at lower temperatures has a higher probability of retaining fluoride in the glass. Decreasing the temperature incrementally from 1150°C to 950°C may provide an observation of any tendency of phases to crystallize from the glass on cooling and the resulting effect on viscosity. Observations of the tendency to devitrify during this part of the procedure provide information useful in determining T_L of the glass.

Temperatures for the viscosity calculation were taken from the thermocouple positioned adjacent to the sample crucible. The viscosity measurement reported at a temperature set point was based on the arithmetic mean of torque readings taken every 15 seconds on the spindle rotating in the glass melt. The glass was held at each setpoint temperature for 15 minutes. The readings were taken over the last five minutes of the 15-minute hold. Mean viscosities were calculated and recorded at each setpoint temperature.

5. CHARACTERIZATION RESULTS AND DISCUSSION

The glasses investigated in this study were characterized with respect to:

1. Composition and homogeneity
2. As fabricated (quenched) homogeneity
3. Effects of CCC heat treatment on homogeneity
4. Liquidus temperature (T_L)
5. Durability as measured by the leaching response to the PCT
6. Viscosity profile.

5.1 Composition and Homogeneity Results

5.1.1 Composition

The main purpose for conducting composition analysis of the Phase 2b glasses was to observe if significant fluorine volatility would occur from the glasses during melting. The results of analyses are given (oxide wt%) in Table 7 and can be compared to the "as-batched" compositions given in Table 4. Fluorine analysis was not performed on glasses batched without it. Fluorine loss was likely during unsuccessful attempts to prepare a homogeneous IG2-03 product. The difference between "as-batched" and "as analyzed" fluorine of IG2-26 can be explained only by fluorine omission during batching. Analysis results also suggest a batching error occurred in the make-up of IG2-22 glass. In this case, it is probable that amounts of K_2O and Na_2O were switched. That this occurred was confirmed through SEM observations of the relative sodium and potassium amounts in the glass product.

5.1.2 Homogeneity of Air Quenched Glasses

Table 8 gives visual and transmitted light microscopy (70X) observations of all air quenched Phase 2b glasses. Twenty-six of the 37 Phase 2b glasses, appeared homogeneous on initial formation. Most of the inhomogeneous glasses appear to lie in the outer layer of the two-layer design used to define Phase 2b of the CVS. Optical observations reveal that nine of the inhomogeneous Phase 2b glasses contain either crystallinity or an amorphous phase separation. Also given in the table are the results of XRD analysis on these glasses. This analysis reveals the presence of crystallinity in eight of the inhomogeneous and two of the glasses observed to be homogeneous by optical techniques. SEM analysis was performed on some glasses to assist in phase identification performed by XRD. In a few glasses, the grain structure of some crystalline species was too small relative to the electron beam size for SEM analysis to be useful. This was the case with $Ca_5(PO_4)_3F$ (fluorapatite) which was identified by XRD in glasses IG2-17, -27 and -34. Crystallinity observed optically in IG2-10 was of too low volume % to be identified by XRD techniques.

In glass IG2-07, SEM analysis easily observed ZrO_2 crystals, but the fluorapatite crystal structure was too small relative to the beam size for SEM analysis to be useful. This condition is illustrated in Figure 3, a SEM micrograph (1994X) of the crystalline structure observed in glass IG2-07. Inspection of the results presented in Table 6 and those of Table 8 reveals that most glasses vitrified at temperatures higher than 1150°C contained crystallinity, as identified by XRD or SEM techniques.

It is possible that inhomogeneity detectable only by application of transmission electron microscopy (TEM) analysis may be present in any optically homogeneous glass. Thus the application of TEM to the glasses that appear optically homogeneous may provide additional information that will be useful in understanding homogeneity composition relationships in vitrified INTEC HLW.

Table 8. Homogeneity properties of air quenched glasses formed in this study.

Sample ID	Density, g/cc	Visual/Optical	XRD
IG2-01	2.49	Inhomogeneous	Na_3AlF_6
IG2-02	2.45	Homogeneous	Amorphous
IG2-03	2.34	Inhomogeneous	Fe_2O_3, $NaAlO_2$
IG2-04	2.45	Homogeneous	Amorphous
IG2-05	2.94	Inhomogeneous	ZrO_2
IG2-06	2.73	Inhomogeneous	ZrO_2
IG2-07	2.78	Inhomogeneous	ZrO_2, $Ca_5(PO_4)_3F$, CaF_2
IG2-08	2.56	Homogeneous	Amorphous
IG2-09	2.66	Inhomogeneous	Amorphous
IG2-10	2.45	Inhomogeneous	Unidentified phase
IG2-11	2.55	Homogeneous	Amorphous
IG2-12	2.63	Homogeneous	Amorphous
IG2-13	2.59	Homogeneous	Amorphous
IG2-14	2.29	Homogeneous	Amorphous
IG2-15	2.56	Homogeneous	Amorphous
IG2-16	2.61	Homogeneous	Amorphous
IG2-17	2.65	Homogeneous	$Ca_5(PO_4)_3F$
IG2-18	2.67	Homogeneous	Amorphous
IG2-19	2.58	Homogeneous	Amorphous
IG2-20	2.58	Homogeneous	Amorphous
IG2-21	2.61	Homogeneous	Amorphous
IG2-22	2.59	Homogeneous	SiO_2, SiP_2O_7, $AlPO_4$
IG2-23	2.62	Homogeneous	Amorphous
IG2-24	2.66	Homogeneous	Amorphous
IG2-25	2.66	Homogeneous	Amorphous
IG2-26	2.60	Homogeneous	Amorphous
IG2-27	2.59	Inhomogeneous	$Ca_5(PO_4)_3F$
IG2-28	2.62	Homogeneous	Amorphous
IG2-29	2.62	Homogeneous	Amorphous

Table 8. (continued).

Sample ID	Density, g/cc	Visual/Optical	XRD
IG2-30	2.41	Homogeneous	Amorphous
IG2-31	2.56	Homogeneous	Amorphous
IG2-32	2.61	Homogeneous	Amorphous
IG2-33	2.62	Homogeneous	Amorphous
IG2-34	2.63	Inhomogeneous	$Ca_5(PO_4)_3F$, $KAlSiO_4$
IG2-35	2.61	Homogeneous	Amorphous
IG2-36	2.64	Homogeneous	Amorphous
IG2-37	2.67	Homogeneous	Amorphous

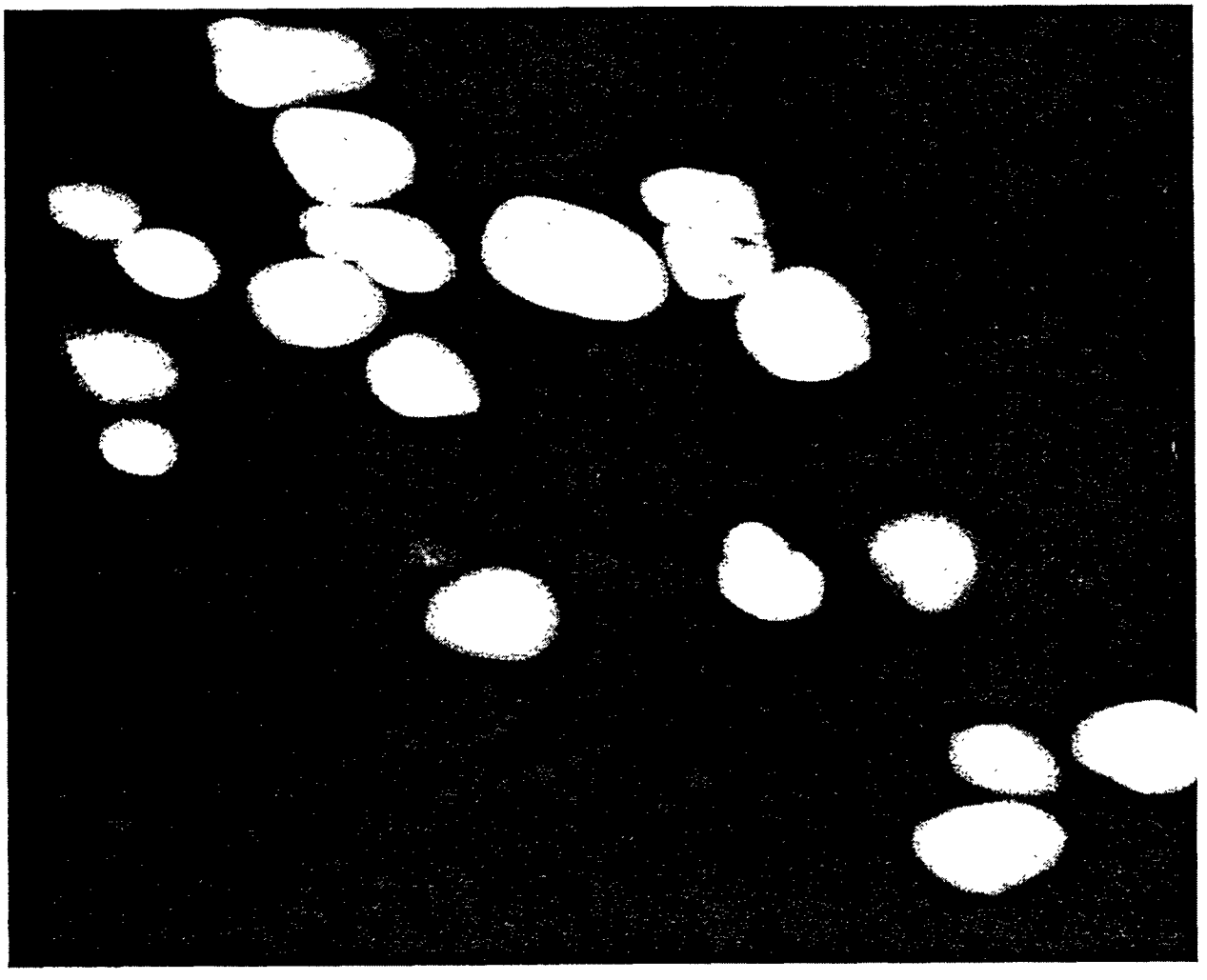

Figure 3. SEM Micrograph (1994 X) of crystalline structure in glass IG2-07 formed by air quenching.

5.1.3 Homogeneity of Glasses Subjected to CCC Heat Treatment

Twelve optically homogeneous air quenched glasses were subjected to the CCC heat treatment. The results with respect to optical and visual appearance and XRD analysis are given in Table 9. This information indicates that six (IG2-11, -15, -19, -20, -26, and -28) of the twelve glasses remained optically homogeneous and were amorphous with respect to XRD after being subjected to the CCC heat treatment.

During homogeneity observations of air quenched glasses, areas of inhomogeneity were identified in IG2-09 and IG2-10 products. The optical, XRD and SEM techniques available at INTEC could not identify if the homogeneity could be attributed to crystallinity. Therefore in an effort to identify hosted crystallinity, inhomogeneous air quenched glasses IG2-09 and IG2-10 were remelted and cooled by the CCC heat treatment. This treatment rate allowed time for crystal growth to a size detectable through XRD and SEM techniques. It also may have provided conditions needed for other phases to crystallize. The results of applying the CCC heat treatment to these glasses and subsequent analysis of each by XRD techniques are also given in Table 9.

Table 9. Homogeneity and phase formation in glasses subjected to CCC experiment.

Glass	Homogeneity by Optical Microscopy (50X) After Test	Major Phase Formed During Test as Determined by XRD
IG2-09	Inhomogeneous	$LiAlSiO_4$ and $NaAlSiO_4$
IG2-10	Inhomogeneous	Li_3PO_4 and LiF
IG2-11	Homogeneous	Amorphous
IG2-12	Inhomogeneous	NaF, $LiAlOCl_2$, and $NaAl2Si_2O_9$
IG2-15	Homogeneous	Amorphous
IG2-19	Homogeneous	Amorphous
IG2-20	Homogeneous	Amorphous
IG2-23	Inhomogeneous	$Ca_5(PO_4)_3F$
IG2-26	Homogeneous	Amorphous
IG2-28	Homogeneous	Amorphous
IG2-29	Inhomogeneous	$Ca_5(PO_4)_3F$
IG2-33	Inhomogeneous	$Ca_5(PO_4)_3F$
IG2-35	Inhomogeneous	$Ca_5(PO_4)_3F$
IG2-36	Inhomogeneous	$Ca_5(PO_4)_3F$

5.2 Liquidus Temperature Results

The T_L obtained for Phases 2b glasses are given in Table 10. Also given are the crystalline phases identified in each glass through the application of XRD. The major phase is considered the primary phase for determination of T_L. The phase known to be of minor presence in each of these glasses is enclosed in parentheses. The reported T_A value provides the lowest temperature at which the sample remained

amorphous as determined by optical microscopy. Likewise, the T_C value provides the highest temperature at which the sample contained crystallinity as determined by optical microscopy. The T_L information given in Table 10 is significant because it is the first obtained on glasses with components representative of INTEC calcined HLW.

Fluorapatite ($Ca_5(PO_4)_3F$) crystallized at T_L in most Phase 2b glasses forming homogeneous products at 1150°C (IG2-16, -20, -21, -23, -28, -29, -32, -33, –35, -36, and -37, inner layer GCER formulations). In glass IG2-15, although fluoride is present, hydroxylapatite ($Ca_5(PO_4)_3$ OH) was identified as the primary phase. In glass IG2-19, lithium silicate (Li_2SiO_3) formed at T_L, and fluorapatite formed at a lower temperature. In IG2-08, and IG2 -11, all outer layer GCER formulations forming homogeneous glasses at 1150°C, calcium silicate ($CaSiO_3$) and lithium silicate (Li_2SiO_3) formed respectively at T_L. Lithium silicate also formed at T_L in IG2-26, an inner layer GCER glass forming an amorphous product at 1150°C. The results of XRD and SEM analysis of glass IG2-04 indicate the formation of Na_2ZrO_3 at T_L. Nickel oxide is also present. The crystalline phase present at T_L in GCER outer layer glass IG2-12 could not be identified by techniques available at INTEC. Villiaumite (NaF), $LiAlOCl_2$ and $Na_4Al_2Si_2O_9$ were detected in IG2-12 when cooled according to the CCC heat treatment. In glass IG2-31, $LiNaZrSi_6O_{15}$ formed at T_L and lithium phosphate (Li_3PO_4) forms at a lower temperature. This glass is equivalent to IG1-38 of the Phase 1b glasses. Only $LiNaZrSi_6O_{15}$ was observed to form at T_L in IG1-38 as a result of the T_L analysis performed in Phase 1b.[3]

Figures 4 and 5 are examples of the SEM micrographs used in the analysis of these glasses. Figure 4 is a micrograph (1000X) of the crystalline phase in IG2-20 determined by XRD to be fluorapatite. Figure 5 is an elemental map of that phase and the surrounding glass. The map reveals the higher concentrations of calcium, phosphorous and fluorine in the crystals than in the surroundings which supports the results of XRD analysis. Figure 6 is a micrograph (460 X) of the NiO crystals in IG2-04. Crystalline Na_2ZrO_3 was too finely dispersed to be analyzed by SEM techniques available at INTEC. Figure 7 is an elemental map displaying Ni content of the crystals in IG2-04.

As discussed in section 5.1, certain Phase 2b glasses (IG2-02, -13, -14, -18, -24 and -25) required temperatures higher than 1150°C for vitrification to homogeneous products. In these glasses zirconium oxide or zirconium silicate was the most common phase forming at T_L. Hydroxylapatite formed in IG2-02 and nepheline formed in IG2-14 at T_L. Figures 8 and 9 are examples of the SEM application used in the analysis of these glasses. Figure 8 is a micrograph (500X) of the crystalline phase in IG2-24 determined by XRD to be ZrO_2. Figure 9 is an elemental map of that phase and the surrounding glass revealing the higher concentrations of zirconium in the crystals than in the surroundings which supports the results of XRD analysis.

Table 10. Results of liquidus temperature measurements (°C) performed on Phase 2b glasses.

Glass	Phase	$T_{amorphous}$	$T_{crystalline}$	T_L
IG2-1	—	—	—	Not determined
IG2-2	$Ca_5(PO_4)_3(OH)$	1138	1128	1133
IG2-3	—	—	—	Not determined
IG2-4	NiO, (Na_2ZrO_3)	918	908	913
IG2-5	—	—	—	Not determined
IG2-6	—	—	—	Not determined
IG2-7	—	—	—	Not determined
IG2-8	$CaSiO_3$	866	856	861
IG2-9	—	—	—	Not determined
IG2-10	—	—	—	Not determined
IG2-11	Li_2SiO_3	778	768	773
IG2-12	Phase not identifiable	828	818	823
IG2-13	$ZrSiO_4$	1228	1213	1223
IG2-14	$NaAlSiO_4$	1138	1128	1133
IG2-15	$Ca_5(PO_4)_3OH$	828	818	823
IG2-16	$Ca_5(PO_4)_3F$	953	943	948
IG2-17	—	—	—	Not determined
IG2-18	ZrO_2	1412	1422	1407
IG2-19	Li_2SiO_3, ($Ca_5(PO_4)_3F$)	846	836	841
IG2-20	$Ca_5(PO_4)_3F$	848	838	843
IG2-21	$Ca_5(PO_4)_3F$	966	956	961
IG2-22	—	—	—	Not determined
IG2-23	$Ca_5(PO_4)_3F$	928	918	923
IG2-24	ZrO_2	1387	1377	1382
IG2-25	ZrO_2	1368	1358	1363
IG2-26	Li_2SiO_3	971	961	966
IG2-27	—	—	—	Not determined
IG2-28	$Ca_5(PO_4)_3F$	943	933	938
IG2-29	$Ca_5(PO_4)_3F$	928	918	923
IG2-30	$LiAlSi_3O_8$	953	943	948
IG2-31	$LiNaZrSi_6O_{15}$, (Li_3PO_4)	888	878	883
IG2-32	$Ca_5(PO_4)_3F$	938	928	933
IG2-33	$Ca_5(PO_4)_3F$	918	908	913
IG2-34	—	—	—	Not determined
IG2-35	$Ca_5(PO_4)_3F$	936	926	931
IG2-36	$Ca_5(PO_4)_3F$	928	918	923
IG2-37	$Ca_5(PO_4)_3F$	943	933	938

Figure 4. SEM micrograph (1000X) of fluorapatite crystal and adjacent glass matrix in IG2-20 with spectra taken from fluorapatite crystal.

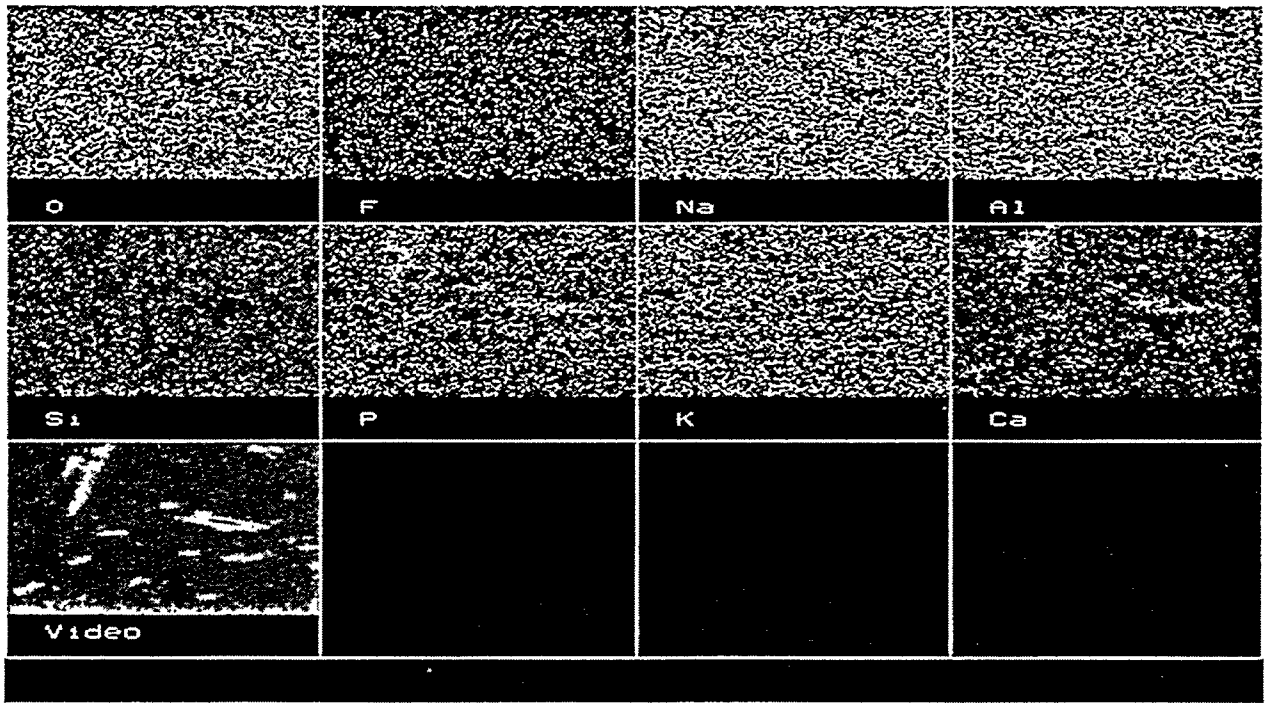

Figure 5. Elemental map of fluorapatite crystal and adjacent glass in IG2-20.

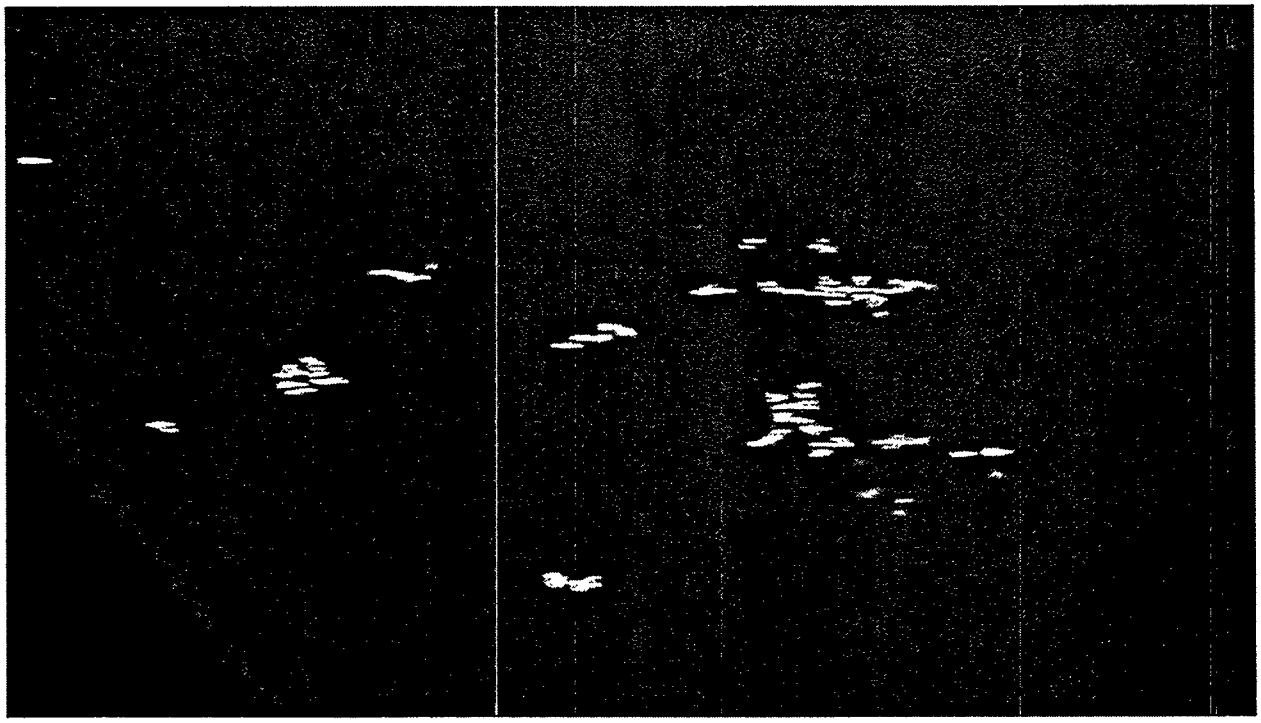

Figure 6. SEM micrograph (1000X) of IG2-04 displaying NiO and Na_2ZrO_3 crystallinity with spectra taken from Na_2ZrO_3 crystal.

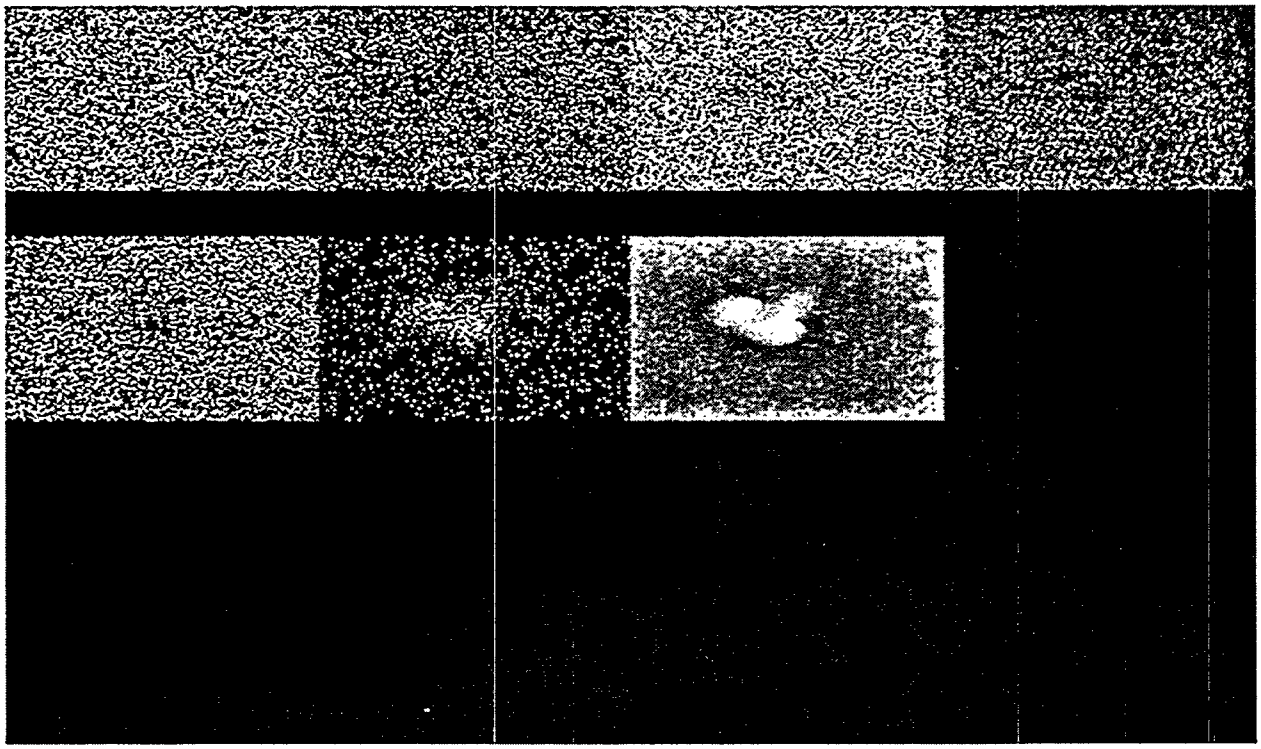

Figure 7. Elemental map of nickel oxide and sodium zirconate crystals and adjacent glass in IG2-04.

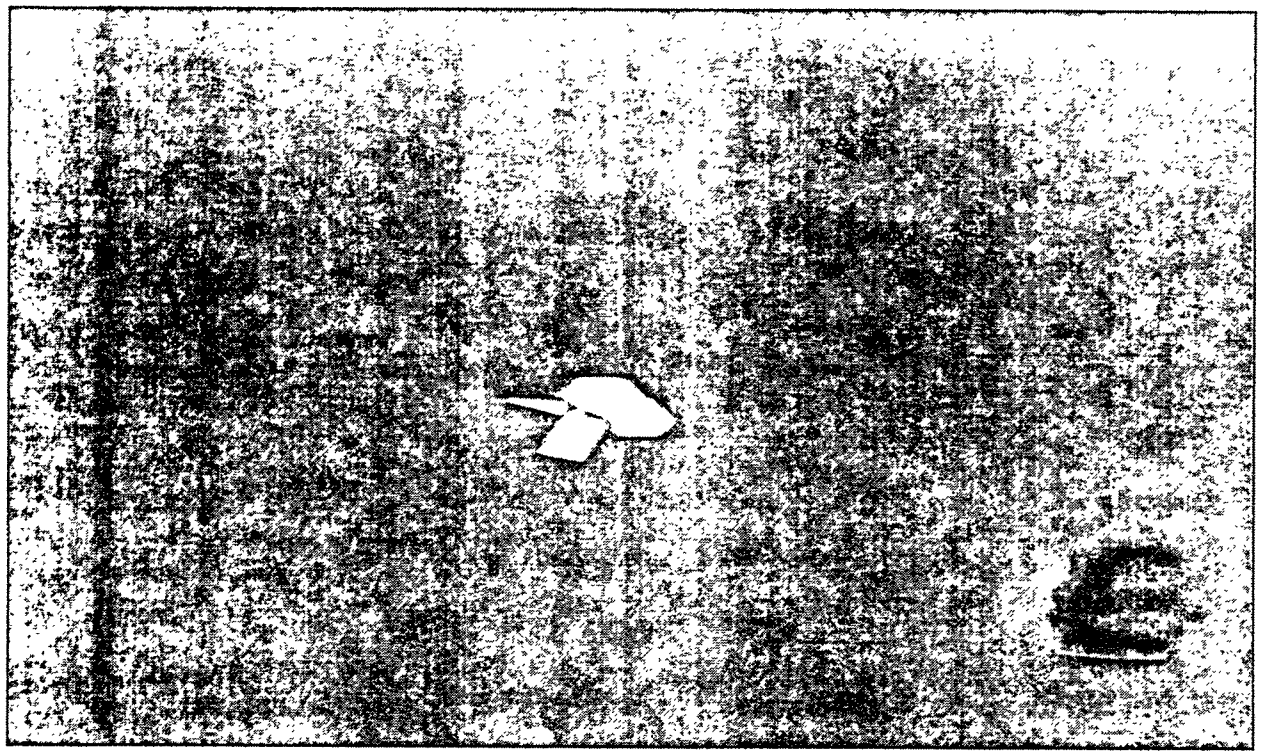

Figure 8. SEM micrograph (500X) of IG2-24 displaying ZrO_2 crystallinity.

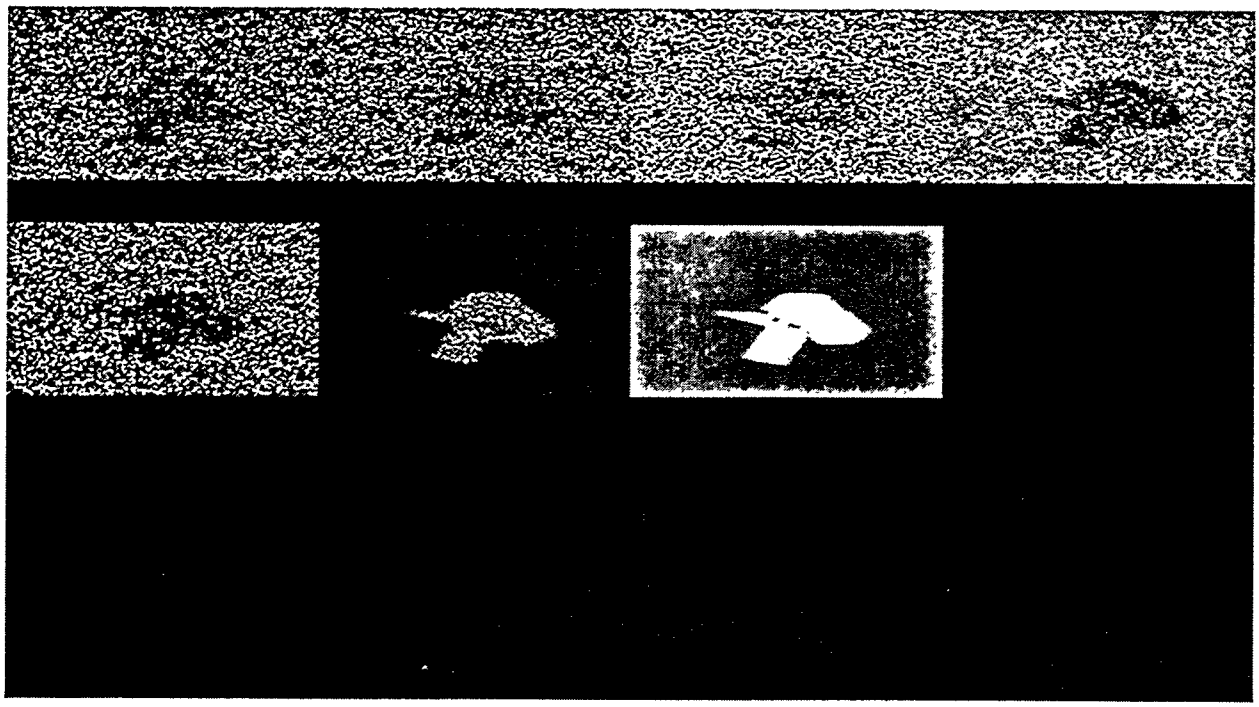

Figure 9. Elemental map of zirconia crystal identified in IG2-24 showing distribution of calcium, oxygen, silicon, and zirconium.

5.3 Durability Results

5.3.1 Results from the Multi-Element Solution Standard

A multi-element solution standard was included for measurement during analysis of Phase 2b glass leachates. The multi-element standard is a 5% HNO_3 solution containing Al, B, Ca, Cr, Fe, K, Li, Mg, Na, Ni, P, S, Si, Sn, Sr, and Zr. An analysis of the standard for this suite of elements was performed after the analysis of each group of five leachates.

Various investigations were performed before and during leachate sample analysis to minimize the chance of analytical error because of spectral and physical effects. The potential for physical effects was assessed prior to analysis by examining the results from spiked matrix sample analysis and by comparing results from different sample dilution levels. To assess and mitigate spectral interference, wavelength scans of each sample were acquired and examined to select appropriate analytical and background correction wavelengths. Independent calibration verifications were performed both initially and periodically during leachate analysis to assess the effect of calibration bias on results. The results of these investigations suggest that the ICP and flame atomic absorption spectrometry (FLAAS) techniques used for leachate analysis were not subject to significant matrix or spectral bias.

The certified (NIST traceable) elemental concentrations of the multi-element solution standard are given in Table 10 where all data are given in mg/L unless other units are indicated. Table 11 includes the number of replicates (N) each element in the standard was run during leachate analysis, the average values for each element run in the standard during leachate analysis, and the standard deviation (sigma) between measured and certified elemental concentrations. Also given are the percent of the relative standard deviation (%RSD) and the average percent recovery (%R). Analysis method is given in the last column of Table 11. Good agreement between the certified elemental values and those experimentally determined for the multi-element standard was observed throughout this study.

Table 11. Analytical results from multi-element solution standard.

	Measured Results						
Analyte	N	Average	Sigma	%RSD	Certified, mg/L	Average %R	Analysis Method
Aluminum	34	2.535	0.071	2.8%	2.50	101.4%	ICP
Boron	38	2.520	0.093	3.7%	2.50	100.8%	ICP
Calcium	33	2.525	0.071	2.8%	2.50	101.0%	ICP
Chromium	32	2.552	0.118	4.6%	2.50	102.1%	ICP
Iron	33	2.552	0.086	3.4%	2.50	102.1%	ICP
Lithium	34	2.489	0.084	3.4%	2.50	99.5%	ICP
Magnesium	29	2.539	0.075	3.0%	2.50	101.5%	ICP
Nickel	31	2.542	0.074	2.9%	2.50	101.7%	ICP
Phosphorous	29	2.540	0.049	1.9%	2.50	101.6%	ICP
Potassium	22	0.509	0.012	2.4%	0.499	102.1%	FLAAS
Silicon	37	2.550	0.079	3.1%	2.50	102.0%	ICP
Sodium	23	0.504	0.018	3.5%	0.502	100.6%	FLAAS

Table 11. (continued).

Strontium	31	2.512	0.048	1.9%	2.50	100.5%	ICP
Sulfur	35	2.467	0.088	3.5%	2.50	98.7%	ICP
Tin	30	2.524	0.094	3.7%	2.50	101.0%	ICP
Zirconium	30	2.562	0.118	4.6%	2.50	102.5%	ICP

5.3.2 Normalized PCTs Using As-Targeted Glass Compositions

The elemental concentrations in a PCT leachate can be normalized to their concentrations in the waste form for comparison of an elemental leachability from the product of one glass formulation (or waste form) to that in another. Normalization can be accomplished using either "as batched" or "as measured" concentrations of those elements of interest. Normalization using "as measured" composition may be preferable in the case of an element suspected of volatilizing from a glass melt. For the purposes of this report, normalization was performed with respect to the "as batched" composition.

Elemental leaching concentrations were normalized through the relationship:

$$N_I = \frac{C_i - Q_i(B)}{1000\,(f_i)}$$

Where:

N_i = Normalized release of element *i* (g/L)

C_i = Concentration of element *i* in the leachate, ppm

$Q_i(B)$ = Concentration of element *i* in the blank, ppm

f_i = Mass fraction of element *i* obtained from the as batched composition in the unleached sample

and 1000 converts μg/ml to g/L. The common logarithm of the leachate concentration was determined from the mean of the duplicate leachate concentrations for an element of interest (see Appendix B). The common logarithms of mean normalized releases with respect to the "as batched" composition (see Table 3) are given in Table 12.

Table 12. PCT and leachate pH results for Phase 2b glasses normalized by "as targeted" composition.

Glass	Log NL [Al (g/L)]	Log NL [B (g/L)]	Log NL [Ca (g/L)]	Log NL [Cr (g/L)]	Log NL [F (g/L)]	Log NL [Fe (g/L)]	Log NL [K (g/L)]	Log NL [Li (g/L)]	Log NL [Mg (g/L)]	Log NL [Na (g/L)]
ARM-A	-0.7715	0.1228	-2.4659	ND	ND	ND	ND	0.1960	ND	0.0602
ARM-B	-0.8119	0.1344	-2.1494	ND	ND	ND	ND	0.1998	ND	0.0607
EA-A	-1.12024	1.0506	-1.8822	ND	ND	-3.4571	0.4967	0.8271	ND	0.9232
EA-B	-1.09166	1.0858	-1.9033	ND	ND	ND	0.4925	0.8320	ND	0.9380
IG2-01	-0.5761	-0.3462	ND	-0.9979	-0.5593	ND	ND	ND	-1.9165	-0.3707
IG2-02	-1.1356	-0.7457	-1.3607	-2.8932	ND	ND	ND	ND	-0.9674	-1.6718
IG2-03	-0.4897	1.3947	ND	-1.1439	0.7717	-1.2186	ND	ND	-0.1850	0.0373
IG2-04	-0.2704	0.7611	ND	-0.5680	ND	ND	0.2525	-0.7162	-0.6426	-0.4960
IG2-05	-0.4992	-0.0091	-2.1158	-1.2331	ND	-2.2674	0.0508	ND	ND	0.4560
IG2-06	-1.6326	0.6164	ND	-1.4830	ND	-1.5226	ND	-3.8055	-1.1422	-0.9793
IG2-07	-2.2697	-0.2126	-1.5117	-0.5799	ND	ND	-0.3790	ND	ND	-1.1552
IG2-08	-0.8519	-0.0563	-1.0988	-0.8298	ND	ND	0.0618	ND	ND	0.1420
IG2-09	-0.9224	-0.7011	-1.1644	-1.6891	-0.9426	-2.8581	ND	-0.3512	ND	-1.7651
IG2-10	-1.0228	0.4460	ND	-0.6969	0.2478	-0.7746	0.0070	0.4399	0.03414	-0.5448
IG2-11	-0.4318	0.5978	-2.1297	-0.1316	ND	ND	ND	0.6999	ND	0.7170
IG2-12	ND	1.3682	ND	-0.5593	1.3527	ND	ND	1.3210	-0.4581	1.1690
IG2-13	-0.3378	-0.2384	ND	-1.2759	ND	ND	ND	0.0279	ND	-1.3525
IG2-14	-0.4187	-0.0711	ND	-0.9824	ND	-0.6768	-0.1355	ND	-1.3628	0.0739
IG2-15	-0.3898	0.1689	-2.5956	-0.4735	-0.1572	-2.0386	-0.1182	0.3077	ND	0.3573
IG2-16	-0.6020	0.1847	-2.6047	-0.8038	-0.1418	-1.7878	-0.3406	0.1063	-1.3564	0.0376
IG2-17	-0.9401	-0.3729	-2.2258	-1.0948	-0.8271	ND	-0.6050	-0.1214	ND	-0.1754
IG2-18	-0.4521	-0.1073	-2.8194	-1.4372	-0.5574	1.8672	-0.2787	-0.0195	ND	0.1947
IG2-19	-0.4337	0.1632	-2.5338	-0.3842	-0.0159	-2.1044	-0.1708	0.2827	ND	0.3432
IG2-20	-0.5746	0.0944	-2.3543	-0.5536	-0.1268	-0.9184	-0.1216	0.2282	-1.6768	0.2768
IG2-21	-0.8628	-0.2981	-1.6839	-1.6969	ND	-2.1682	-0.3443	0.0215	ND	-0.0687
IG2-22	-0.4537	0.0728	-2.8966	-0.6345	-0.0723	-2.1726	0.9256	0.3766	ND	-0.8504
IG2-23	-0.6894	0.2603	-2.3560	-0.8140	0.1095	-2.4645	-0.4036	0.1669	-1.4963	0.1957
IG2-24	-0.5401	-0.1209	-2.2600	-0.7171	-0.7794	-2.0813	-0.2088	0.1469	ND	0.0513
IG2-25	-0.4796	-0.0650	-2.2775	-0.7988	-0.5702	-2.2427	-0.1662	0.2218	ND	0.0925
IG2-26	-0.5725	-0.2085	-2.6712	-1.4161	ND	-1.2225	-0.3935	0.0382	-1.4963	-0.0067
IG2-27	-1.9032	-0.2418	-1.7739	-1.3765	-0.5227	-2.3823	-0.5056	-0.0010	ND	-0.1301
IG2-28	-0.7327	-0.1201	-1.9555	-1.5622	-0.8676	-2.6288	-0.1636	0.1643	ND	0.1625
IG2-29	-1.6492	-0.0176	-2.5060	ND	-0.2597	-2.1100	-0.3336	0.0025	ND	0.0399
IG2-30	-0.1009	0.0476	ND	ND	ND	ND	ND	0.1121	ND	-1.1025
IG2-31	-0.4776	0.5104	ND	ND	ND	ND	-0.3940	-0.4793	ND	0.2756

Table 12. (continued).

Glass	Log NL [Al (g/L)]	Log NL [B (g/L)]	Log NL [Ca (g/L)]	Log NL [Cr (g/L)]	Log NL [F (g/L)]	Log NL [Fe (g/L)]	Log NL [K (g/L)]	Log NL [Li (g/L)]	Log NL [Mg (g/L)]	Log NL [Na (g/L)]
IG2-32	-0.6138	0.0203	-2.3304	-1.2612	-0.1445	-2.1597	-0.2698	0.1339	ND	0.1156
IG2-33	--0.6632	-0.0330	-2.5961	-1.4595	-0.1891	-2.3279	-0.3294	0.0387	ND	0.0648
IG2-34	-0.6606	-0.0030	-2.3542	-1.5921	-0.1554	-2.0478	-0.3268	0.1252	-1.7182	0.0593
IG2-35	-0.6632	-0.1014	-2.5884	-2.7383	-0.3036	-2.4944	-0.3836	-0.0076	ND	0.0134
IG2-36	-0.7173	-0.1550	-2.4145	-2.7383	-0.4158	-2.3544	-0.4047	-0.0359	-1.8334	-0.0314
IG2-37	-0.7059	-0.0795	-2.4397	-1.7089	-0.2906	-2.4650	-0.2851	0.0713	-1.9648	-0.0247

Glass	Log NL [Ni (g/L)]	Log NL [P (g/L)]	Log NL [S (g/L)]	Log NL [Sn (g/L)]	Log NL [Sr (g/L)]	Log NL [Si (g/L)]	Log NL [Zr (g/L)]	Leachate pH
ARM-A	ND	-0.2049	ND	ND	-2.5485	-0.3026	ND	10.01
ARM-B	ND	-0.2049	ND	ND	-2.5485	-0.2896	ND	10.00
EA-A	ND	ND	ND	ND	ND	0.3746	ND	11.36
EA-B	ND	ND	ND	ND	ND	0.3668	ND	11.35
IG2-01	-1.0584	ND	-0.5563	-1.1659	ND	-0.5975	ND	8.50
IG2-02	ND	-2.1433	ND	ND	-2.4358	-1.1446	ND	7.68
IG2-03	-2.0251	ND	ND	-1.0879	-2.3831	-0.3758	ND	6.79
IG2-04	-0.8772	ND	-0.2363	-0.7553	ND	-0.3133	-0.988	10.88
IG2-05	ND	ND	-0.0880	ND	ND	-0.5050	ND	11.27
IG2-06	-1.4422	0.0004	-0.0313	ND	ND	-0.4664	-2.0531	9.50
IG2-07	ND	ND	-0.1024	ND	-2.5847	-0.8874	-3.9332	9.34
IG2-08	ND	ND	-0.3496	ND	-1.8553	-0.3919	ND	10.11
IG2-09	ND	ND	-0.8484	ND	-2.4500	-0.9817	ND	9.67
IG2-10	ND	0.4564	0.1942	-0.2980	-2.4087	-0.3161	ND	10.44
IG2-11	ND	-0.3167	-0.5180	ND	-2.8132	0.4381	ND	11.72
IG2-12	ND	ND	0.4458	-1.4071	-2.8132	-0.6309	-2.3344	8.60
IG2-13	ND	ND	-0.3983	-0.8982	-3.6261	-0.3853	-1.3451	10.19
IG2-14	ND	-0.3979	-0.4046	-0.7311	-2.5122	-0.4485	-0.8421	10.44
IG2-15	-2.2933	-0.4064	-0.0637	-1.2523	ND-	-0.2773	-2.9059	11.12
IG2-16	-1.6376	-0.5405	-0.2245	ND	ND	-0.7947	-2.3009	10.01
IG2-17	-2.6166	-2.1906	-0.5480	ND	ND	-0.7901	ND	9.90
IG2-18	-2.3390	-0.2418	-0.2450	-1.5041	ND	-0.5214	-3.3982	10.78
IG2-19	-2.2143	-0.4134	0.0044	ND	ND	-0.2902	-2.7692	11.23
IG2-20	-2.0882	-0.5310	0.1068	-1.4741	ND	-0.3417	--1.7394	11.13
IG2-21	ND	-2.4137	-0.3841	ND	-2.927	-0.7078	-3.2921	10.26
IG2-22	-2.6400	-0.4599	-0.2556	-1.1000	ND	-0.4807	-3.5021	11.30

Table 12. (continued).

Glass	Log NL [Ni (g/L)]	Log NL [P (g/L)]	Log NL [S (g/L)]	Log NL [Sn (g/L)]	Log NL [Sr (g/L)]	Log NL [Si (g/L)]	Log NL [Zr (g/L)]	Leachate pH
IG2-23	-2.6400	-0.3056	-0.3307	ND	ND	-0.6596	-2.6847	10.23
IG2-24	-2.4361	-1.8647	-0.3121	ND	ND	-0.7483	-3.9911	10.68
IG2-25	-3.4182	-1.8095	-0.2216	ND	ND	-1.0831	ND	10.83
IG2-26	2.3638	-0.3495	-0.4071	-1.6960	ND	-0.5448	-2.7736	10.54
IG2-27	-2.9367	ND	-0.4682	ND	-3.149	-0.6947	-3.379	10.05
IG2-28	-3.5899	-2.8952	-0.2887	ND	-3.2282	-0.6789	ND	10.54
IG2-29	-2.1311	-0.5213	ND	ND	ND	-0.6367	-2.7372	10.27
IG2-30	ND	ND	ND	ND	ND	-0.1480	-0.1712	9.23
IG2-31	ND	0.3780	-0.7443	ND	ND	-0.1856	-3.1542	9.99
IG2-32	-2.3273	-0.4716	-0.0831	ND	ND	-0.5841	-2.6356	10.11
IG2-33	-2.4915	-0.5311	-0.3328	ND	ND	-0.6013	-2.8809	10.26
IG2-34	-1.9673	0.5388	-0.2809	ND	ND	-0.5869	-2.5213	10.22
IG2-35	-2.6265	-0.5178	-0.3035	ND	ND	-0.6125	-2.8662	10.13
IG2-36	-2.4409	-0.7438	-0.2605	ND	-2.1212	-0.6433	-3.1356	10.14
IG2-37	-2.5852	-0.9985	-0.2511	ND	-1.8166	-0.6209	-4.6571	10.18

A significant database exists for the leachability of boron, lithium and sodium from the EA glass subjected to the PCT. With respect to the leachability of these elements, only IG2-03 and IG2-12 performed worse than the EA glass when subjected to the PCT. Both these glasses are from the GCER outer layer. Glass IG2-12 contained the highest amount of alkali oxides (Li_2O+Na_2O) of the Phase 2b glasses prepared and characterized, and it melted to a homogeneous product at 1150°C. Glass IG2-03 contained a high amount of alkali oxides (Li_2O+Na_2O), compared to other Phase 2b glasses, but it could not be melted to a homogeneous product within the thermal capability of the furnace used.

The compositions of the Phase 2b glasses are unlike that of the EA glass. Thus their leachates are impacted differently by composition than is the EA glass leachate. Given this difference, only IG2-11 performed worse than the EA glass with respect to silicon leachability when subjected to the PCT. Also, of the Phase 2b glasses, only the IG2-11 leachate was of higher pH than that of the EA glass. Glass IG2-11 is a GCER outer layer glass, and it melted to a homogeneous product at 1150°C.

A comparison of the Phase 2b glasses and the EA glass with respect to leachability of other elements needs more data than obtained in this study. This is particularly required for elements present in small amounts in both the EA and Phase 2b glasses or for elements present in greatly different mass fractions in the two glass types.

The comparison of Phase 2b glass leaching properties to those of the ARM glass when both are subjected to the PCT is more difficult than the comparison to the EA glass. With respect to major elements present in both glasses (boron, lithium, sodium and silicon), the data in Table 12 suggest that the PCT leachabilities of most Phase 2b glasses compare well with those of the ARM glass. Most Phase 2b glass leachates are of a higher pH than that from the ARM glass.

Blank analyses performed for fluorine analysis were below limits of detection. Therefore the lower detection limit of the ICP instrument was used as the blank analysis. Phase 2b leachates were also analyzed for chlorine, but amounts present were below detection limits.

5.4 Viscosity Characterization

Viscosity as a function of melt temperature ($\eta - T_M$) was observed on Phase 2b glasses, according to the procedure described in Section 4. The result of the IG2-03 formulation was not a glass and therefore was not characterized with respect to viscosity. Glasses that were melted at higher temperatures than 1150°C (see Table 5) were measured over the range of 950°C to 1350°C. Table C-1, Appendix C contains the raw η data for the Phase 2b test glasses.

The glass $\eta - T_M$ data was fitted to the Arrhenius model:

$$\ln\eta = E + \frac{F}{T},$$

where E, and F, are temperature independent coefficients and T is absolute temperature. The raw data for most glasses (see Table C-1), fits the Arrhenius model well (R2>0.98). Figure 10 showing the fit of all $\eta - T_M$ data points from IG2-19 to the Arrhenius model is an example. Occasionally data points were omitted from the Arrhenius fits in order to obtain lower standard error on coefficients E and F. The omitted points are identified in Table C-1 with a strikeout. These data were influenced by crystallization or phase separation in each of the glasses IG2-6, -10, -17, and -27 during viscosity measurement. Data points for IG2-1, -5, -7, and -14 were omitted from the Arrhenius fit because of mechanical problems identified during viscosity measurement. The impact of data removal is best illustrated by example. Figure 11 shows the $\eta - T_M$ data from IG2-27 fitted to the Arrhenius model with all data points. Figure 12 shows the $\eta - T_M$ data from IG2-27 fitted to the Arrhenius model with three data points removed.

Table 13 gives the coefficients (E and F) from the fit of raw data to the Arrhenius model. For the purpose of viscosity characterization, the crucible melt temperatures, T_M, were established as central temperatures. Therefore, the viscosity at the melting temperature (T_M °C) was calculated for each test glass using the Arrhenius model. In addition, the temperature at a glass viscosity of 2 Pa-sec (T_2) and 10 Pa-sec (T_{10}), were calculated using the Arrhenius model for Phase 2b test glasses and are given in Table 13.

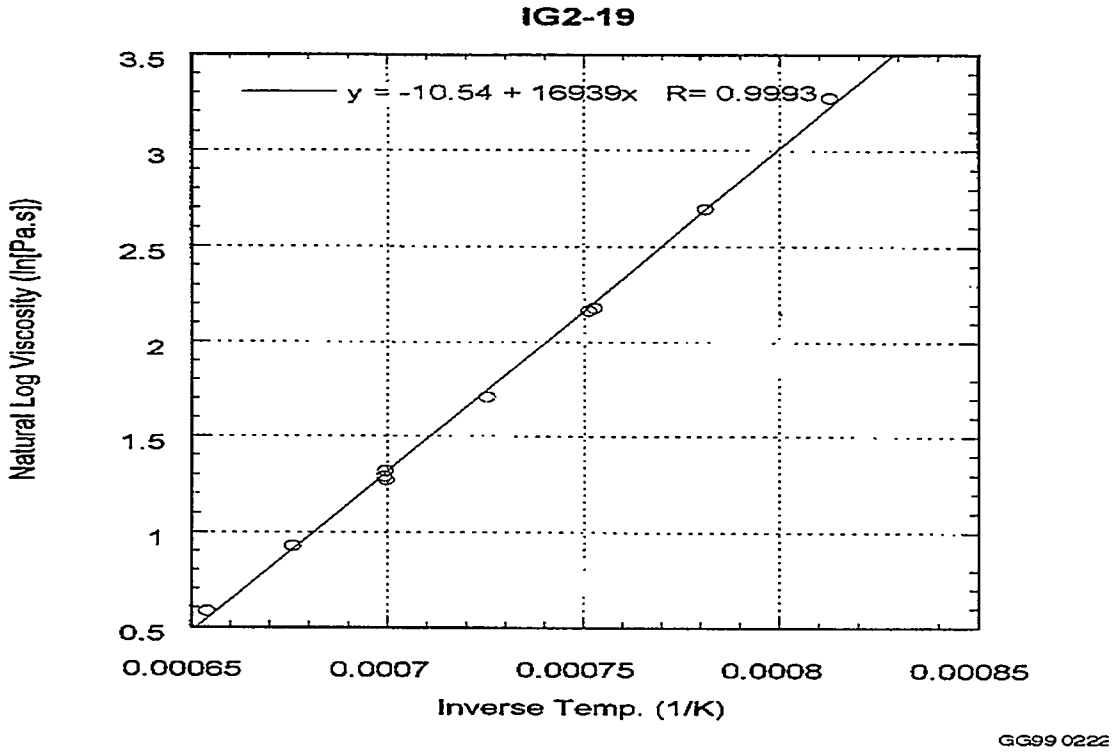

Figure 10. Fit of Arrhenius equation to IG2-19 viscosity data.

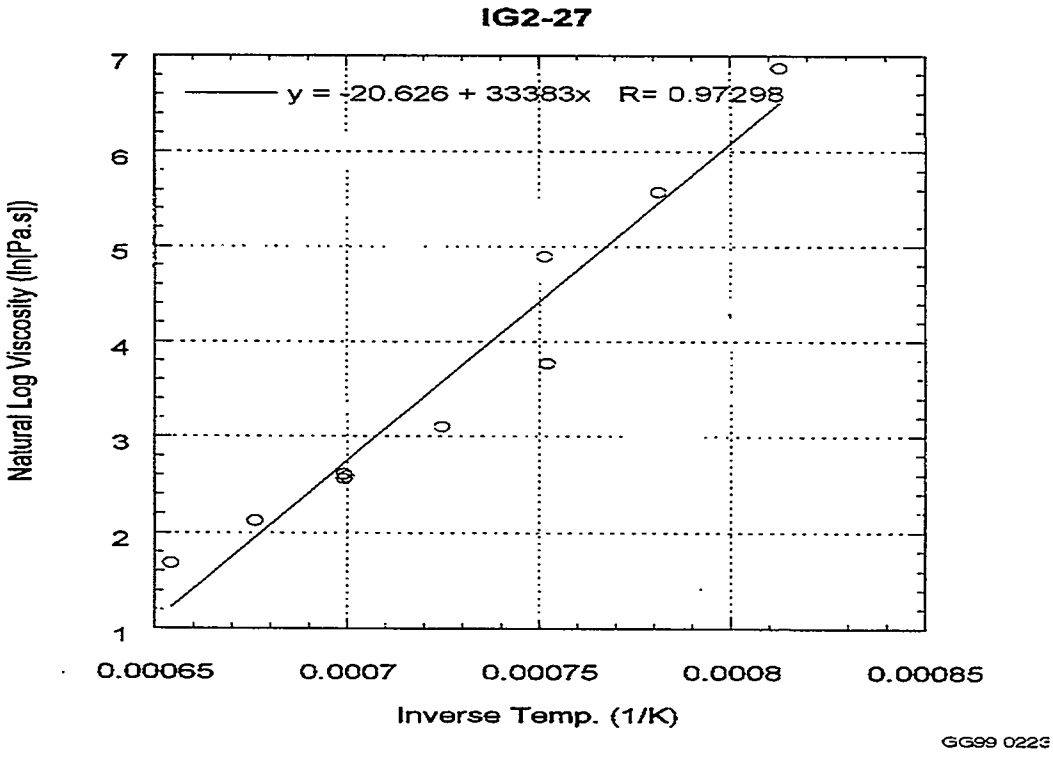

Figure 11. Fit of Arrhenius equation to IG2-27 viscosity data showing discontinuity.

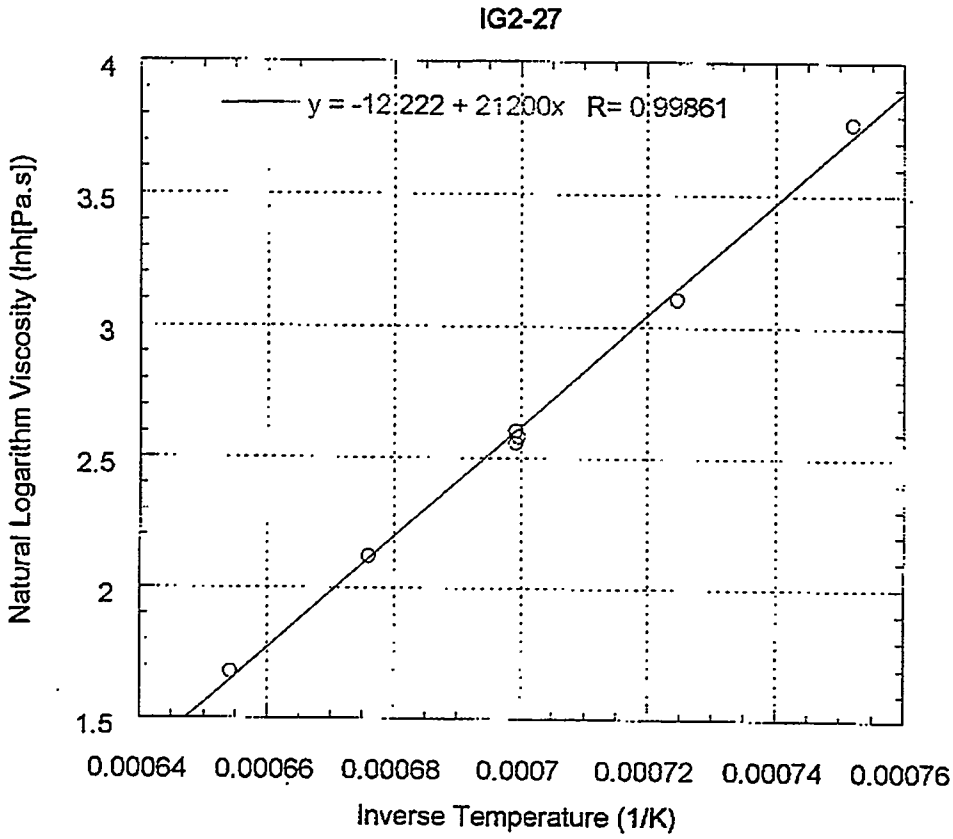

Figure 12. Fit of Arrhenius equation to IG2-27 viscosity data.

Table 13. Viscosity Profile at T_M °C using Arrhenius model.

Sample ID	A	B (K)	Pa-sec at T_M	T_M °C	T_2 °C	T_{10} °C
IG2-01*	-8.170	16658	15.90	1250	1606	1317
IG2-02	-14.189	26621	26.81	1250	1516	1341
IG2-03*	—	—	—	1550	—	—
IG2-04	-9.382	14154	1.76	1150	1132	938
IG2-05*	-15.185	23393	1.19	1250	1200	1065
IG2-06*	-11.684	16591	0.45	1250	1067	913
IG2-07*	-28.627	47213	10.70	1250	1337	1253
IG2-08	-12.226	17998	1.52	1150	1120	966
IG2-09*	-12.414	18290	1.55	1150	1122	970
IG2-10*	-11.331	17744	3.12	1150	1203	1028
IG2-11	-10.121	15057	1.58	1150	1119	939

Table 13. (continued).

Sample ID	A	B (K)	Pa-sec at T_M	T_M °C	T_2 °C	T_{10} °C
IG2-12	-13.868	20742	2.03	1150	1151	1010
IG2-13	-12.412	22091	8.10	1250	1413	1228
IG2-14	-12.483	24733	42.74	1250	1604	1400
IG2-15	-10.366	16800	4.22	1150	1246	1053
IG2-16	-11.982	19284	4.80	1150	1248	1077
IG2-17*	-12.163	20998	5.07	1250	1360	1178
IG2-18	-12.183	20260	3.06	1250	1300	1125
IG2-19	-10.540	16939	3.91	1150	1235	1046
IG2-20	-11.146	18736	7.53	1150	1309	1120
IG2-21	-11.831	20386	12.10	1150	1355	1169
IG2-22*	-13.137	21426	2.53	1250	1276	1115
IG2-23	-12.176	19270	3.91	1150	1224	1058
IG2-24	-12.327	19490	1.60	1250	1224	1059
IG2-25	-12.059	19182	1.71	1250	1231	1062
IG2-26	-11.848	20409	12.09	1150	1354	1169
IG2-27*	-12.222	21200	5.45	1250	1368	1186
IG2-28	-11.922	19929	8.02	1150	1307	1128
IG2-29	-11.180	18085	4.61	1150	1250	1068
IG2-30	-10.119	17829	11.12	1150	1376	1162
IG2-31	-12.345	20636	8.63	1150	1310	1136
IG2-32	-11.396	18555	5.17	1150	1262	1081
IG2-33	-11.584	18437	3.94	1150	1229	1055
IG2-34*	-11.549	18751	2.14	1250	1259	1081
IG2-35	-11.353	18313	4.55	1150	1247	1068
IG2-36	-11.228	18100	4.44	1150	1245	1065
IG2-37	-11.400	18422	4.69	1150	1250	1071

* Inhomogeneous air quenched product.

6. SUMMARY OF PHASE 2B GLASS CHARACTERISTICS

The data in Table 14 presents a comparison of Phase 2b glass characteristics with performance constraints given in Section 3. Those glasses for which higher melt temperatures were required should not necessarily be expected to meet lower temperature processing constraints. The data indicates that glasses IG2-15, -16, -19, -20, -28, -31, -32, and -37 perform in a manner that meets or exceeds all performance constraints used in the study. Each of these samples is a GCER inner layer glass. These results are consistent with the intent stated in Subsection 2.2.1 of limiting the inner layer component ranges of the GCER to increase the probability of yielding glasses that would meet an arbitrary set of processing and performance specifications.

Table 14. Summary of Phase 2b glass characteristics compared to performance criteria.

Sample ID	Homogeneous by XRD analysis		Liquidus Temperature	PCT Durability compared to EA glass			Viscosity Profile at T_M °C (2-10 Pa-s)			
				r_B (g/L)	r_{Li} (g/L)	r_{Na} (g/L)				
	Quenched	CCC	$T_L<T_M$-100°C	1.0682	0.8296	0.9306	Pa-s	T_M °C	T_2 °C	T_{10} °C
IG2-01	No	ND	ND	-0.3462	ND	-0.3707	15.90	1250	1606	1317
IG2-02	Yes	ND	1133	-0.7457	ND	-1.6718	26.81	1250	1516	1341
IG2-03	No	ND	ND	1.3947	ND	0.0373	ND	1550	ND	ND
IG2-04	Yes	ND	913	0.7611	-0.7162	-0.4960	1.76	1150	1132	938
IG2-05	No	ND	ND	-0.0091	ND	0.4560	1.19	1250	1200	1065
IG2-06	No	ND	ND	0.6164	-3.8055	-0.9793	0.45	1250	1067	913
IG2-07	No	ND	ND	-0.2126	ND	-1.1552	10.70	1250	1337	1253
IG2-08	Yes	ND	861	-0.0563	ND	0.1420	1.52	1150	1120	966
IG2-09	No	No	ND	-0.7011	-0.3512	-1.7651	1.55	1150	1122	970
IG2-10	No	No	ND	0.4460	0.4399	-0.5448	3.12	1150	1203	1028
IG2-11	Yes	Yes	773	0.5978	0.6999	0.7170	1.58	1150	1119	939
IG2-12	Yes	No	823	1.3683	1.3210	1.1690	2.03	1150	1151	1010
IG2-13	Yes	ND	1223	-0.2384	0.0279	-1.3525	8.10	1250	1413	1228
IG2-14	Yes	ND	1133	-0.0711	ND	0.0739	42.74	1250	1604	1400
IG2-15	Yes	Yes	823	0.1689	0.3077	0.3573	4.22	1150	1246	1053
IG2-16	Yes	ND	948	0.1847	0.1063	0.0376	4.80	1150	1248	1077
IG2-17	No	ND	ND	-0.3729	-0.1214	-0.1754	5.07	1250	1360	1178
IG2-18	Yes	ND	1407	-0.1073	-0.0195	0.1947	3.06	1250	1300	1125
IG2-19	Yes	Yes	841	0.1632	0.2827	0.3432	3.91	1150	1235	1046
IG2-20	Yes	Yes	843	0.0944	0.2282	0.2768	7.53	1150	1309	1120
IG2-21	Yes	ND	961	-0.2981	0.0215	-0.0687	12.10	1150	1355	1169

Table 14. (continued).

Sample ID	Homogeneous by XRD analysis		Liquidus Temperature $T_L<T_M$-100°C	PCT Durability compared to EA glass			Viscosity Profile at T_M °C (2-10 Pa-s)			
				r_B (g/L)	r_{Li} (g/L)	r_{Na} (g/L)				
	Quenched	CCC		1.0682	0.8296	0.9306	Pa-s	T_M °C	T_2 °C	T_{10} °C
IG2-22	No	ND	ND	0.0728	0.3766	-0.8504	2.53	1250	1276	1115
IG2-23	Yes	No	923	0.2603	0.1669	0.1957	3.91	1150	1224	1058
IG2-24	Yes	ND	1382	-0.1209	0.1469	0.0513	1.60	1250	1224	1059
IG2-25	Yes	ND	1363	-0.0650	0.2218	0.0925	1.71	1250	1231	1062
IG2-26	Yes	Yes	966	-0.2085	0.0382	-0.0067	12.09	1150	1354	1169
IG2-27	No	ND	ND	-0.2418	-0.0010	-0.1301	5.45	1250	1368	1186
IG2-28	Yes	Yes	938	-0.1201	0.1643	0.1625	8.02	1150	1307	1128
IG2-29	Yes	No	923	-0.0176	0.0025	0.0399	4.61	1150	1250	1068
IG2-30	Yes	ND	948	0.0476	0.1121	-1.1025	11.12	1150	1376	1162
IG2-31	Yes	ND	883	0.5104	-0.4793	0.2756	8.63	1150	1310	1136
IG2-32	Yes	ND	933	0.0203	0.1339	0.1156	5.17	1150	1262	1081
IG2-33	Yes	No	913	-0.0330	0.0387	0.0648	3.94	1150	1229	1055
IG2-34	No	ND	ND	-0.0030	0.1252	0.0593	2.14	1250	1259	1081
IG2-35	Yes	ND	931	-0.1014	-0.0076	0.0134	4.55	1150	1247	1068
IG2-36	Yes	ND	923	-0.1550	-0.0359	-0.0314	4.44	1150	1245	1065
IG2-37	Yes	ND	938	-0.0795	0.0713	-0.0247	4.69	1150	1250	1071

ND (Not Determined)

7. CONCLUSIONS AND RECOMMENDATIONS

About two-thirds of the formulations defined in Phase 2b of the INTEC CVS resulted in optically homogeneous products when vitrified at 1150°C and cooled under air quenching conditions. All of these glasses producing homogeneous products have melt viscosities at 1150°C falling within the range of 2-10 Pa-sec., T_Ls 100°C or more below 1150°C and PCT leaching responses well below those of the EA glass. The Phase 2b matrix also included glasses anticipated to require a vitrification temperature higher than 1150°C. These formulations typically contained higher zirconium and aluminum contents and lower alkali oxide contents. About half of these yielded optically homogeneous products when melted at temperatures as high as 1550°C. These glasses had leaching responses well below those of the EA glass and viscosities at 1150°C falling within the range of 2-10 Pa-sec. However, Only two of these glasses (IG2-02 and IG2-14) had T_Ls 100°C or more below their melt temperature. The results discussed above provide evidence that the CVS approach is progressing towards acquiring significant composition-product characteristic information. With further effort, information can be acquired on the compositional boundaries of formulations yielding homogeneous products that meet T_L, durability and viscosity constraints established for this study. Thus, more data is needed for defining optimized formulations required for developing a vitrification process for INTEC HLW. Rigorous investigation of composition related characteristics are outside the scope of this study but must be addressed through future studies. The mechanism for effects such as these and the possibility of similar relationships from other major elements on durability, viscosity and T_L must be completed before optimized glasses are defined for vitrifying INTEC HAW.

Through the formation of Phase 2b glasses under air quenched and CCC heat treatments, it was revealed that phase separation and crystallization also depends on cooling rate. Determining the relationship between composition and tendency to devitrify on cooling must be part of future composition-product characteristic investigation phases of this CVS. Because during production, molten glass poured into a disposal canister will be cooled to ambient temperature at a rate as slow as the CCC. Glasses remaining homogeneous when cooled at these rates should more easily qualify for repository storage than those that phase separate or devitrify. Data is being collected through this study will be input for a technically based decision on whether inhomogeneity significantly impacts product performance. For the purposes of this phase of the CVS, it is also assumed that that 1150°C is the nominal melter operating temperature for vitrifying INTEC HLW. Thus only Phase 2b glasses that could be vitrified to optically homogeneous products at 1150°C were subjected to the CCC heat treatment. Six of the glasses subjected to the CCC treatment remained optically homogeneous. Analysis of these glasses (those not remaining homogeneous after the CCC treatment) indicate that fluorapatite is the predominant phase that crystallizes at slow cooling rates when phosphate is present. Nepheline analogs and lithium phosphate or silicate were also observed crystallizing from Phase 2b glasses not containing phosphate. Phase 2b glasses requiring a higher vitrification temperature than 1150°C to yield optically homogeneous products should also be subjected to a CCC treatment. The results of such testing would provide information on the homogeneity properties of glasses needing a system different than a joule heated ceramic walled melter for forming vitrified products. Electronic microscopy, including TEM techniques, could be performed on glasses subjected to the CCC heat treatment regardless of temperature of formation in order to observe

glass-in-glass separation as well the presence of crystallinity not detectable by the means used in this study.

A more thorough estimate of INTEC calcined waste compositions has been published after Phase 2 of the INTEC CVS began.[20] These estimates fall within the composition range on which the Phase 2b matrix is based. Composition with respect to major and minor components as well as radionuclides are included in this updated estimate. The estimates do not include the chemical and phase composition of undissolved solids within the calcines. Nevertheless, these newest INTEC calcined waste composition estimates must be used to develop glass formulations for use in future phases of this CVS. Each of the components by themselves or in combination with others, could have significant effects on the processability or acceptability for repository storage of the glasses being developed.

As observed in this study, cooling at rapid rates such as air quenching does not always provide the conditions required for the phase separation or crystallization that could occur at slower cooling rates. Cooling rate influences phase separation and crystalline phase formation in glasses. Both these phenomena could impact product durability. Therefore, studies of HAW glasses must also include observations of the effects of cooling rates down to the CCC on homogeneity and durability. Such information is required for the development and optimization of processable HAW glasses that have high probability of being acceptable for disposal. It also provides data for the development of generalized models for defining the tendency of a glass to phase separate as a function of cooling rates and of composition.

Recommendations for other important areas of attention with respect to the four product properties investigated in Phase 2b CVS for INTEC HAW glasses include:

1. Obtaining more data for the definition of primary phase fields of the crystalline species that determine T_L of glasses investigated

Much of the information obtained from T_L investigations performed in this study is new because of the waste compositions (and thus glass compositions) used. The result is that different crystalline species were formed at T_L than formed in Phase 1 of the CVS or in Hanford, DWPF and WVDP investigations. Fluorapatite appears to be the most common phase to crystallize at T_L from phase 2b glasses containing calcium, flourine and phosphate. Hydroxylapatite appears at T_L in these glasses containing phosphate. However other crystalline phases such as alkali aluminosilicates or phosphates also form at T_L in these glasses when fluorine is absent. Likewise, in glasses requiring a temperature higher than 1150°C to achieve a homogeneously vitrified product, zirconium oxide and silicate phases form at T_L. Occasionally, other phases formed in these glasses at T_L. Insufficient data is available to define the primary phase fields for crystalline forms encountered at T_L, but obtaining such information will be required for optimizing glasses for vitrifying INTEC HAW and calcine.

2. Studying the effects of composition and phase changes and on durability

Many of the air quenched Phase 2b formulations yield durable products as determined by responses to the PCT. As observed in Phase 1 of the CVS, the leaching data obtained in this phase also suggests relationships between glass composition and leachability. More waste components were included in formulating the Phase 2b matrix than in the Phase 1 matrix. Because of the presence of more components used in formulating Phase 2b glasses, their durability has a more complex relationship to waste composition. Likewise, the durability of glasses subjected to the CCC heat treatment should be

determined and compared to their air quenched versions. This comparison could reveal the effects of cooling rate on durability, particularly if phase changes occur. More data will be needed to define all these relationships. This requirement must be addressed because better knowledge of the waste compositions will be acquired in the future.

3. Defining the influence of composition on the ability to retain a homogeneous product

The Phase 1 results indicated that the relative amounts of refractory components and borosilicate glass forming additives in formulations greatly influence product homogeneity. This observation is reinforced by the results obtained in Phase 2b of the CVS. Most obvious is the effect of the relative amounts of these components on vitrification temperature required for achieving an optically homogeneous product. Several of the Phase 2b formulations anticipated to need higher vitrification temperatures did not produce optically homogeneous products. Likewise, the results of subjecting optically homogeneous air quenched glasses to the CCC heat treatment reveals that cooling rate impacts the ability of a formulation to retain a homogeneous product. A further consideration must be the impact of inhomogeneity resulting from cooling on product durability. Thus there is significant reason for investigating compositional boundaries for practical vitrification temperatures and for retention of homogeneity with cooling rate particularly as knowledge of INTEC HLW composition improves. Those component-homogeneity relationships that are significant must be defined before INTEC HAW glasses can be optimized.

4. Defining the influence of composition on glass viscosity-melt temperature profile

In the first phase of this CVS, phosphate content was observed to have a major influence on the continuity of glass viscosity as a function of melt temperature. Phosphate was not a major glass component in this phase of the CVS, and viscosity continuity at lower temperatures of Phase 2b glasses was improved over those produced in Phase 1b. Calcium fluoride is the major component of zirconia calcine and therefore an important component of the Phase 2b glasses. The data obtained in this phase of the CVS suggest that its presence could have a significant impact on the viscosity-melt temperature profile (and other properties). As with the other characteristics investigated to date, the effects of composition on viscosity as a function of melt temperature must be defined before formulation optimization can be performed.

5. Performing electron microscopy and durability testing of glasses cooled at the CCC rate

Microscopy by TEM techniques should be applied to selected Phase 2b glasses remaining optically homogeneous when formed using the CCC heat treatment. This analysis would detect the presence of glass-in-glass separation as well as the formation of crystalline phases too diffuse to be detected by optical means, SEM and XRD. Likewise, these glasses should be subjected to the PCT and the results compared to those obtained on their air quenched versions. Such a comparison would help reveal any influence of glass-in-glass separation or crystalline phase formation on durability.

8. REFERENCES

1. *Code of Federal Regulations*, Office of the Federal Registrar, Vol. 57, pgs. 22046-22047, 40CFR268, May 26, 1992.

2. The INEEL Spent Nuclear Fuel and Environmental Restoration and Waste Management Programs Environmental Impact Statement, DOE\EIS-0203-F, April, 1995.

3. B. A. Staples, D. K. Peeler, J. D. Vienna, B. A. Scholes and C. A. Musick, *The Preparation and Characterization of INTEC Phase 2 Composition Variation Study Glasses*, INEEL/EXT-98-00970, Rev. 1, March, 1999.

4. T. B. Edwards, D. K. Peeler, I. A. Reamer, G. F. Piepel, J. D. Vienna, and H. Li, *Phase 2b Experimental Design for the INEEL Glass Composition Variation Study (U)*, WSRC-TR-99-00224, Rev. 0, March 30, 1999.

5. American Society for Testing and Materials, "Standard Test Method for Determining Chemical Durability of Nuclear Waste Glasses, The Product Consistency Test (PCT)," ASTM-C-1285-94, 1994

6. G. F. Piepel, J. D. Vienna and P. Hrma, *Phase 1 Experimental Design for the INEEL HLW Glass Composition Variation Study*, PNNL-SA-29594, Rev. 2, January, 1999.

7. P. Hrma, G. F. Piepel, M. J. Schweiger, D. F. Smith, D. S. Kim, P. E. Redgate, J. D. Vienna, C. A. LoPresti, D. B. Simpson, D. K. Peeler, and N. H. Lagowski, *Property-Composition Relationships for Hanford, High-Level Waste Glass Melting at 1150°C*, PNL-10359, vol. 1 and 2, Pacific Northwest National Laboratory, Richland, Washington, 1994.

8. B. A. Staples and C. A. Musick, *Workshop for Conducting Phase 2 of the INTEC Glass Composition Variation Study*, INEEL/EXT-99-00574, June 1999.

9. American Society for Testing and Materials, "Standard Practices for Measurement of Liquidus Temperature of Glass by the Gradient Furnace Method," ASTM C-829-81, 1998.

10. D. K. Peeler, I. A. Reamer, J. D. Vienna and J. V. Crum, Technical Status Report: Preliminary *Glass Formulation Report for the INEEL HAW*, WSRC-TR-98-0012, Rev. 1, March, 1998.

11. R. H. Doremus, "Glass Science," John Wiley & Sons, New York, 1973.

12. Waste Acceptance Product Specifications for Vitrified High-Level Waste Forms, Office of Environmental Restoration and Waste Management, U.S. Department of Energy, Washington, D.C. February, 1993.

13. S. L. Marra and C. M. Jantzen, *Characterization of Projected DWPF Glasses Heat Treated to Simulate Canister Centerline Cooling (U)*, WSRC-TR-92-142, Rev. 1, June, 1993.

14. Westinghouse Savannah River Company, *Glass Melting Procedure*, GTOP-3-004, Savannah River Technology Center, Aiken, SC, 1996.

15. Westinghouse Savannah River Company, *Laboratory-Scale Glass Preparation Procedure*, GTOP-3-016, Savannah River Technology Center, Aiken, SC, 1998.

16. T. B. Edwards and D. K. Peeler, *Analytical Plan for Measuring Chemical Compositions of INEEL Phase 2 Glasses*, WSRC-RP-99-00522, Rev. 0, June 15, 1999.

17. EPA Method 200.62-A CLP, "Dissolution of Industrial Waste Materials for Elemental Analysis by Potassium Hydroxide Fusion."

18. J. D. Vienna, D. K. Peeler, C. M. Jantzen, J. V. Crum and Larry Bruckner, "Standard Test Methods for Determining the Liquidus Temperature (T_L) of Waste and Simulated Waste Glasses," Submitted to ASTM C26.13 for Committee Ballot, 1998 American Society for Testing and Materials.

19. "Standard Practice for Measuring Viscosity of Glass Above the Softening Point," ASTM C-965-95, 1995.

20. M. D. Staiger, *Calcine Waste Storage at the Idaho Nuclear Technology and Engineering Center*, INEL/EXT-98-00455, June, 1999.

Appendix A

X-Ray Diffraction Patterns for Air Quenched Glasses and for those Cooled at Canister Centerline Heat Treatment

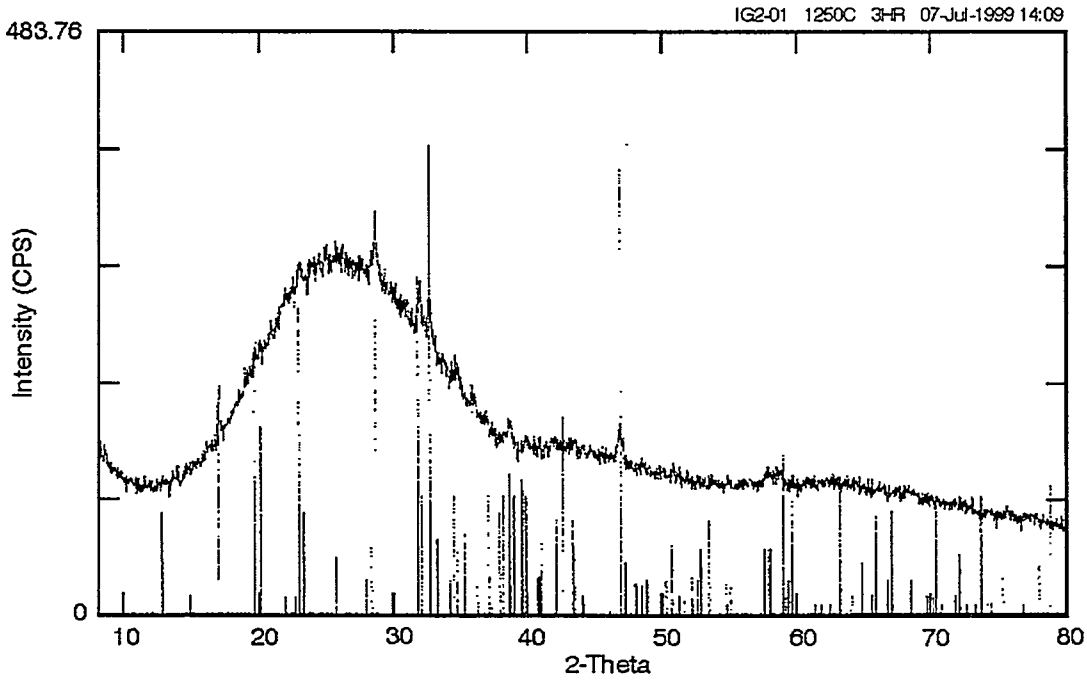

Figure A1-1. Four-hour XRD spectra of IG2-01 showing presence of cryolite

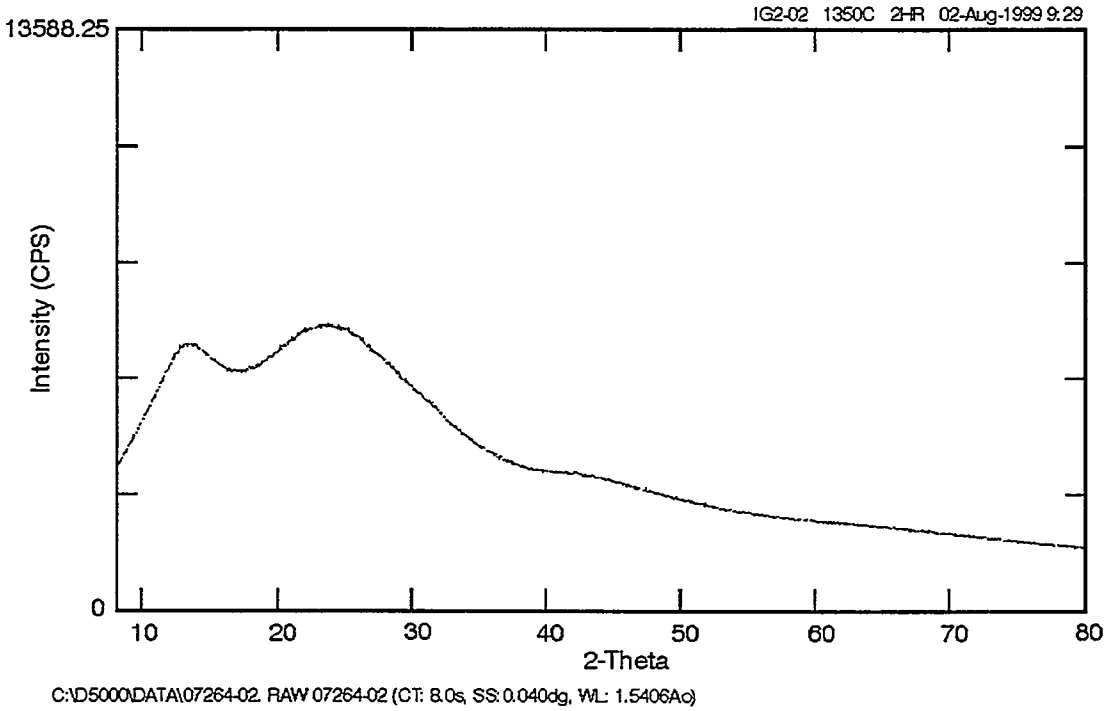

Figure A1-2. Four-hour XRD spectra of IG2-02 showing absence of crystallinity.

GG990196

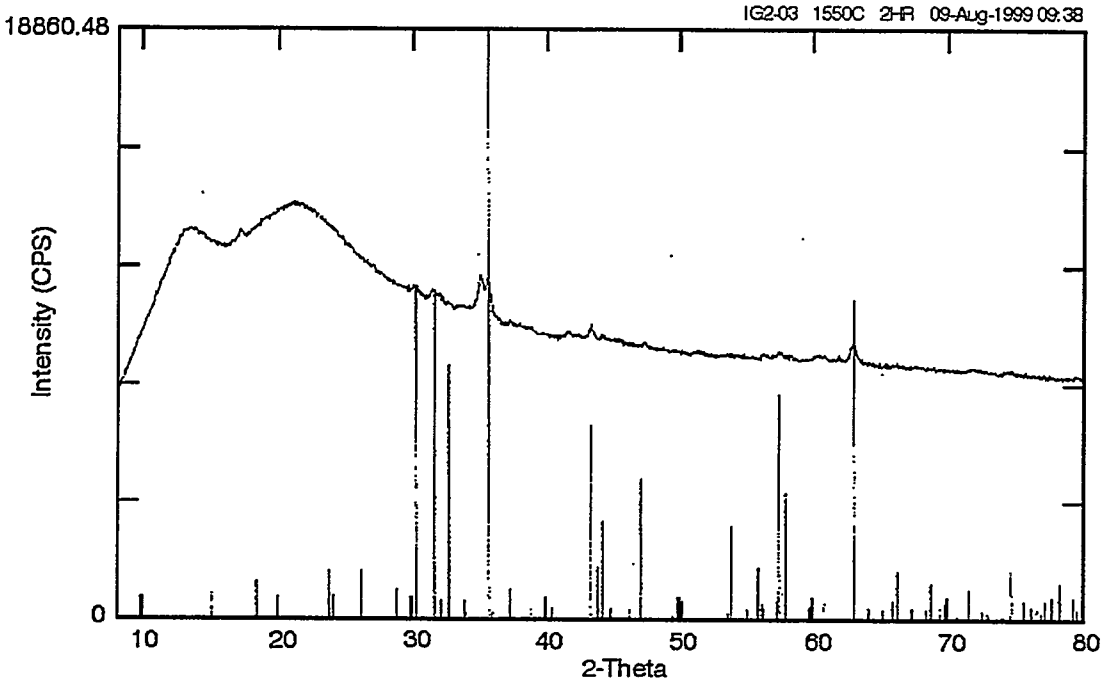

Figure A1-3. Four-hour XRD spectra of IG2-03 showing presence of iron oxide crystallinity.

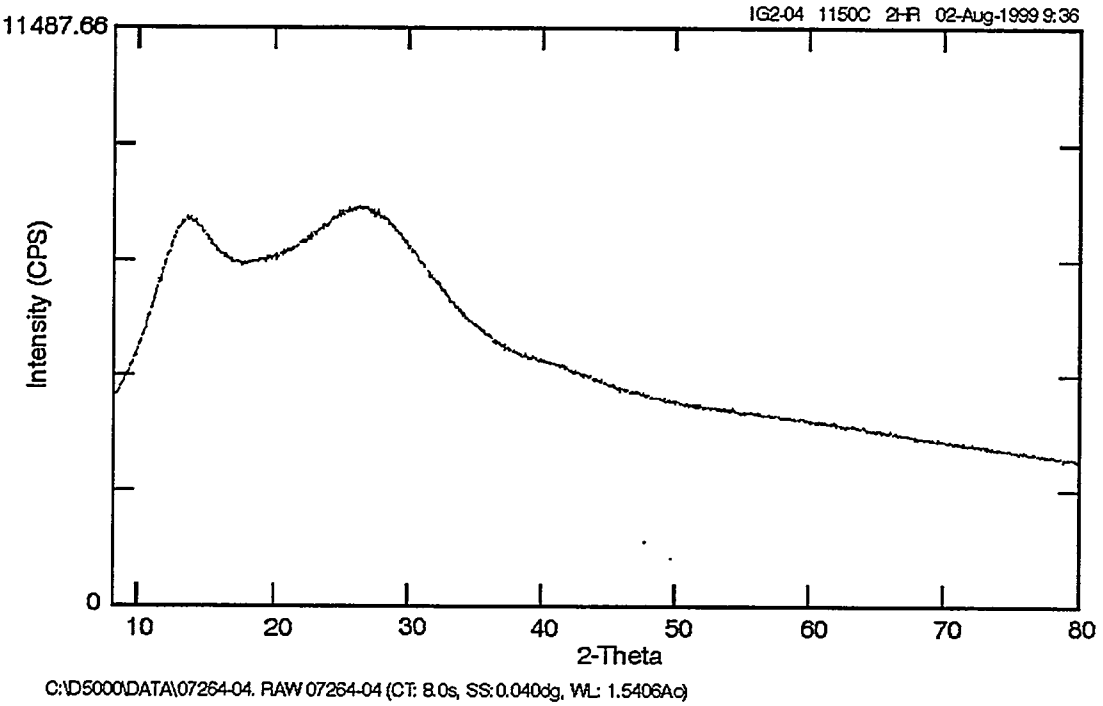

Figure A1-4. Four-hour XRD spectra of IG2-04 showing absence of crystallinity.

GG99 01 97

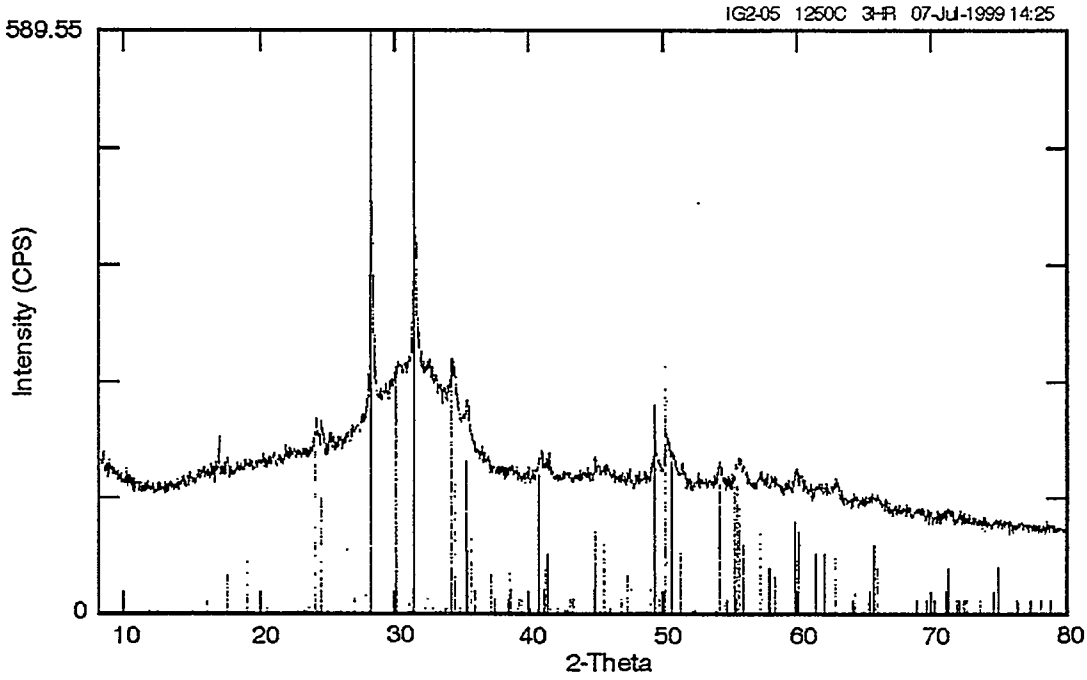

Figure A1-5. Four-hour XRD spectra of IG2-05 showing presence of zirconium oxide.

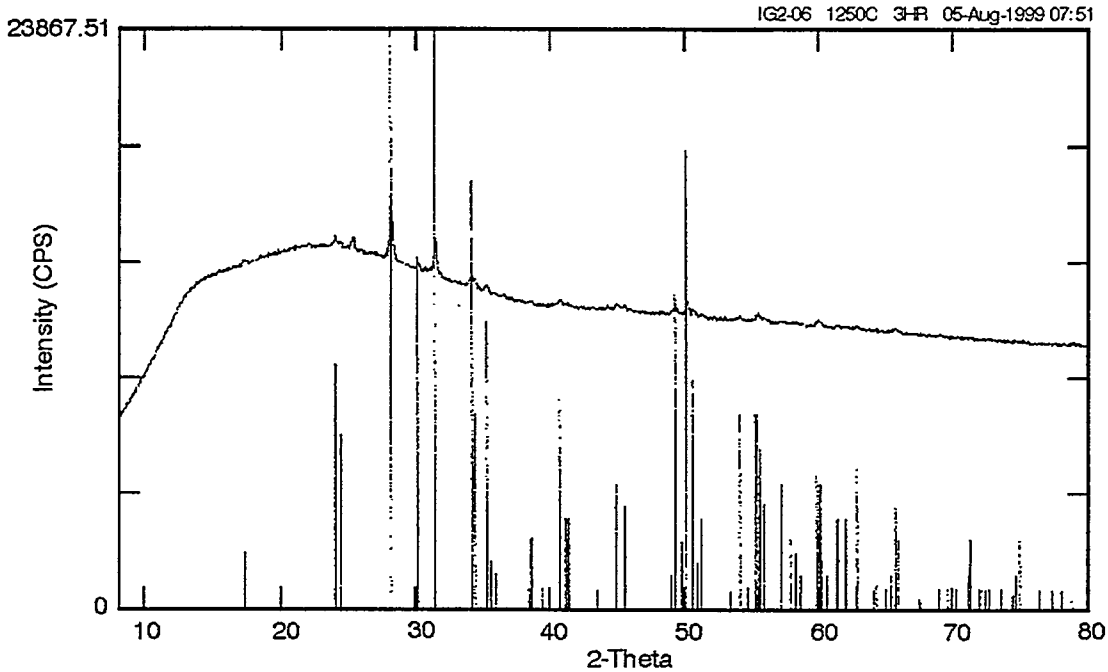

Figure A1-6. Four-hour XRD spectra of IG2-06 showing presence of zirconium oxide.

GG99 01 98

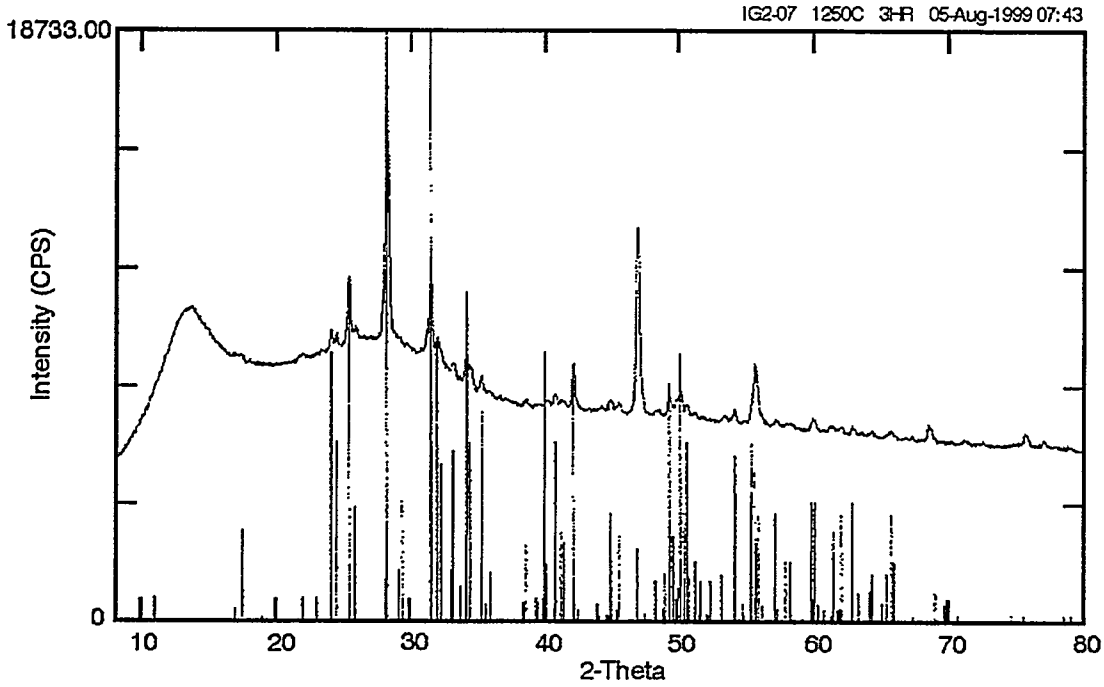

Figure A1-7. Four-hour XRD spectra of IG2-07 showing presence of zirconium oxide fluorapatite, and fluorite.

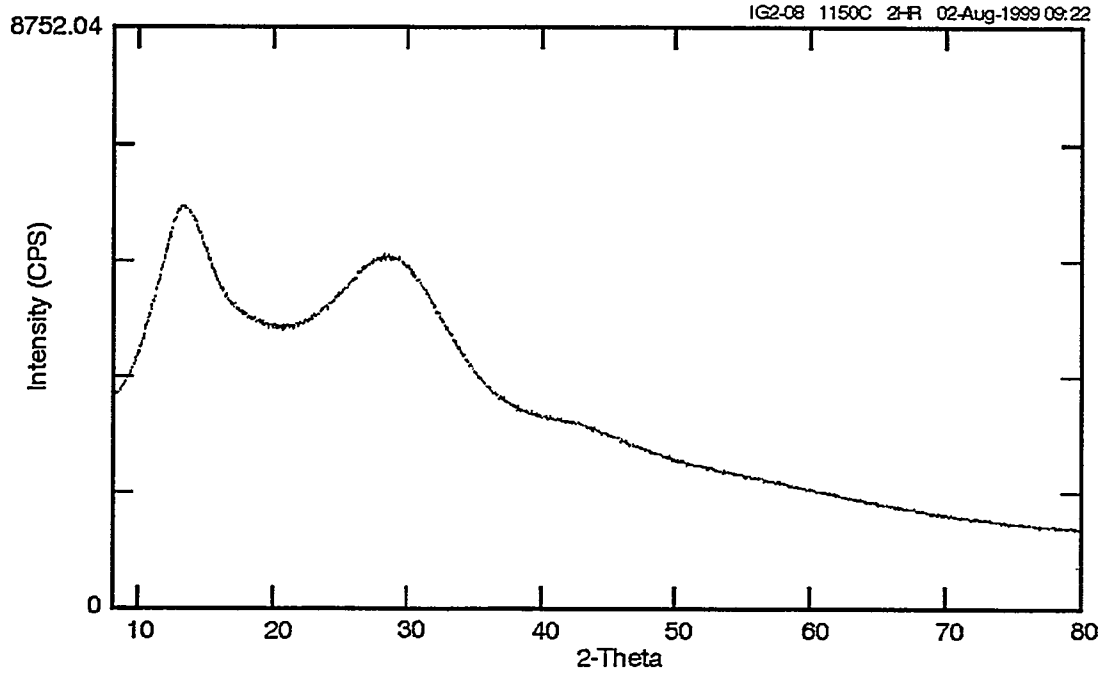

Figure A1-8. Four-hour XRD spectra of IG2-08 showing absence of crystallinity.

GG99 0199

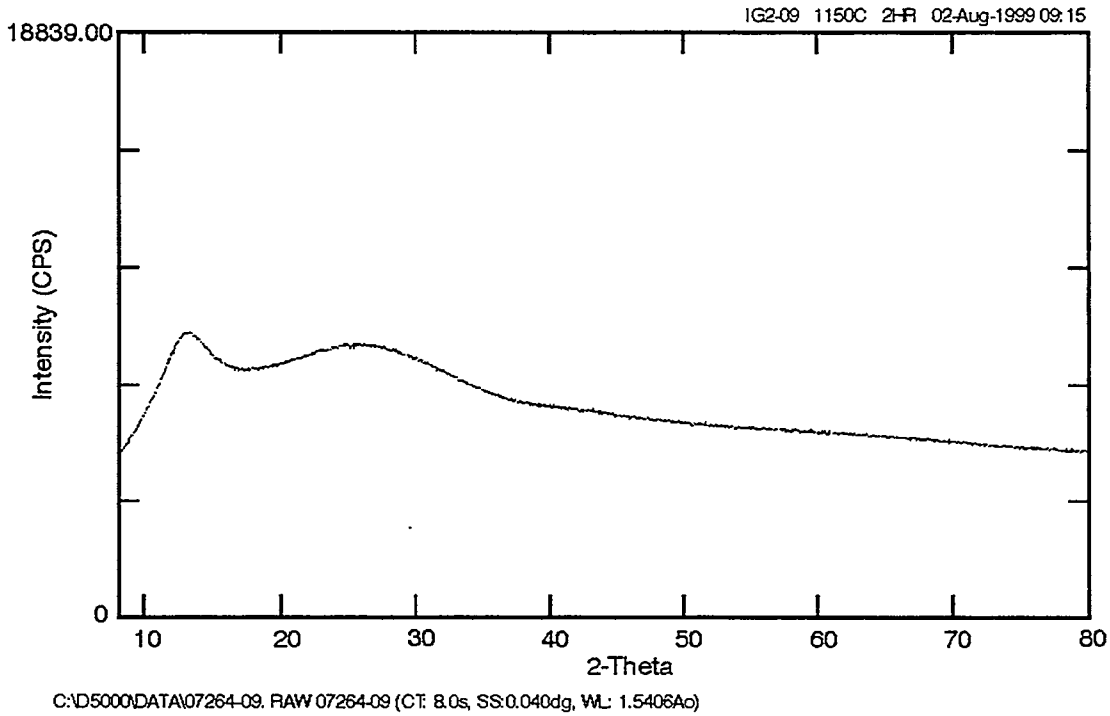

Figure A1-9. Four-hour XRD spectra of IG2-09 showing absence of crystallinity.

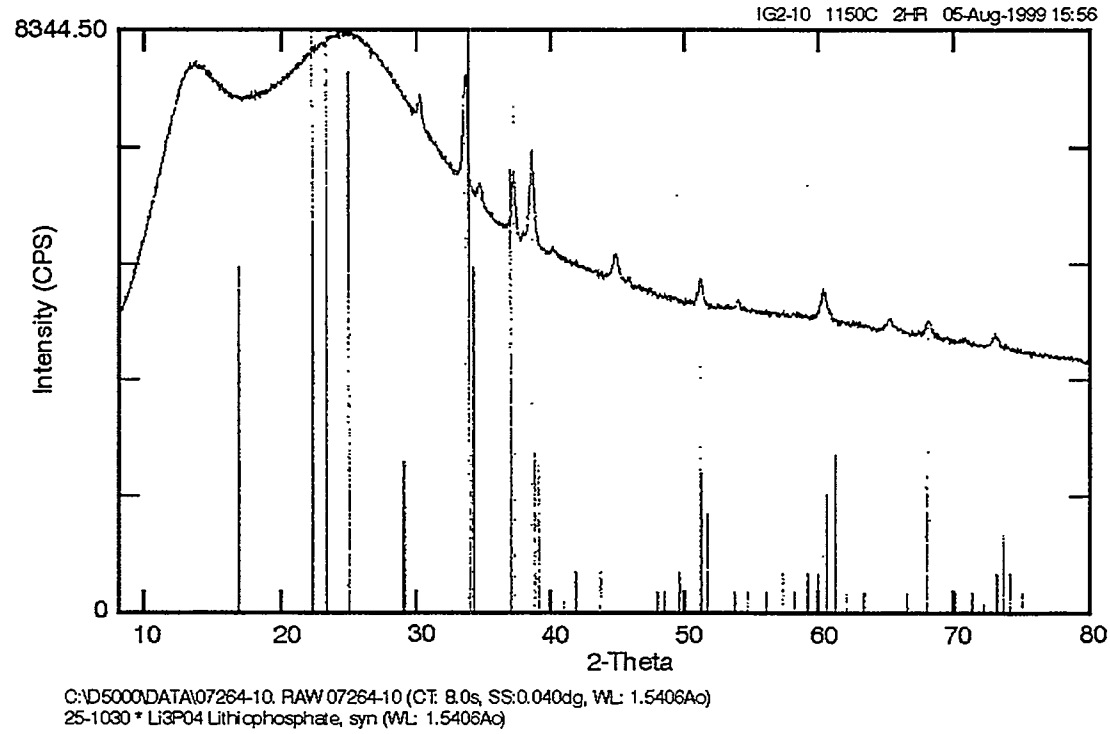

Figure A1-10. Four-hour XRD spectra of IG2-10 showing presence of lithium phosphate.

GG99 020C

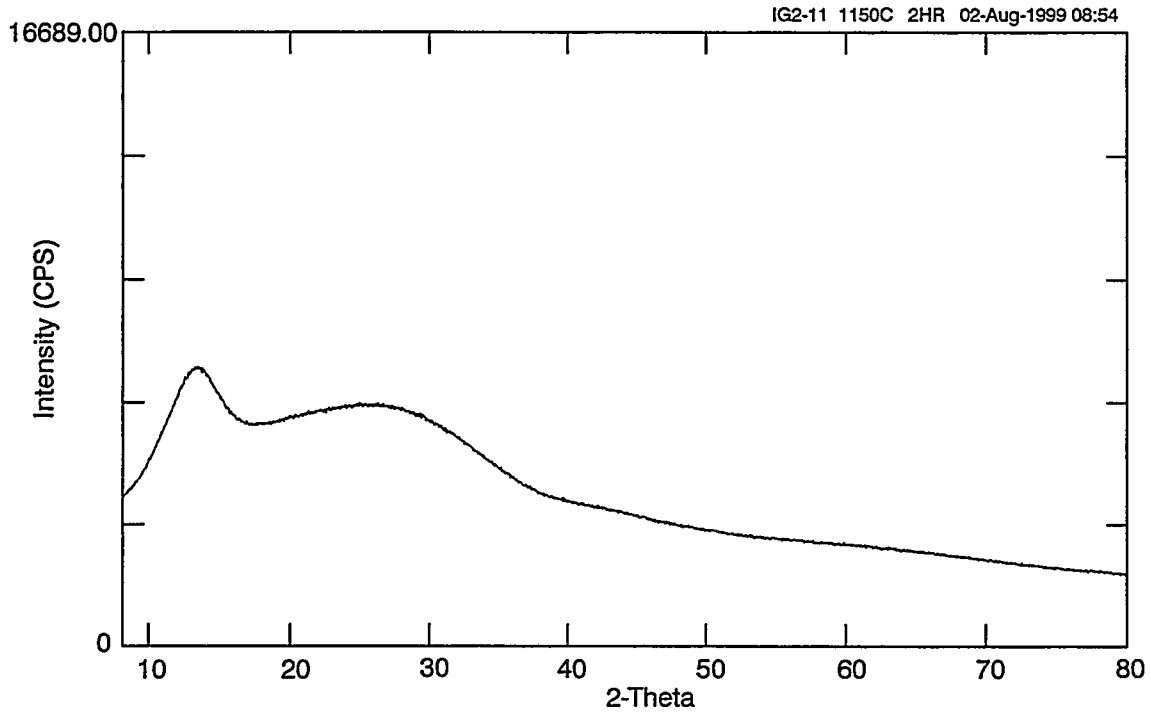

Figure A1-11. Four-hour XRD spectra of IG2-11 showing absence of crystallinity.

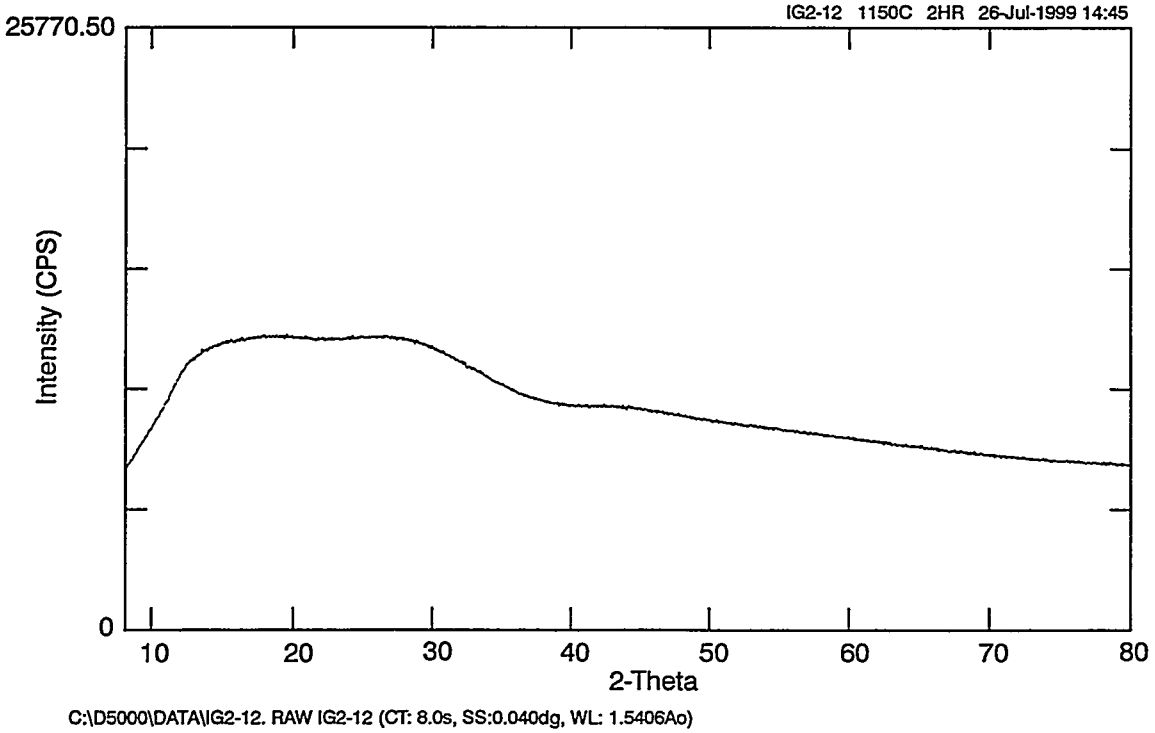

Figure A1-12. Four-hour XRD spectra of IG2-12 showing absence of crystallinity.

GG99 0201

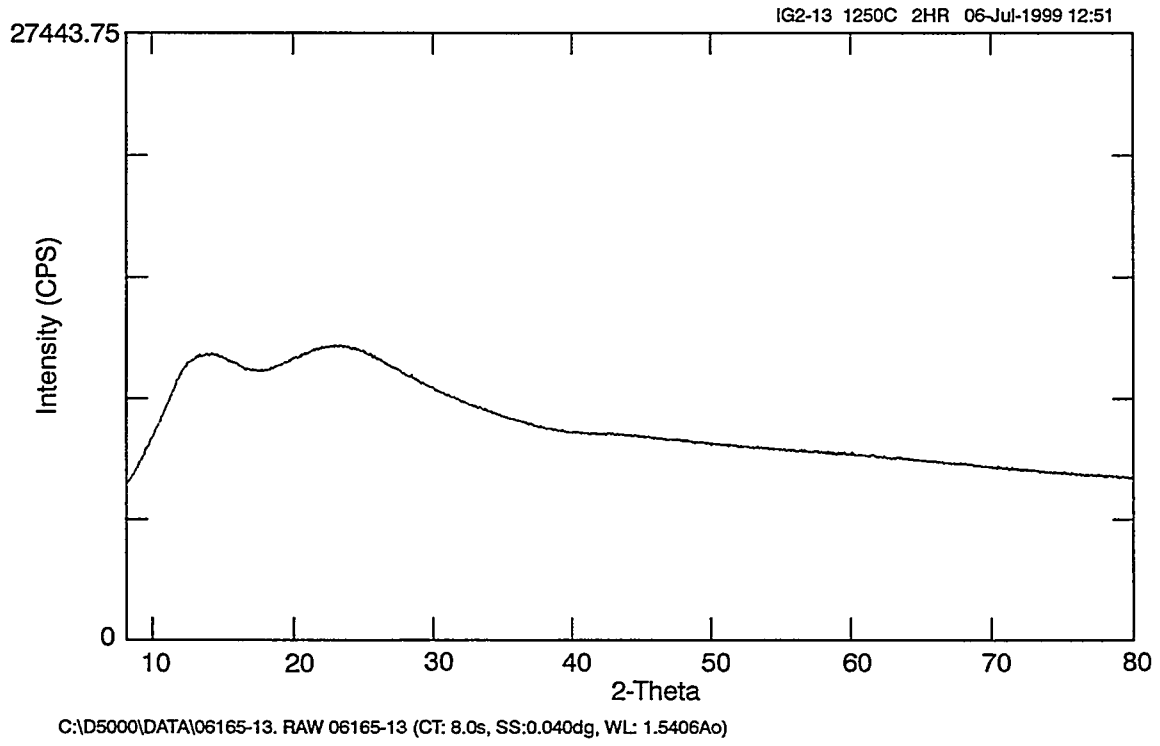

Figure A1-13. Four-hour XRD spectra of IG2-13 showing absence of crystallinity.

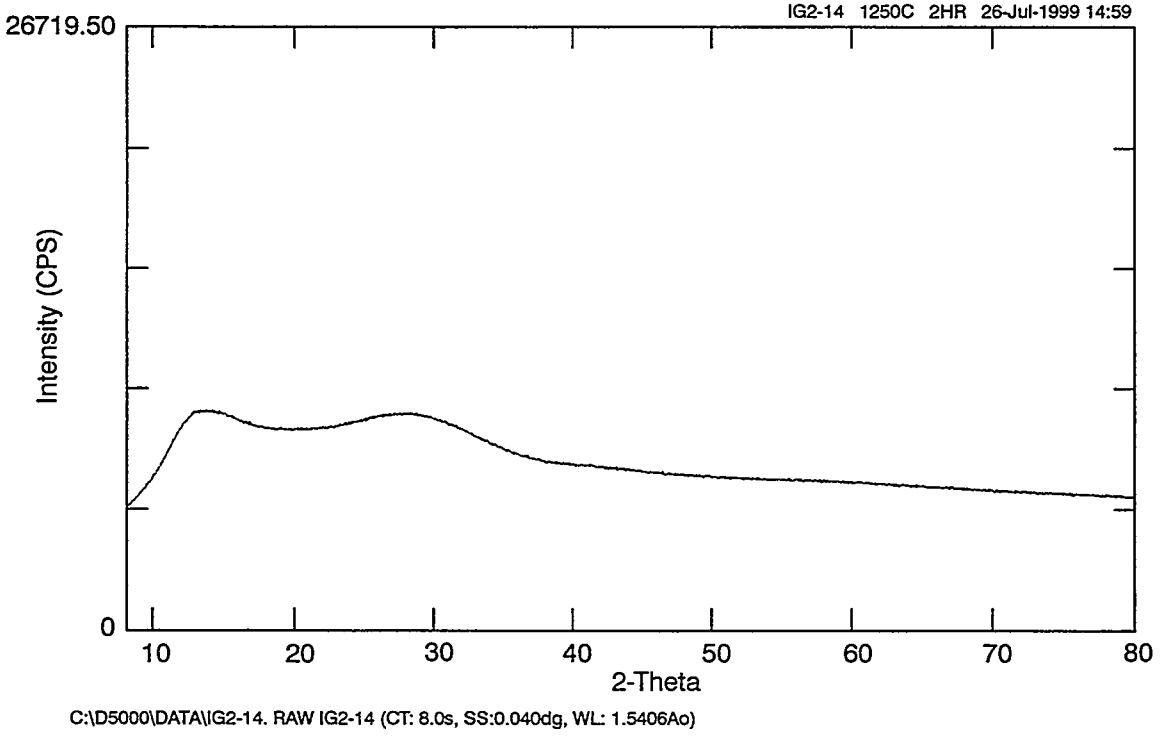

Figure A1-14. Four-hour XRD spectra of IG2-14 showing absence of crystallinity.

GG99 0203

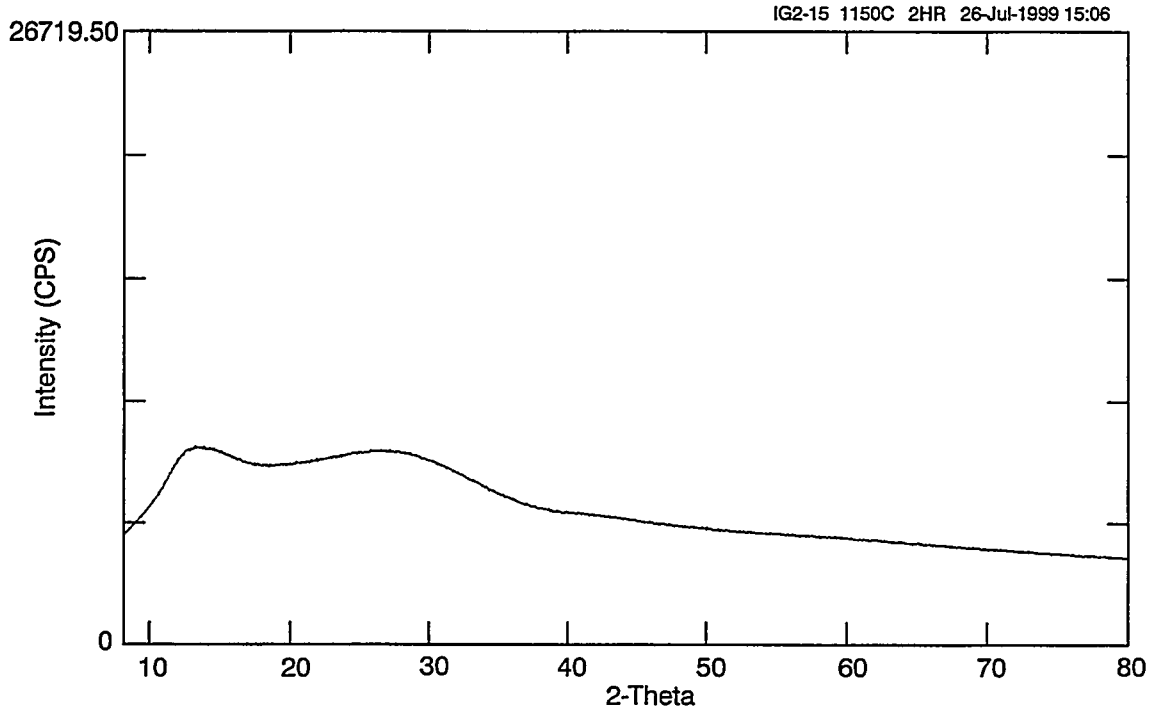

Figure A1-15. Four-hour XRD spectra of IG2-15 showing absence of crystallinity.

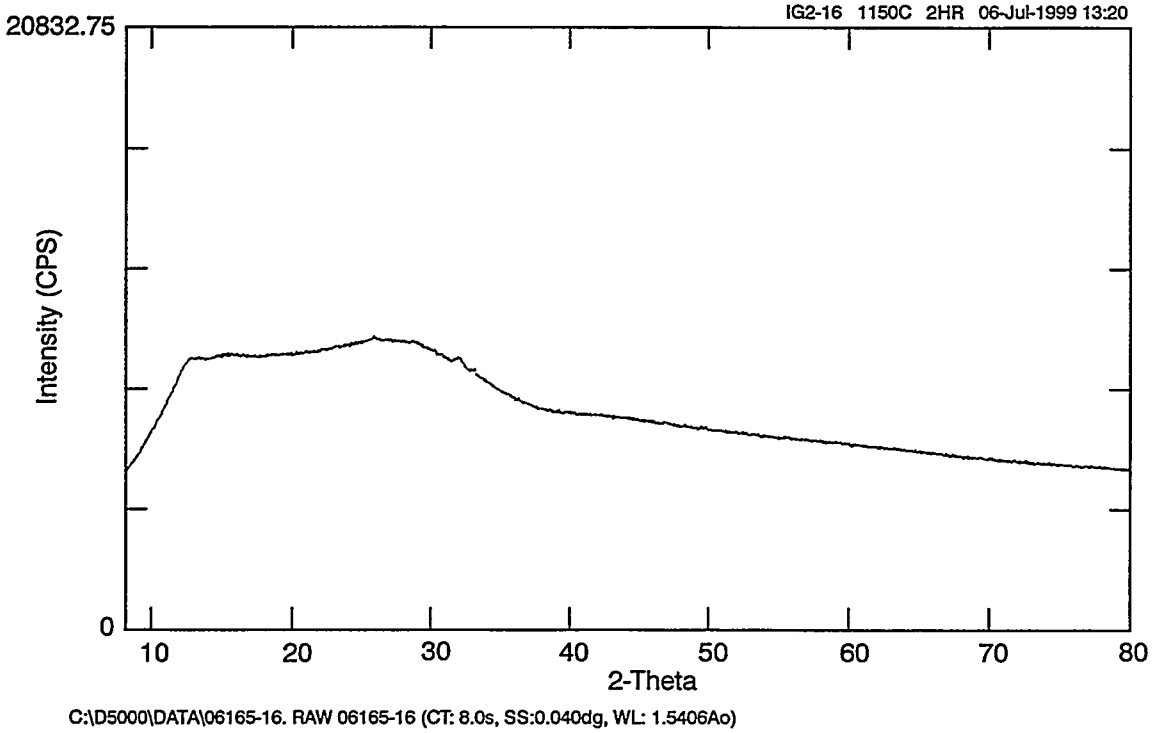

Figure A1-16. Four-hour XRD spectra of IG2-16 showing absence of crystallinity.

GG99 0204

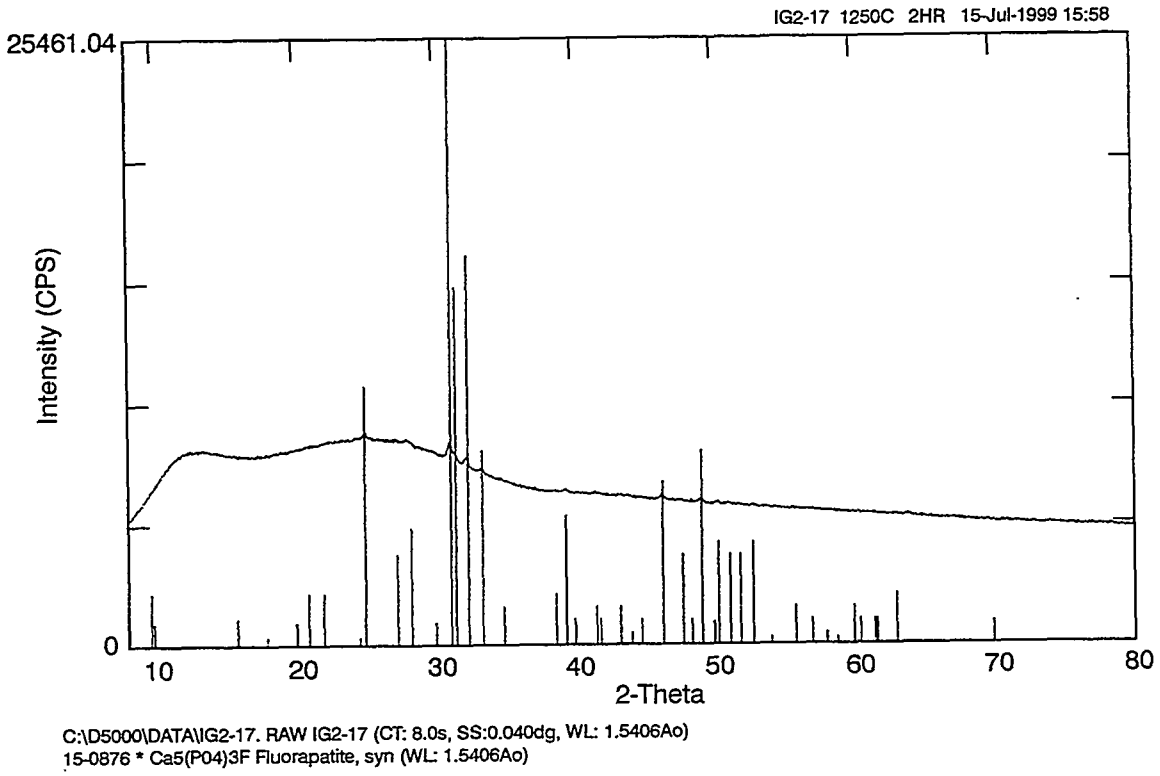

Figure A1-17. Four-hour XRD spectra of IG2-17 showing presence of fluorapatite.

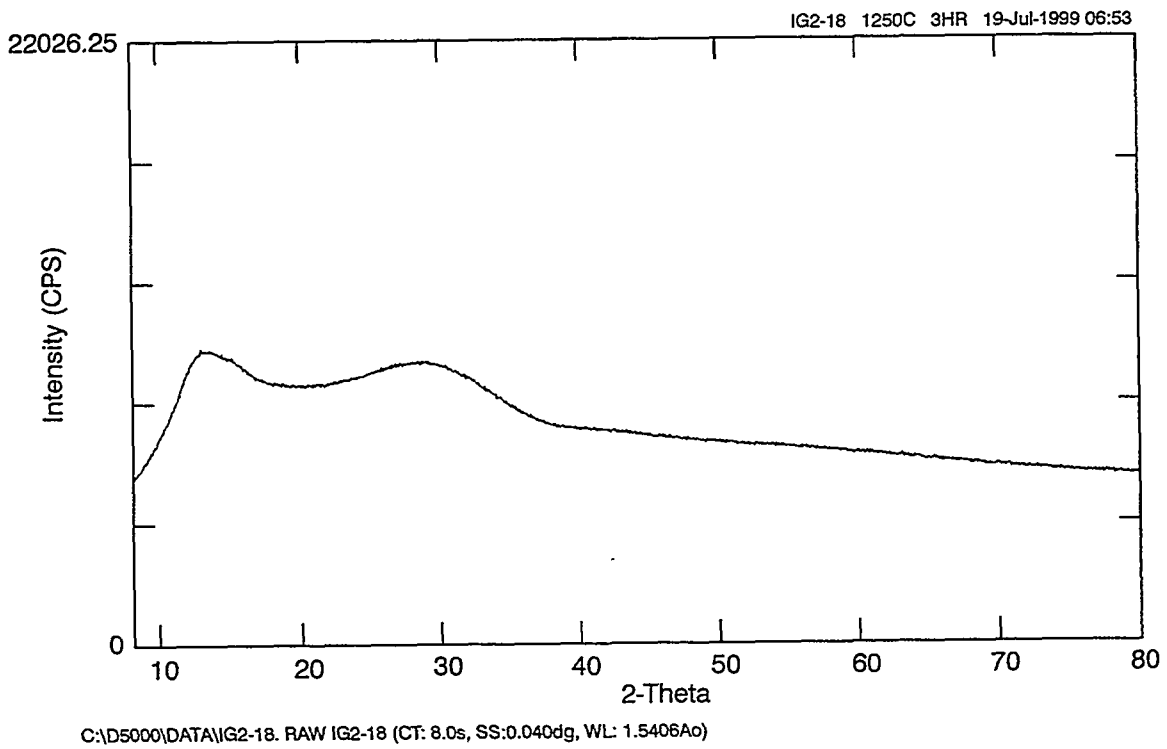

Figure A1-18. Four-hour XRD spectra of IG2-18 showing absence of crystallinity.

GG99 0205

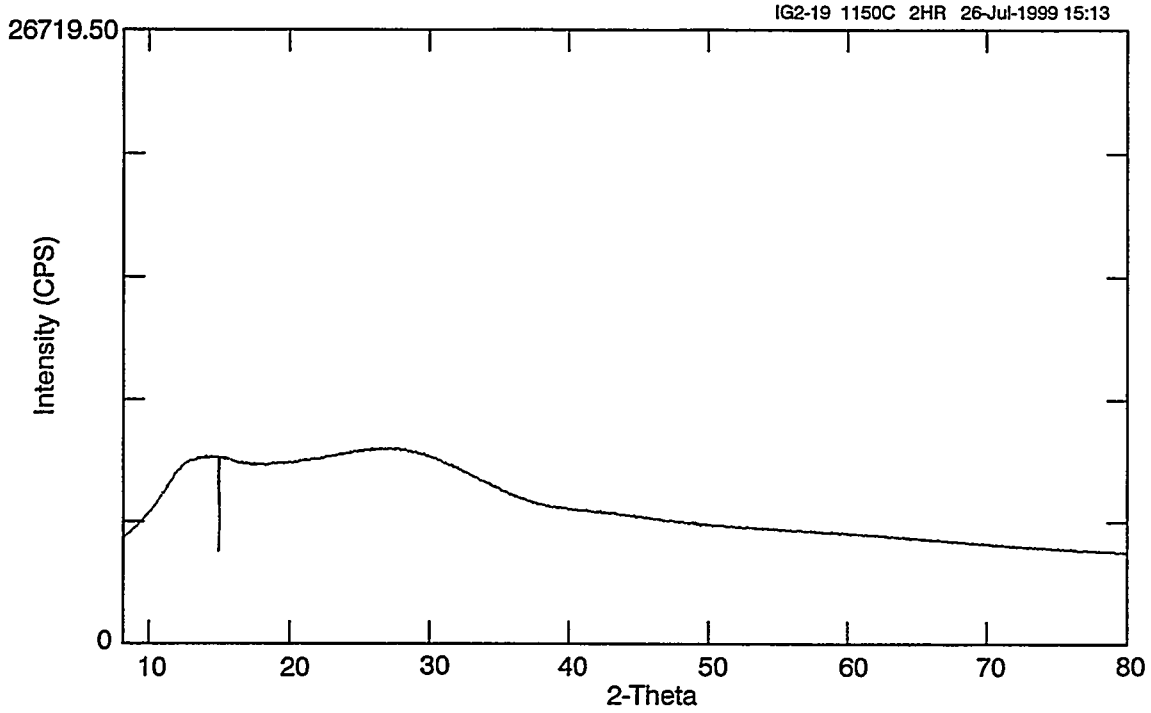

Figure A1-19. Four-hour XRD spectra of IG2-19 showing absence of crystallinity.

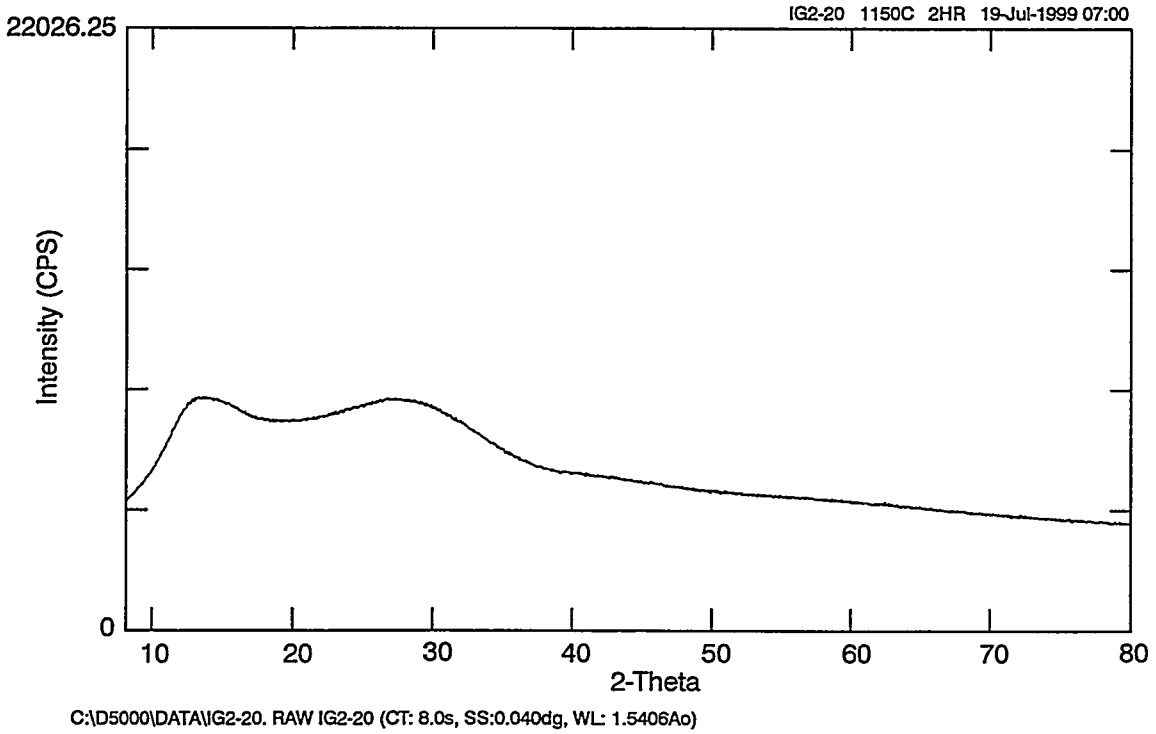

Figure A1-20. Four-hour XRD spectra of IG2-20 showing absence of crystallinity.

GG99 0206

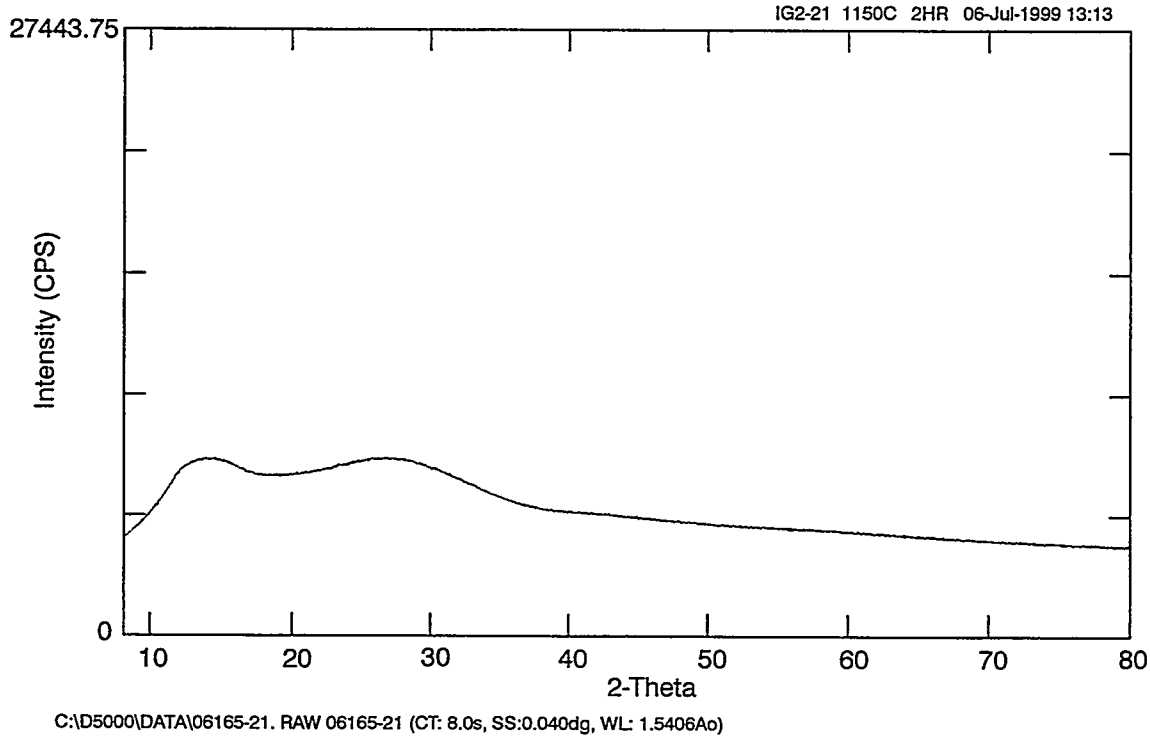

Figure A1-21. Four-hour XRD spectra of IG2-21 showing absence of crystallinity.

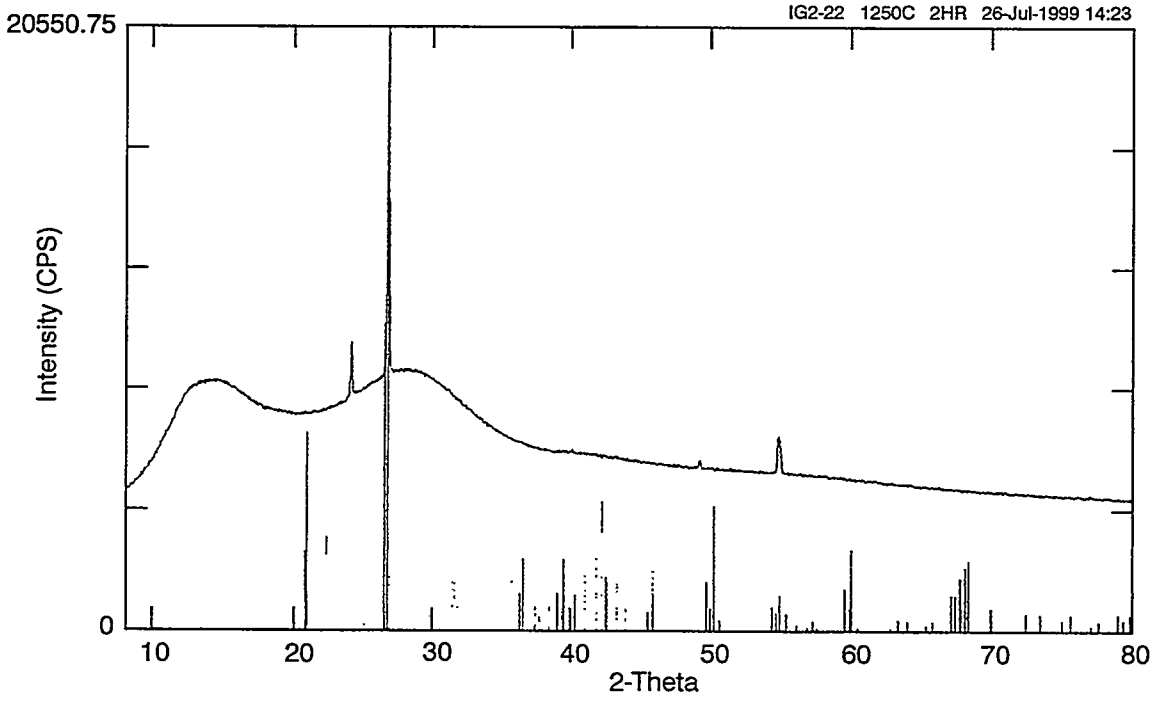

Figure A1-22. Four-hour XRD spectra showing presence of quartz and berlinite.

GG99 0207

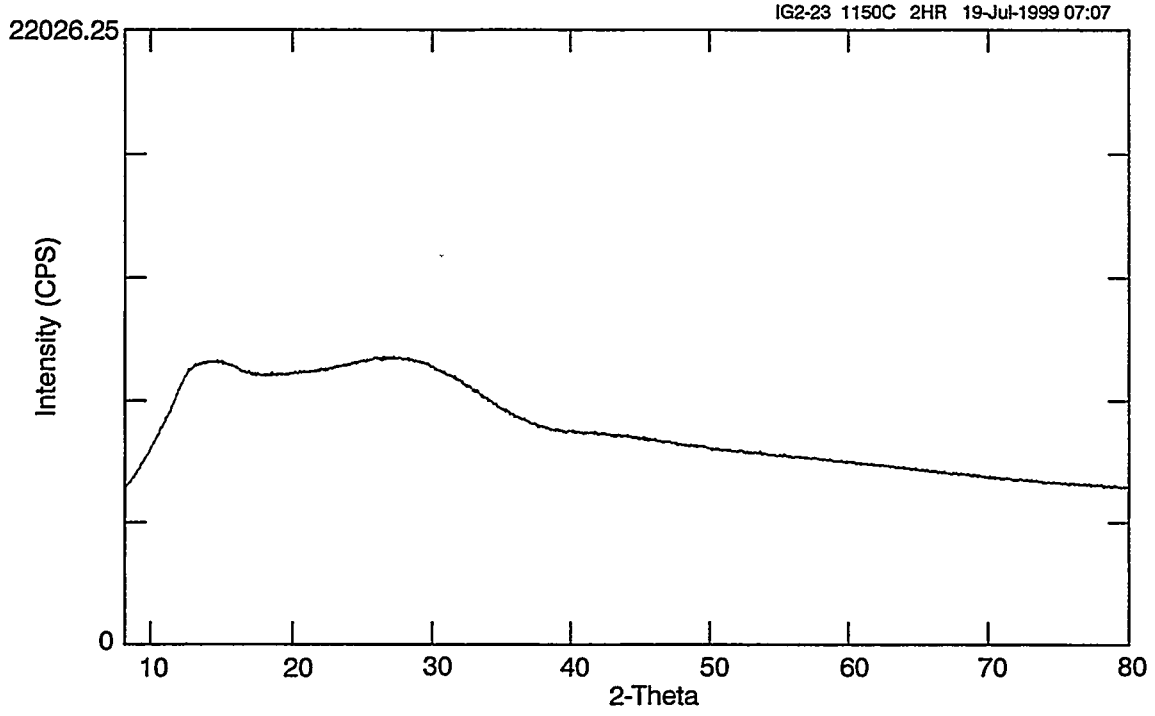

Figure A1-23. Four-hour XRD spectra of IG2-23 showing absence of crystallinity.

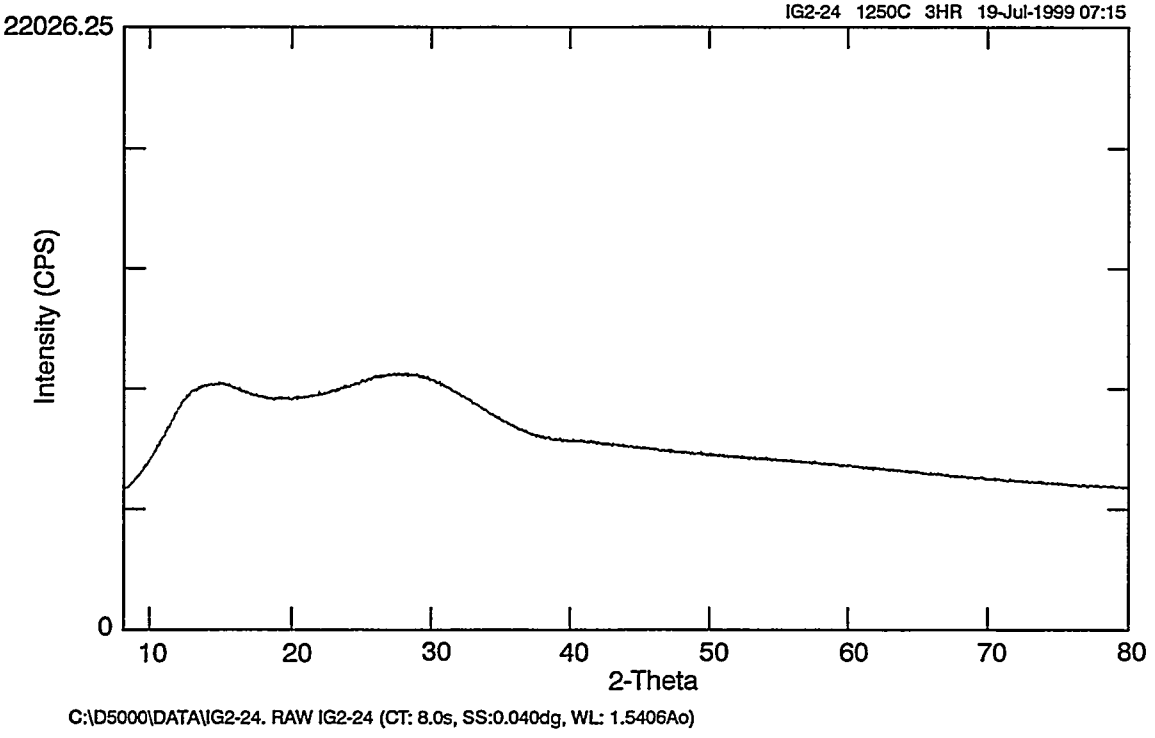

Figure A1-24. Four-hour XRD spectra of IG2-24 showing absence of crystallinity.

GG99 0208

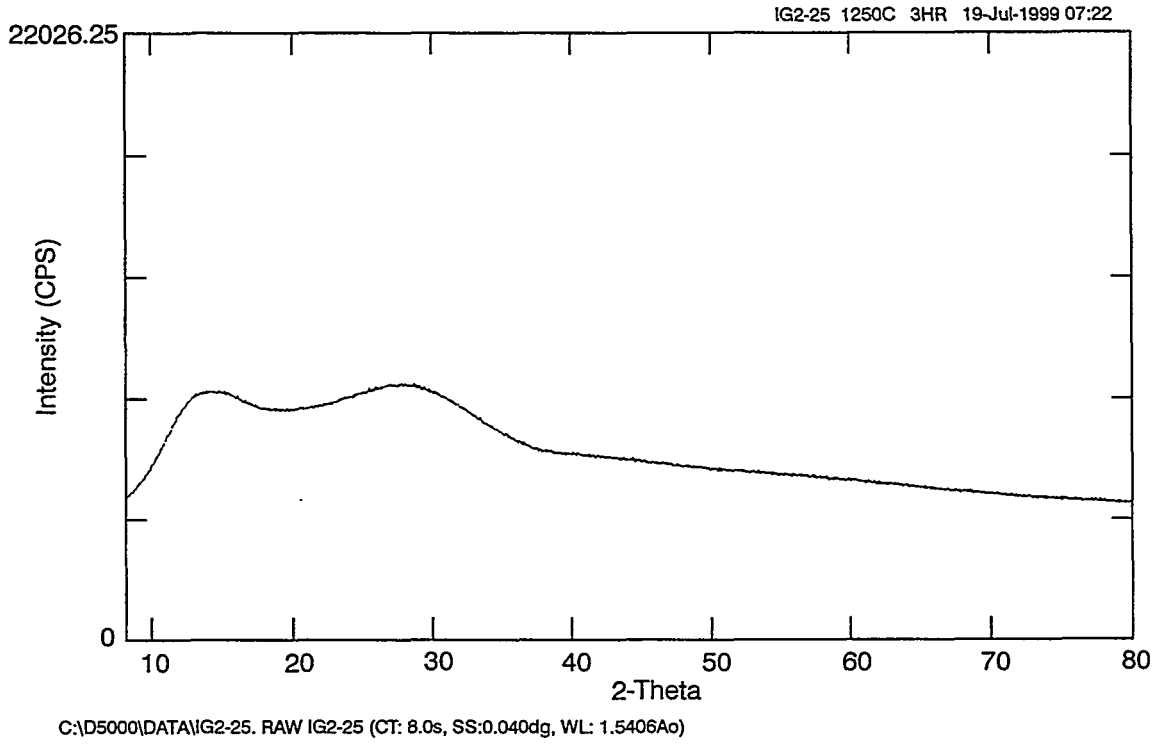

Figure A1-25. Four-hour XRD spectra of IG2-25 showing absence of crystallinity.

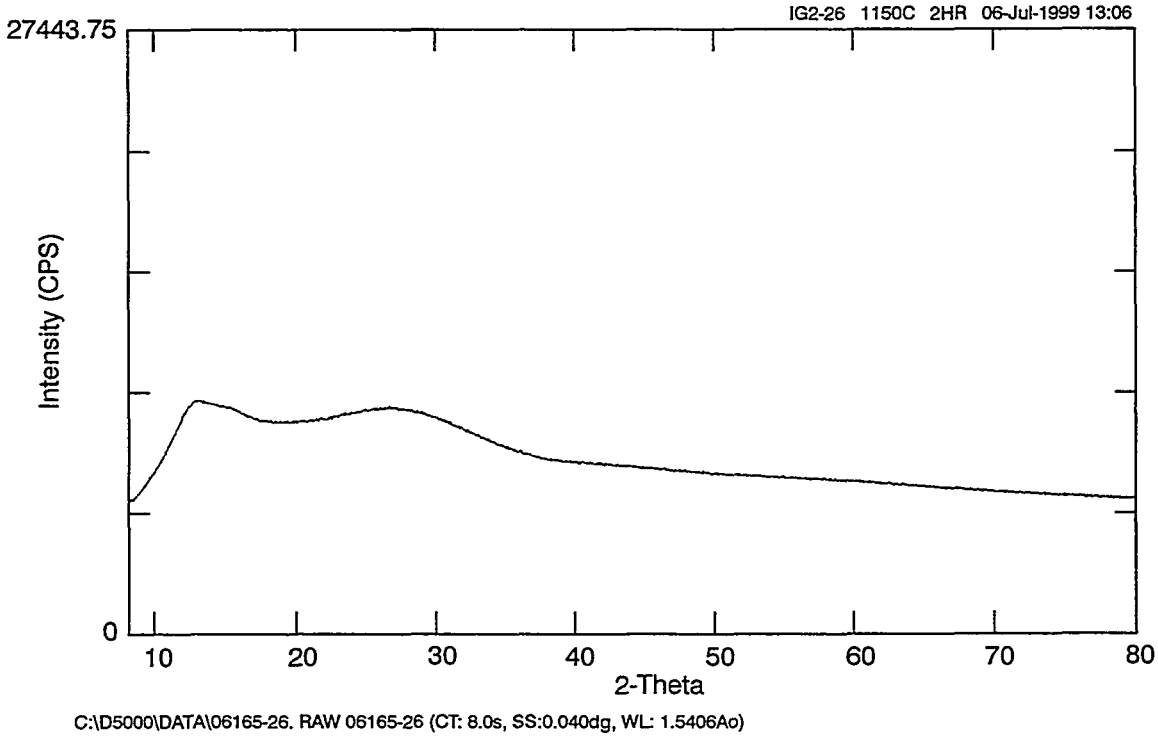

Figure A1-26. Four-hour XRD spectra of IG2-26 showing absence of crystallinity.

GG99 0209

Appendix B

Raw Data from PCT Leachate Analyses of INTEC Phase 2b CVS Glasses

Table B-1. PCT leachate analyses (μ g/ml) for EA and ARM standard glasses.

Glass	Al	B	Ca	Cr	F	Fe	K	Li	Mg	Na	Ni
ARM-1	5.16	47.11	0.14	0.00	0.00	0.02	0.14	37.51	0.00	83.40	0.00
ARM-2	4.71	48.38	0.20	0.00	0.00	0.01	0.17	37.84	0.00	83.50	0.01
EA-1	1.58	393.52	0.19	0.00	0.00	0.04	1.10	132.91	0.00	1045.00	0.00
EA-2	1.69	426.80	0.19	0.00	0.00	0.02	1.09	134.43	0.00	1081.00	0.00

Glass	P	S	Si	Sn	Sr	Zr
ARM-1	1.89	0.20	111.64	0.00	0.01	0.00
ARM-2	1.89	0.21	114.97	0.00	0.01	0.00
EA-1	0.45	0.61	541.94	0.00	0.00	0.00
EA-2	0.45	0.62	532.28	0.00	0.00	0.00

Table B-2. PCT leachate analyses (μ g/ml) for leachant blanks.

Glass	Al	B	Ca	Cr	F	Fe	K	Li	Mg	Na	Ni
Blank-A	0.14	0.00	0.14	0.00	0.00	0.05	0.07	0.01	0.00	0.03	0.01
Blank-B	0.07	0.00	0.08	0.00	0.00	0.01	0.07	0.01	0.00	0.08	0.00
Blank-C	0.07	0.00	0.10	0.00	0.00	0.01	0.06	0.00	0.00	0.04	0.00
Blank-D	0.05	0.30	0.09	0.00	0.00	0.01	0.05	0.01	0.02	0.04	0.00
Blank-E	0.15	0.08	0.05	0.00	0.00	0.02	0.05	0.01	0.00	0.07	0.00
Blank-F	0.15	0.04	0.05	0.00	0.00	0.01	0.06	0.01	0.00	0.10	0.00

Glass	P	S	Si	Sn	Sr	Zr
Blank-A	0.00	0.00	2.28	0.00	0.00	0.01
Blank-B	0.00	0.00	2.02	0.00	0.00	0.00
Blank-C	0.00	0.00	1.72	0.00	0.00	0.00
Blank-D	0.02	0.00	2.33	0.00	0.00	0.00
Blank-E	0.02	0.00	2.14	0.00	0.00	0.00
Blank-F	0.02	0.00	2.28	0.00	0.00	0.00

Table B-3. PCT leachate analyses (μg/ml) for phase 2b glasses.

Glass	Al	B	Ca	Cr	F	Fe	K	Li	Mg	Na	Ni
IG2-01-1	28.89	6.96	0.06	0.03	21.90	0.03	0.06	0.01	0.03	61.60	1.18
IG2-01-2	27.10	6.96	0.06	0.03	24.80	0.03	0.46	0.03	0.00	64.00	0.87
IG2-02-1	7.50	9.34	3.75	0.00	0.00	0.02	0.17	0.02	0.09	7.34	0.00
IG2-02-2	8.08	10.63	3.84	0.00	0.00	0.01	0.25	0.04	0.08	8.45	0.00
IG2-03-1	5.55	1197.89	0.07	0.00	206.10	3.04	0.69	1.17	0.37	337.00	0.12
IG2-03-2	6.49	1555.91	0.15	0.04	277.00	3.71	0.31	0.25	0.66	465.00	0.11
IG2-04-1	56.06	320.89	0.04	0.07	0.00	0.04	147.00	217.13	0.18	117.00	1.61
IG2-04-2	56.91	319.35	0.05	0.07	0.00	0.04	148.00	215.03	0.18	118.00	1.50
IG2-05-1	5.69	14.72	0.07	0.02	0.00	0.32	9.21	0.15	0.00	419.00	0.00
IG2-05-2	6.15	15.48	0.07	0.02	0.00	0.31	9.36	0.17	0.00	423.00	0.00
IG2-06-1	12.14	217.60	0.06	0.01	0.00	0.65	0.25	0.01	0.00	33.5	0.09
IG2-06-2	13.76	241.24	0.05	0.01	0.00	2.72	0.31	0.01	0.12	43.8	0.76
IG2-07-1	2.35	9.57	2.69	0.07	0.00	0.01	33.60	0.28	0.00	24.90	0.00
IG2-07-2	2.37	9.35	2.72	0.07	8.50	0.02	35.40	0.29	0.00	26.70	0.00
IG2-08-1	2.67	48.57	6.92	0.04	0.00	0.03	96.70	0.21	0.00	132.00	0.00
IG2-08-2	2.69	48.95	6.81	0.04	0.00	0.00	93.50	0.22	0.00	129.00	0.00
IG2-09-1	12.74	3.12	5.84	0.01	13.00	0.09	0.35	15.55	0.00	6.50	0.00
IG2-09-2	12.59	3.05	5.99	0.01	14.50	0.10	0.32	14.89	0.00	6.26	0.00
IG2-10-1	1.93	42.48	0.08	0.06	112.90	9.74	84.60	104.82	0.84	105.00	0.02
IG2-10-2	1.76	43.57	0.08	0.05	111.80	9.03	83.10	108.59	0.86	105.00	0.02
IG2-11-1	6.32	62.73	0.56	0.38	0.00	0.00	0.61	211.26	0.00	620.00	0.00
IG2-11-2	7.47	59.30	0.40	0.36	0.00	0.01	1.26	205.01	0.00	608.00	0.00
IG2-12-1	0.074	1289.37	0.10	0.08	1343.00	0.02	0.25	50.05	0.27	2139.00	0.00
IG2-12-2	0.096	1301.62	0.13	0.08	1356.00	0.02	0.18	51.15	0.29	2210.00	0.00
IG2-13-1	12.58	13.00	0.04	0.02	0.00	0.12	0.31	45.05	0.00	1.77	0.01
IG2-13-2	10.23	12.36	0.06	0.01	0.00	0.09	0.24	43.55	0.00	1.62	0.00
IG2-14-1	40.94	16.82	0.06	0.03	0.00	13.24	63.40	0.02	0.04	136.00	0.01
IG2-14-2	39.41	15.54	0.05	0.03	0.00	10.17	57.40	0.03	0.04	126.00	0.01
IG2-15-1	17.45	28.20	0.15	0.09	13.20	0.05	19.40	57.63	0.00	255.00	0.03
IG2-15-2	17.00	26.45	0.17	0.09	14.40	0.05	18.40	54.86	0.00	248.00	0.01
IG2-16-1	14.53	56.96	0.16	0.04	13.90	0.05	11.30	17.87	0.04	122.00	0.05
IG2-16-2	14.57	56.25	0.15	0.04	14.20	0.10	11.40	17.51	0.04	119.00	0.14
IG2-17-1	4.81	7.76	0.44	0.01	10.60	0.02	6.08	10.21	0.00	47.50	0.00
IG2-17-2	5.03	7.96	0.40	0.04	10.60	0.09	6.32	10.74	0.00	51.00	0.02
IG2-18-1	22.75	14.63	0.12	0.01	9.90	0.31	24.20	13.61	0.00	173.00	0.01

Table B-3. (continued).

Glass	Al	B	Ca	Cr	F	Fe	K	Li	Mg	Na	Ni
IG2-18-2	21.96	14.32	0.13	0.01	9.40	0.29	28.00	12.88	0.00	173.00	0.02
IG2-19-1	15.86	26.79	0.19	0.11	15.40	0.06	16.90	53.58	0.00	249.00	0.08
IG2-19-2	15.30	27.15	0.15	0.12	17.50	0.03	16.60	52.62	0.00	238.00	0.01
IG2-20-1	11.07	22.92	0.16	0.08	15.10	0.02	37.90	24.47	0.00	212.00	0.02
IG2-20-2	11.51	23.12	0.26	0.08	13.50	0.07	37.00	22.37	0.04	206.00	0.11
IG2-21-1	6.27	9.79	1.31	0.01	0.00	0.04	23.50	15.40	0.00	66.70	0.00
IG2-21-2	5.46	8.88	1.21	0.00	0.00	0.02	21.40	13.71	0.00	59.40	0.00
IG2-22-1	21.46	22.76	0.11	0.06	15.60	0.04	209.00	65.54	0.00	15.80	0.01
IG2-22-2	23.09	21.05	0.13	0.06	16.50	0.04	208.00	66.30	0.00	15.50	0.01
IG2-23-1	11.70	68.21	0.21	0.04	25.20	0.04	10.10	21.47	0.03	179.00	0.01
IG2-23-2	11.22	66.50	0.21	0.04	24.90	0.02	9.55	19.21	0.03	168.00	0.01
IG2-24-1	19.14	14.88	0.36	0.06	9.50	0.06	33.30	39.35	0.00	89.70	0.01
IG2-24-2	17.41	13.18	0.43	0.05	7.90	0.04	28.00	34.16	0.00	76.20	0.05
IG2-25-1	21.34	16.34	0.39	0.04	9.50	0.03	34.60	44.88	0.00	97.70	0.00
IG2-25-2	20.64	15.59	0.38	0.04	11.90	0.05	33.00	42.28	0.00	84.70	0.01
IG2-26-1	10.81	9.68	0.10	0.01	0.00	0.23	18.10	20.94	0.00	59.30	0.02
IG2-26-2	11.88	13.26	0.20	0.02	0.00	0.23	22.00	29.10	0.06	85.90	0.02
IG2-27-1	6.66	10.70	1.06	0.01	13.00	0.02	7.79	14.58	0.00	53.00	0.01
IG2-27-2	6.51	10.55	1.02	0.01	15.70	0.04	7.77	14.24	0.00	56.30	0.01
IG2-28-1	7.72	13.47	0.62	0.01	8.50	0.07	34.40	20.50	0.00	109.00	0.01
IG2-28-2	8.03	14.64	0.71	0.01	8.00	0.07	33.60	19.94	0.00	105.30	0.00
IG2-29-1	11.92	27.99	0.19	0.00	17.80	0.14	17.10	18.68	0.00	93.80	0.03
IG2-29-2	11.71	26.62	0.19	0.00	19.00	0.18	16.90	17.97	0.00	94.00	0.06
IG2-30-1	64.11	50.91	0.06	0.00	0.00	0.36	0.11	49.76	0.00	3.14	0.01
IG2-30-2	62.01	53.15	0.06	0.00	0.00	0.39	0.10	51.91	0.00	2.84	0.01
IG2-31-1	64.13	123.93	0.04	0.00	0.00	0.02	8.59	89.28	0.00	122.00	0.01
IG2-31-2	68.21	127.51	0.04	0.00	0.00	0.02	8.28	87.52	0.00	123.00	0.01
IG2-32-1	12.63	31.05	0.22	0.01	20.50	0.10	19.40	24.20	0.00	116.00	0.02
IG2-32-2	12.80	32.76	0.27	0.02	23.00	0.18	19.70	25.01	0.00	106.00	0.03
IG2-33-1	11.21	27.15	0.18	0.01	19.30	0.10	17.00	19.18	0.00	95.50	0.02
IG2-33-2	11.51	29.32	0.17	0.01	21.30	0.10	17.10	20.35	0.00	102.50	0.02
IG2-34-1	11.35	30.03	0.24	0.01	21.30	0.11	16.90	23.88	0.00	97.50	0.03
IG2-34-2	11.05	29.24	0.23	0.01	20.90	0.24	16.70	23.37	0.04	93.60	0.10
IG2-35-1	10.70	22.59	0.16	0.00	16.80	0.07	14.00	16.44	0.00	81.20	0.01
IG2-35-2	10.89	23.23	0.18	0.00	16.60	0.08	14.60	17.36	0.00	85.40	0.02
IG2-36-1	9.78	20.82	0.20	0.00	15.10	0.10	14.20	16.29	0.03	77.80	0.02

Table B-3. (continued).

Glass	Al	B	Ca	Cr	F	Fe	K	Li	Mg	Na	Ni
IG2-36-2	9.90	20.94	0.23	0.00	14.30	0.09	13.90	16.32	0.00	77.30	0.02
IG2-37-1	10.13	26.85	0.23	0.01	18.20	0.10	19.50	22.36	0.00	87.10	0.02
IG2-37-2	9.65	21.80	0.18	0.01	16.00	0.05	16.70	18.50	0.03	67.20	0.01

Glass	P	S	Si	Sn	Sr	Zr
IG2-01-1	0.03	0.30	60.38	0.03	0.00	0.01
IG2-01-2	0.14	0.33	55.27	0.03	0.00	0.01
IG2-02-1	0.19	0.00	16.06	0.00	0.01	0.00
IG2-02-2	0.18	0.00	16.15	0.00	0.01	0.00
IG2-03-1	0.09	0.00	112.25	0.03	0.02	0.10
IG2-03-2	0.23	0.00	126.51	0.04	0.04	0.03
IG2-04-1	0.10	0.66	80.51	0.08	0.00	1.23
IG2-04-2	0.02	0.65	81.65	0.08	0.00	1.04
IG2-05-1	0.15	0.90	51.67	0.00	0.00	0.00
IG2-05-2	0.10	0.94	54.20	0.00	0.00	0.00
IG2-06-1	12.73	1.00	57.63	0.00	0.00	0.77
IG2-06-2	13.49	1.10	61.44	0.02	0.00	1.05
IG2-07-1	0.08	0.89	22.85	0.00	0.01	0.03
IG2-07-2	0.05	0.90	24.12	0.00	0.01	0.00
IG2-08-1	0.02	0.51	83.13	0.00	0.06	0.00
IG2-08-2	0.03	0.50	85.80	0.00	0.06	0.00
IG2-09-1	0.00	0.16	19.96	0.00	0.01	0.00
IG2-09-2	0.00	0.16	19.73	0.00	0.01	0.00
IG2-10-1	37.15	1.70	107.77	0.23	0.02	0.02
IG2-10-2	37.42	1.83	125.60	0.22	0.01	0.01
IG2-11-1	6.96	3.79	711.66	0.00	0.01	0.00
IG2-11-2	5.77	3.65	679.73	0.00	0.01	0.00
IG2-12-1	0.14	3.06	46.76	0.02	0.01	0.36
IG2-12-2	0.11	3.24	45.95	0.01	0.01	0.40
IG2-13-1	0.21	0.47	117.40	0.06	0.00	5.54
IG2-13-2	0.15	0.43	116.21	0.05	0.00	3.76
IG2-14-1	5.49	0.45	62.87	0.09	0.01	2.37
IG2-14-2	5.10	0.44	59.77	0.07	0.01	1.87
IG2-15-1	3.50	1.26	130.85	0.03	0.00	0.04

Table B-3. (continued).

Glass	P	S	Si	Sn	Sr	Zr
IG2-15-2	3.50	1.15	118.45	0.02	0.00	0.04
IG2-16-1	2.65	0.69	33.28	0.00	0.00	0.28
IG2-16-2	2.54	0.67	30.55	0.00	0.00	0.31
IG2-17-1	0.15	0.33	38.13	0.00	0.00	0.00
IG2-17-2	0.15	0.31	39.12	0.00	0.00	0.00
IG2-18-1	2.65	0.65	58.50	0.03	0.00	0.04
IG2-18-2	2.49	0.64	58.93	0.00	0.00	0.01
IG2-19-1	3.40	1.14	114.21	0.00	0.00	0.07
IG2-19-2	3.49	1.14	125.60	0.00	0.00	0.03
IG2-20-1	2.60	0.90	104.49	0.01	0.00	0.03
IG2-20-2	2.70	0.87	108.97	0.01	0.00	0.10
IG2-21-1	0.20	0.60	36.17	0.00	0.01	0.03
IG2-21-2	0.06	0.34	59.06	0.00	0.00	0.00
IG2-22-1	3.15	0.69	66.35	0.03	0.00	0.02
IG2-22-2	3.06	0.68	66.50	0.05	0.00	0.02
IG2-23-1	4.45	0.57	42.12	0.00	0.00	0.12
IG2-23-2	4.33	0.53	43.44	0.00	0.00	0.13
IG2-24-1	0.17	0.62	19.30	0.00	0.00	0.00
IG2-24-2	0.14	0.48	52.62	0.00	0.00	0.01
IG2-25-1	0.17	0.68	16.67	0.00	0.00	0.00
IG2-25-2	0.15	0.67	19.17	0.00	0.00	0.00
IG2-26-1	1.69	0.39	60.54	0.00	0.00	0.02
IG2-26-2	2.36	0.50	76.12	0.02	0.00	0.18
IG2-27-1	0.09	0.38	48.62	0.00	0.00	0.02
IG2-27-2	0.09	0.39	49.36	0.00	0.00	0.01
IG2-28-1	0.10	0.58	45.85	0.00	0.00	0.00
IG2-28-2	0.10	0.59	55.29	0.00	0.00	0.00
IG2-29-1	1.99	0.00	50.38	0.00	0.00	0.08
IG2-29-2	1.98	0.00	48.00	0.00	0.00	0.08
IG2-30-1	0.05	0.00	176.56	0.00	0.00	14.73
IG2-30-2	0.04	0.00	180.61	0.00	0.00	15.32
IG2-31-1	13.24	0.13	157.97	0.00	0.00	0.04
IG2-31-2	13.00	0.11	165.36	0.00	0.00	0.07
IG2-32-1	2.20	0.95	52.81	0.00	0.00	0.09
IG2-32-2	2.22	0.91	56.96	0.00	0.00	0.11
IG2-33-1	2.00	0.52	47.66	0.00	0.00	0.06

Table B-3. (continued).

Glass	P	S	Si	Sn	Sr	Zr
IG2-33-2	1.86	0.53	58.01	0.00	0.00	0.05
IG2-34-1	1.89	0.61	53.53	0.00	0.00	0.11
IG2-34-2	1.83	0.57	53.43	0.00	0.00	0.14
IG2-35-1	1.86	0.55	48.97	0.00	0.00	0.05
IG2-35-2	1.93	0.57	49.07	0.00	0.00	0.06
IG2-36-1	1.12	0.63	47.11	0.00	0.03	0.02
IG2-36-2	1.27	0.61	47.34	0.00	0.03	0.04
IG2-37-1	0.77	1.19	50.53	0.00	0.06	0.02
IG2-37-2	0.62	0.76	46.74	0.00	0.07	0.00

Appendix C

Raw Data from Viscosity Measurements on Phase 2b Glasses

Table C-1. Viscosities calculated from temperatures (°C) measured by viscometer thermocouple.

Sample No.	Measured Viscosity (Pa-sec) at Sample Temperature (C)											
IG2-01*												
Temp (C)	1156.7	1105.7	1055.4	1006.5	956.6	1155.6	1204.6	1254.5	1303.8	1353.8	~~1156.2~~	~~1254.9~~
η (Pa-sec)	29.94	46.49	76.18	130.91	237.94	31.02	21.84	15.76	11.31	8.56	~~41.16~~	~~19.67~~
IG2-02												
Temp (C)	1254.9	1205.0	1155.5	1105.8	1056.1	1156.6	1205.9	1255.0	1304.5	1354.7	1405.5	1255.6
η (Pa-sec)	23.36	42.21	81.00	170.14	415.42	84.56	42.01	23.46	13.93	9.39	6.62	22.74
IG2-04												
Temp (C)	1157.1	1106.2	1056.1	1006.4	956.8	1156.5	1205.6	1255.7	1156.9			
η (Pa-sec)	1.64	2.35	3.47	5.35	8.64	1.66	1.22	0.91	1.70			
IG2-05*												
Temp (C)	1256.3	1205.8	1156.1	1106.7	~~1057.3~~	~~1156.3~~	~~1205.2~~	1254.7	1304.2	1254.6		
η (Pa-sec)	1.17	1.98	3.24	5.83	~~17.78~~	~~4.92~~	~~2.32~~	1.02	0.71	1.15		
IG2-06*												
Temp (C)	~~1157.7~~	~~1107.3~~	~~1057.5~~	1007.7	958.0	1157.4	1206.7	1256.1	1157.1			
η (Pa-sec)	~~1.28~~	~~2.07~~	~~2.96~~	3.84	5.77	0.85	0.63	0.45	0.92			
IG2-07*												
Temp (C)	~~1256.5~~	~~1206.5~~	~~1156.9~~	1107.2	1057.2	1157.4	1206.4	1255.2	1304.5	1354.0	1255.8	
η (Pa-sec)	~~5.54~~	~~37.23~~	~~122.15~~	338.10	749.13	99.78	29.18	7.22	2.94	1.91	8.86	
IG2-08												
Temp (C)	1157.8	1107.4	1057.3	1007.5	957.7	1058.7	1157.9	1206.7	1255.6	1156.8		
η (Pa-sec)	1.37	2.11	3.46	6.21	12.36	3.41	1.39	0.97	0.70	1.43		

Table C-1. (continued).

Sample No.	Measured Viscosity (Pa-sec) at Sample Temperature (C)													
IG2-09*														
Temp (C)	1159.4	1108.1	1057.7	1007.9	958.3	1059.1	1158.2	1207.4	1256.6	1157.6				
η (Pa-sec)	1.34	2.10	3.40	5.97	13.25	3.93	1.42	0.98	0.70	1.46				
IG2-10*														
Temp (C)	1059.1	1007.7	956.8	906.8	~~857.3~~	~~957.8~~	1057.3	1106.8	1156.2	1205.5	1254.8	1155.7	1056.3	1156.7
η (Pa-sec)	6.92	11.73	21.69	46.76	~~138.01~~	~~26.48~~	7.28	4.25	2.86	2.04	1.45	3.04	7.13	3.02
IG2-11														
Temp (C)	1059.4	1007.4	956.9	906.9	857.1	957.5	1057.1	1106.7	1156.3	1205.7	1255.2	1156.0	1056.3	1156.6
η (Pa-sec)	3.05	4.88	8.06	14.19	27.45	8.02	3.17	2.15	1.53	1.10	0.82	1.54	3.28	1.53
IG2-12														
Temp (C)	1061.8	957.6	907.3	857.3	958.1	1007.3	1057.4	1106.9	1156.3	1205.5	1254.8	1155.7	1056.2	1156.7
η (Pa-sec)	4.34	18.06	42.00	112.57	18.82	9.33	4.82	2.85	1.84	1.25	0.88	2.06	5.96	2.08
IG2-13														
Temp (C)	1254.8	1204.7	1155.2	1105.6	1055.7	1156.1	1205.5	1254.9	1304.4	1354.3	1255.1			
η (Pa-sec)	7.54	12.19	20.65	36.93	71.19	20.72	12.36	7.70	4.96	3.37	7.70			
IG2-14														
Temp (C)	1255.5	1204.9	1155.4	1205.1	1254.3	1303.8	~~1354.4~~	1403.0	1452.9	1353.7	1254.7	1353.8	1452.8	
η (Pa-sec)	44.31	68.02	120.90	66.89	39.05	24.58	~~17.66~~	9.21	6.09	15.54	44.17	15.97	6.31	
IG2-15														
Temp (C)	1157.1	1106.4	1056.1	956.4	1057.4	1156.6	1205.7	1254.9	1155.6					
η (Pa-sec)	3.86	5.90	9.48	28.44	9.44	3.93	2.76	1.97	4.01					
IG2-16														
Temp (C)	1156.1	1105.3	1054.8	1004.9	955.2	1055.7	1155.3	1204.7	1254.2	1155.4				
η (Pa-sec)	4.37	7.14	12.25	22.29	44.05	12.20	4.45	2.95	2.03	4.64				

Table C-1. (continued).

Sample No.	Measured Viscosity (Pa-sec) at Sample Temperature (C)												
IG2-17*													
Temp (C)	1254.3	1204.1	1154.4	1104.7	1054.8	~~1005.1~~	1155.2	1204.5	1253.9	1303.5	1253.9		
η (Pa-sec)	4.74	7.51	12.40	21.58	40.11	~~99.00~~	12.55	7.61	4.89	3.33	5.07		
IG2-18													
Temp (C)	1254.9	1205.1	1155.6	1106.1	1056.3	1006.6	956.9	1057.8	1157.0	1255.1	1304.4	1354.0	1255.0
η (Pa-sec)	2.86	4.42	7.10	11.88	20.72	39.00	79.49	20.41	6.89	2.89	1.99	1.42	3.04
IG2-19													
Temp (C)	1156.1	1105.6	1055.5	1007.0	957.3	1058.2	1157.3	1206.5	1255.7	1156.6			
η (Pa-sec)	3.57	5.52	8.84	14.81	26.43	8.72	3.64	2.53	1.79	3.74			
IG2-20													
Temp (C)	1158.7	1107.3	1056.9	1006.9	957.2	1058.2	1157.6	1206.6	1255.8	1156.6			
η (Pa-sec)	6.65	10.93	18.44	32.56	62.00	18.51	6.96	4.64	3.14	7.27			
IG2-21													
Temp (C)	1158.7	1108.0	1057.7	1007.5	957.6	1058.8	1158.1	1207.1	1256.1				
η (Pa-sec)	10.79	17.95	31.62	59.57	120.82	31.53	11.11	7.17	4.69				
IG2-22*													
Temp (C)	1158.1	1116.7	1058.4	1007.6	957.9	1059.3	1158.4	1207.2	1256.2	1157.0			
η (Pa-sec)	6.00	9.29	18.49	35.81	75.12	19.21	6.40	3.83	2.52	6.30			
IG2-23													
Temp (C)	1158.4	1107.5	1057.2	1007.4	957.7	1058.8	1157.9	1206.9	1256.0	1156.8			
η (Pa-sec)	3.51	5.68	9.75	17.65	34.49	9.73	3.56	2.37	1.63	3.64			
IG2-24													
Temp (C)	1159.2	1108.9	1058.7	1008.9	959.3	1060.1	1158.5	1207.1	1256.2	1157.0			
η (Pa-sec)	3.56	5.85	9.95	17.85	33.40	9.70	3.59	2.33	1.56	3.66			

Table C-1. (continued).

Sample No.	Measured Viscosity (Pa-sec) at Sample Temperature (C)									
IG2-25										
Temp (C)	1158.9	1108.3	1058.2	1008.3	958.6	1059.7	1158.8	1207.8	1256.6	1157.3
η (Pa-sec)	3.73	6.15	10.46	18.65	34.14	10.04	3.79	2.46	1.65	3.87
IG2-26										
Temp (C)	1156.7	1106.6	1056.6	1006.8	957.1	1057.9	1157.3	1206.5	1255.7	1156.3
η (Pa-sec)	11.00	18.27	32.31	60.42	121.48	31.70	10.98	7.16	4.79	11.15
IG2-27*										
Temp (C)	1157.2	1106.8	1056.7	~~1007.0~~	~~957.4~~	~~1058.0~~	1157.2	1206.3	1255.4	1156.2
η (Pa-sec)	12.94	22.34	43.41	~~263.20~~	~~961.09~~	~~133.31~~	13.54	8.33	5.37	13.23
IG2-28										
Temp (C)	1158.5	1107.5	1056.7	1006.8	957.0	1057.7	1157.0	1206.2	1255.3	1156.2
η (Pa-sec)	7.38	12.07	20.88	38.38	76.51	20.63	7.16	4.72	3.29	7.42
IG2-29										
Temp (C)	1158.5	1107.2	1056.3	1006.4	956.5	1057.4	1156.6	1205.6	1254.8	1155.7
η (Pa-sec)	4.11	6.56	11.04	19.21	35.85	10.91	4.30	2.90	2.03	4.48
IG2-30										
Temp (C)	1157.7	1107.7	1057.6	1007.9	958.2	1059.3	1158.4	1207.0	1255.9	1156.8
η (Pa-sec)	10.22	15.80	25.80	44.42	82.84	25.46	10.26	6.96	4.89	10.45
IG2-31										
Temp (C)	1158.3	1107.1	1056.9	1008.2	958.5	1059.6	1156.9	1205.7	1254.5	1155.5
η (Pa-sec)	7.75	12.90	22.80	43.08	88.52	22.54	7.89	5.10	3.45	8.08

Table C-1. (continued).

Sample No.	Measured Viscosity (Pa-sec) at Sample Temperature (C)									
IG2-32										
Temp (C)	1160.2	1108.7	1058.0	1008.0	958.2	1059.3	1158.4	1207.2	1256.3	1157.1
η (Pa-sec)	4.54	7.31	12.29	21.89	41.66	12.37	4.72	3.18	2.19	4.94
IG2-33										
Temp (C)	1157.6	1106.4	1056.1	1006.3	956.6	1057.4	1156.9	1206.0	1255.2	1155.8
η (Pa-sec)	3.53	5.69	9.54	16.86	32.02	9.59	3.62	2.46	1.72	3.79
IG2-34*										
Temp (C)	1157.3	1106.8	1056.6	1006.7	956.9	1057.8	1157.1	1206.1	1255.3	1156.0
η (Pa-sec)	4.58	7.38	12.47	22.31	42.80	12.26	4.67	3.14	2.18	4.90
IG2-35										
Temp (C)	1156.7	1106.7	1056.8	1006.9	957.2	1058.3	1157.5	1206.6	1255.7	1156.4
η (Pa-sec)	4.16	6.56	10.91	19.21	36.18	10.69	4.19	2.83	1.96	4.35
IG2-36										
Temp (C)	1158.4	1107.4	1057.1	1007.2	957.4	1058.3	1157.6	1206.7	1256.0	1156.8
η (Pa-sec)	3.94	6.26	10.41	18.35	34.72	10.35	4.10	2.78	1.95	4.26
IG2-37										
Temp (C)	1157.1	1107.3	1057.4	1007.6	957.8	1058.8	1158.0	1207.3	1256.5	1157.4
η (Pa-sec)	4.25	6.69	11.19	19.76	37.61	11.03	4.29	2.88	2.01	4.49